

Programa de Doctorado en Hidrología y Gestión de los Recursos Hídricos

Wastewater Treatment by Membrane-Based Systems: Removal of Emerging Contaminants and Water Reuse using Recycled Membranes

TESIS DOCTORAL

Anamary Pompa Pernía

2025



Programa de Doctorado en Hidrología y Gestión de los Recursos Hídricos

Wastewater Treatment by Membrane-Based Systems: Removal of Emerging Contaminants and Water Reuse using Recycled Membranes

Tesis Doctoral presentada por:

Anamary Pompa Pernía

Dirigida por:

Dra. Serena Molina Martínez Dra. Junkal Landaburu Aguirre

Departamento de Química Analítica, Química Física e Ingeniería Química

Alcalá de Henares, 2025

Acknowledgments

The research work presented in this doctoral thesis is part of the national projects INREMEM 2.0 (Hybrid wastewater treatments based on recycled membranes with the objective of zero liquid discharge (ZLD), grant RTI2018-096042-B-C21) and nanoCLEAN (Quantification, treatment and environmental impact of micronanoplastics in WWTPs, grant PID2019-111519RA-I00), which are funded by MICIU/AEI /10.13039/501100011033.

I would like to express my gratitude to the program of predoctoral contracts for training doctors (FPI), grant PRE2019-088421 funded by MICIU/AEI /10.13039/501100011033 and by ESF Investing in your future.

I also would like to express my sincere gratitude to the Department of Hydro Systems of Technische Universität Dresden, Germany, for hosting me as a visiting scholar in its institution, where a part of the presented investigation was carried out. Lastly, the support from the University of Alcalá and IMDEA Water are particularly acknowledged.

















Como es característico en toda investigación, esta tesis representa la colaboración de numerosas personas e instituciones, a quienes deseo expresar mi gratitud.

En primer lugar, agradezco al instituto IMDEA Agua por brindarme la oportunidad de desarrollar este trabajo. Un reconocimiento especial al exdirector y jefe de línea, el Prof. Eloy García-Calvo.

Quiero extender un agradecimiento muy especial a mis directores de tesis, la Dra. Serena Molina y la Dra. Junkal Landaburu Aguirre, ya que sin su apoyo esta investigación no habría sido posible. A Serena, por confiar en mí para dar continuidad a su proyecto. A Junkal, por redireccionar mi camino, por compartir sus ideas conmigo y hacerme ver los matices. A ambas, les agradezco profundamente toda su dedicación durante estos años, así como sus infinitas revisiones y correcciones, que han enriquecido significativamente este trabajo. He tenido la fortuna de contar con su cercanía y disponibilidad, sin olvidar el coaching tan necesario durante estos años de formación como investigadora.

I want to acknowledge Prof. André Lerch for allowing me to work in his research group at TU-Dresden. To Dr. Kristin Kerst, for welcoming me so warmly (including our trips together), and for our fruitful collaboration. To Ana Alemán, for developing all the image processes and for her company.

Al grupo de Tecnología de Membranas de IMDEA, en particular a la ya doctora Amaia Ortiz, por todo su apoyo al inicio de mi tesis (tanto dentro como fuera del instituto) y a la también reciente doctora Laura Rodríguez por ser una fuente de inspiración en el ámbito MBR. A Imane, por su asistencia en el laboratorio y, sobre todo, por el tiempo compartido tanto dentro como fuera de IMDEA, así como por continuar con este trabajo.

A todos mis excompañeros de IMDEA Agua, por hacer el instituto un lugar agradable para trabajar.

A los amigos que me han brindado su apoyo durante estos años. A mi familia, especialmente a Ángel, por traerme hasta aquí. A Denis, por estar a mi lado en este viaje. Por todo, gracias.

Contents

List of Figures	i
List of Tables	iii
List of Abbreviations	iv
Resumen	vii
Abstract	X
Publications	xiiii
Other Contributions	xiii
Research stay	xiviv
CHAPTER I: General Introduction	1
1.1 Water scarcity	1
1.2 Desalination and Wastewater Regeneration and Reuse	1
1.3 Microplastic and Nanoplastic Pollution: Emerging contaminants	3
1.4 Membrane-based technologies	5
1.5 Membrane-based Technologies: advantages and drawbacks	11
1.6 Membrane recycling	12
CHAPTER II: Scope and outline of the Thesis	17
2.1 Justification of the Thesis	17
CHAPTER III: Nutrient recovery from urban wastewater: recycled validations.	membrane 23
1. Introduction	21
2. Materials and Methods	23
2.1. Wastewater Sample	23
2.2. Chemical Reagents	23
2.3. Preparation of Membranes	23
2.3.1. Recycled Nanofiltration Membranes	24
2.3.2. Recycled Anion-Exchange Membranes	25
2.4. Membrane Performance in UWW Treatment	25
2.4.1. Nanofiltration Experiments	25
2.4.2. Electrodialysis Experiments	27
2.5. Irrigation of Lettuce	28
2.5.1. Statistical Analysis	29
2.6. Analytical Methods	29

3. R	esults	30
3	.1. UWW Treatment by rNF Membranes	30
3	.2. UWW Treatment by ED Applying rAEM	31
	3.2.1. Determination of the Operating Voltage and LCD	31
	3.2.2. rAEM Evaluation	32
3	.3. Water Quality for Crop Irrigation.	34
3	.4. Lettuce Yield and Macronutrient Uptake in Dry Weight	34
4. C	onclusions	36
5. S	upplementary Materials	37
	APTER IV: Fouling study of Ultrafiltration Membranes by Optical Coherence and the company for membrane selection	nce 48
1. Ir	ntroduction	41
2. N	faterials and Methods	43
2	.1 Membranes and plastic foulants	43
2	.2 Crossflow filtration experiments	45
2	.3 Real-time observations of fouling formation	46
	2.3.1 Optical Coherence Tomography (OCT)	46
	2.3.2 Images processing	46
2	.4 Membrane characterization	47
	2.4.1Scanning Electron Microscopy (SEM)	47
	2.4.2 Confocal laser scanning microscopy (CLSM)	47
3. R	esults and discussions	47
3	.1 Membranes and Foulants properties	47
	3.2.1 Fouling phenomena of single PS foulant	48
	3.2.2 Fouling phenomena of combined foulants PS and BSA	49
	3.2.3 Comparison of fouling behavior	52
3	.3 Permeability Recovery	53
4.	Conclusion	55
5.	Supplementary Materials	56
	APTER V: Emerging pollutants removal from urban wastewater: study nbrane Bioreactor.	of 48
1.	Introduction	61
2. N	faterials and Methods	63
2	.1. Chemicals	63

2.2. Membranes	63
2.3. Aerobic Membrane Bioreactor (aMBR) System	64
2.4. Permeate and Sludge Characterization	65
2.4.1. Analytical Methods for Wastewater Parameters	65
2.4.2. Microbial Community Analysis and SMP	66
2.4.3. Semi-Quantification of PS Nanoplastics by Pyrolysis Gas Chromatography-Mass Spectrometry (Py-GC-MS)	66
Sampling and Sampling Treatment	66
Identification and Semi-Quantification	67
2.5. Membrane Characterization	68
2.5.1. RIS Analysis	68
2.5.2. Scanning Electron Microscopy (SEM)	69
2.5.3. Confocal Laser Scanning Microscopy (CLSM)	69
3. Results	69
3.1. Activated sludge	69
3.1.1. Changes to Settleability of Sludge and SMP	69
3.1.2. Microbial Community Analysis	71
3.2. Membrane Operation	73
3.2.1. Permeate Quality	73
3.2.2. Transmembrane Pressure (TMP) Evolution	75
3.2.3. RIS Analysis and Surface Characterizations	77
3.2.4. Membrane Characterization	78
4. Conclusions	80
5. Supplementary Materials	80
CHAPTER VI: General conclusions and future research	83
Future research lines	84
References	87

List of Figures

Figure 1. Schematic representation of micronanoplastics circulation in the
environment
Figure 2. Illustration of the separation process of pressure-driven polymeric
membranes
Figure 3. Scheme of a spiral wound module configuration
Figure 4. Representation of an automatized aerobic MBR of submerged flat-sheet
membrane configuration9
Figure 5. Scheme illustrating the distribution of the co- and counter-ions between the
membranes and the bulk solution
Figure 6. (a) Operating principle of OCT. (b) Comparison of techniques to investigate
fouling structure at different scales
Figure 7. Schematic representation of EoL RO membrane transformation to NF and
UF membranes. 14
Figure 8. The research framework of the present thesis
Figure 9. Schematic representation of membrane preparations (rNF and rAEM
membranes). PA, polyamide; PSF, polysulfone; PET, polyester
Figure 10. Diagram of (a) NF system (T, temperature; EC, electric conductivity; P,
pressure) and (b) ED system (C, cation-exchange membranes; A, anion-exchange
membranes)
Figure 11. Conductivity rejection (CR) and permeance (Jv) in the function of time (t)
for the recycled NF membrane.
Figure 12. (a) Current-voltage and (b) Cowan-Brown method for the determination of
LCD with recycled anion-exchange membranes (rAEMs) (flow rate of 20 mL min-1
and 4 cell pairs).
Figure 13. Comparison of demineralization rate (DR, %) of AMH-PES and rAEM
based on specific energy consumption (SEC, kW h m-3) by electrodialysis treatment.
Figure 14. Comparison of the different treatments (TW: tap water; IRR: treated
wastewater by NF; FRT: treated wastewater by ED) (a) according to the average
biomass fresh weight (FW) and (b) water content (WC, %) in lettuce leaves. Error bars
are reported
Figure 15. Schematic diagram of the filtration and monitoring
Figure 16. Normalized flux decline behavior of the permeate and fouling layer
thickness of (a) RC 30 kDa, (b) PES 30 kDa, (c) PES 150 kDa, and (d) recycled
membranes used to treat the solution containing PS
Figure 17. Normalized flux decline behavior of the permeate and fouling layer
thickness of (a) RC 30 kDa, (b) PES 30 kDa, (c) PES 150 kDa, and (d) Recycled
membrane used to treat the solution containing PS and BSA
Figure 18. Normalized permeate flux (J/J0) declines from the cross-flow filtration
experiments. (a) BSA protein, (b) polystyrene (PS), and (c) combination of PS and
BSA
Figure 19. B-scans depicting the fouling on each membrane surface at the end of the
experiment (150 minutes). RC 30 kDa, PES 30 kDa, PES 150 kDa, and Recycled
membrane, during the filtration of the solution containing PS and PS+BSA,
respectively
r

Figure 20. SEM and 3D-projection CLSM images of studied membranes after the physical cleaning of their surfaces with MilliQ Water. The red color in the 3D projections represents the fluorescent PS nanospheres
List of Supplementary Figures
Figure S 1. Attenuated total reflectance-Fourier transform infrared comparison images to verify the end-of-life transformation

List of Tables

Table 1. Summary of the general characteristics of pressure-driven membranes.	6
Table 2. Chemical and physical characteristics of standard soil 5 M ¹ .	29
Table 3. Characteristics of the synthetic solution and the effluents of NF and E	D
technologies	30
Table 4. Macronutrient concentrations of leave-in dry weight	35
Table 5. Technical data, MWCO, and ζ-Potential of the analyzed membranes an	nd
volumetric particle diameter (D) and ζ -potential of the foulants measured in the working	ng
solution (synthetic wastewater).	14
Table 6. Hydraulic permeability recovery (PR) of the UF membranes evaluated wi	th
different foulants in the synthetic solution.	
Table 7. Technical data of the studied membranes	53
Table 8. Characteristic pyrolytic products obtained for polystyrene and m/z ions selected	ed
as indicators for each peak	57
Table 9. Average effluent quality and removal capacity of MBR	74
Table 10. Summary of the PS quantification in sludge by Py-GC/MS.	75
List of Supplementary Tables	
Table S 1. WHO guidelines of wastewater reuse for irrigation	39
Table S 2. Preparation of the calibration curve.	
Table S 3. Instrumental LOQ and LOD established for each matrix	32

List of Abbreviations

AEM Anion-Exchange Membrane

AFM Atomic Force Microscopy

ATR-FTIR Attenuated Total Reflectance Fourier Transform Infrared Spectroscopy

aMBR Aerobic membrane bioreactor

CEM Cation-Exchange Membrane

CLSM Confocal laser scanning microscopy

COD Chemical oxygen demand

c-UF Commercial Ultrafiltration

DLS Dynamic light scattering

ED Electrodialysis

EDX Energy Dispersive X-ray spectroscopy

EoL End-of-life

Eq. Equation

EPS Extracellular polymeric substances

Fig. Figure

HRT Hydraulic retention time

IEM Ion-Exchange Membrane

LCD Limiting Current Density

MF Microfiltration

MNPs Micronanoplastics

MPs Microplastics

MWCO Molecular weight cut-off

NF Nanofiltration

NPs Nanoplastics

PA Polyamide

PET Polyester

PP Polypropylene

PSF Polysulfone

PS polystyrene

Pyr-GC-MS Pyrolysis gas chromatography-mass spectrometry

RO Reverse Osmosis

r-UF Recycled Ultrafiltration

SBR Sequencing batch reactor

SRT Sludge retention time

SEM Scanning Electron Microscopy

SEC Size Exclusion Chromatography

±SD Standard deviations

TFC Thin Film Composite

THF Tetrahydrofuran

TMP Transmembrane pressure (Pa)

TSS Total suspended solid

UF Ultrafiltration
WC Water content

WCA Water Contact Angle

WWTPs Wastewater treatment plants

Symbols

 P_A^B Permselectivity towards B in respect to A

 Δn_{dil} , Variation of the mol number in the dilute compartment

 ΔV_{m} Measured potential difference (V)

 ΔV_t Theoretical potential difference (V)

A Area

a_i Activity coefficient of the ion i

C_i Concentration of component i

D Diameter

E Energy consumption (kWh·m⁻³)

E_m Potential difference (V)

I Current (A)

I_d Current density (mA·cm²)

J Flux of fresh water, freshwater production or nominal

desalination rate (L·m⁻²·h⁻¹)

J_i Flux of the component i (mol·m⁻²·h⁻¹)

1 Thickness

NaOCl Sodium hypochlorite

PR Permeability recovery

q Circulated charge (Cul·m⁻³)

R Electrical resistance (Ω)

 R_m Membrane electrical resistance ($\Omega \cdot cm^2$)

Rt Total resistance (m⁻¹)

Rc Cake layer resistance (m⁻¹)

Rf Fouling resistance (m⁻¹)

Rpb Pore blocking resistance (m⁻¹)

Rwt Total resistance measured with clean water after physical

cleaning (m⁻¹)

Rm Membrane resistance (m⁻¹)

S Separation Efficiency (%)

 t_i^m Ion transport number in the membrane phase

W_{dry} Weight of dry membrane (g)

W_{wet} Weight of wet membrane (g)

z_i Ion charge

α Permselectivity (%)

η Current efficiency (%)

Resumen

La escasez de agua es un desafío global creciente y, para 2050, se estima que miles de millones de personas residirán en regiones con estrés hídrico. Factores como el cambio climático, el crecimiento poblacional y la contaminación intensifican el problema, afectando particularmente a áreas vulnerables como el Mediterráneo. En respuesta a esta problemática, han surgido diversas soluciones para abordarla, entre las que destacan la desalinización y la regeneración de aguas residuales.

La desalinización es un proceso ampliamente utilizado para proveer de agua potable y agua de procesos en zonas con importante escasez hídrica. La regeneración de aguas residuales, por su parte, permite la reutilización y consecuente reducción del consumo de agua potable para actividades como el riego de cultivos y además ofrece una fuente alternativa de nutrientes. Así, la recuperación de sustancias como el nitrógeno permite aprovechar el agua residual no sólo como un recurso hídrico sino también como una fuente de elementos esenciales. Sin embargo, esta práctica enfrenta desafíos, principalmente debido a problemáticas tan variadas como las cargas salinas presentes en las aguas residuales y la emergente presencia de contaminantes tales como micronanoplásticos (MNPs). De estos últimos, especialmente, los plásticos de menor tamaño (nanoplásticos, NPs) presentan una mayor complejidad tanto para su remoción como para su análisis (detección y cuantificación), debido a las bajas concentraciones en masas de aguas y las limitaciones de las técnicas de análisis actuales.

Para el desarrollo y la implantación de ambos procesos: desalinización y tratamiento de aguas residuales, la tecnología de membranas mantiene un papel central en la gestión del agua, evolucionando en su uso e implantación hacia el desarrollo de estrategias más sostenibles en su tratamiento. Un ejemplo de estas estrategias sostenibles es el reciclaje de membranas de Ósmosis Inversa (OI) al final de su vida útil, a través de métodos directos e indirectos. Estos procesos de reciclaje no sólo extienden la vida útil de las membranas, sino que reducen la generación de desechos, alineándose con los principios de economía circular y promoviendo prácticas de gestión del agua más sostenibles. Así mismo, la versatilidad que facilita el uso de las membranas ha permitido, además, la introducción de esta tecnología para el pretratamiento y/o tratamiento de muestras para su posterior análisis. Un ejemplo es el uso de membranas en la concentración de contaminantes como los MNPs en muestras ambientales para la posible detección y cuantificación de los mismos.

Esta tesis explora enfoques innovadores en el tratamiento del agua mediante el uso de tecnología de membranas, empleando membranas recicladas, así como abordando cuestiones críticas en la escasez de agua y la sostenibilidad ambiental. La investigación se centra en tres áreas claves. En primer lugar, se aborda la problemática de la intrusión salina en instalaciones de aguas residuales, lo que confiere un desafío añadido y requiere del desarrollo de alternativas en el tratamiento de aguas residuales, especialmente cuando el agua tratada se destina al riego agrícola. En este contexto, se estudió la factibilidad de implementación de membranas recicladas en procesos de tratamiento de agua residual con alto contenido salino. Para ello, se obtuvieron membranas de nanofiltración recicladas (rNF) y membranas de intercambio aniónico recicladas (rAEM) a partir de

membranas de OI descartadas al final de su vida útil. Estas membranas recicladas fueron empleadas en el tratamiento de aguas residuales urbanas con alto contenido salino para el riego de cultivos. Las membranas rNF demostraron un alto rechazo selectivo de iones divalentes, mientras que las rAEM mostraron tasas de desmineralización comparables a las membranas comerciales en sistemas de electrodiálisis. Ambos sistemas produjeron efluentes adecuados para el riego, como se validó en un estudio de cultivo de lechugas.

Por otro lado, en esta tesis se estudia la problemática emergente de los NPs en aguas residuales, cuya presencia y comportamiento en los sistemas de tratamiento es una preocupación creciente, abordando dos aspectos complementarios. En primer lugar, se evaluó el comportamiento de diferentes membranas en la concentración de NPs con el objetivo de identificar la membrana más adecuada para una etapa de pretratamiento de muestras para su posterior detección y cuantificación. Para ello, se estudió el comportamiento de diferentes tipos de membranas mediante la filtración de agua tratada con contenido de NPs. Estos plásticos, como el poliestireno (PS), presentan un desafío para las membranas en términos de ensuciamiento y reducción de eficiencia. Por ello, se llevó a cabo un estudio del comportamiento de ensuciamiento de membranas de polietersulfona (PES), celulosa regenerada (CR) y PES reciclada durante la filtración de agua residual tratada que contenía nanopartículas de PS y seroalbúmina bovina (BSA por sus siglas en inglés). Para comprender mejor estos efectos, se empleó la tomografía de coherencia óptica, una técnica que permite observar en tiempo real la formación de ensuciamiento y acumulación de partículas en la superficie de la membrana. Los hallazgos sugirieron que las propiedades de las membranas influyen en la reversibilidad del ensuciamiento, destacando las membranas de CR, las cuales lograron una recuperación total de la permeabilidad tras la limpieza física. De este modo, las membranas de CR resultaron ser las más adecuadas para el pretratamiento de muestras de aguas que contienen poliestireno.

Finalmente, el estudio se extendió al segundo de los aspectos: la remoción de NPs. Se estudió la implementación de biorreactores aeróbios de membrana (BRM) para la remoción de NPs presente en aguas residuales a escala de laboratorio. Se utilizaron membranas comerciales de microfiltración (MF), ultrafiltración (UF) y membranas de UF recicladas. La remoción de PS se monitoreó mediante pirólisis gases-masas (Pyr-GS-MS) en las dos matrices: licor mezcla y permeado. Para el análisis de las muestras de permeado mediante Pyr-GS-MS, se llevó a cabo un paso previo de preconcentración utilizando membranas de CR. Se seleccionaron membranas de CR para este paso de preconcentración ya que en el estudio anterior fueron las más adecuadas por su reversibilidad frente al ensuciamiento. Los resultados mostraron que todas las membranas estudiadas en el sistema BRM lograron una alta eliminación de materia orgánica. Sin embargo, la presencia de PS-NPs tuvo un impacto en el rendimiento de las membranas y en la composición de la comunidad microbiana. Un hallazgo destacable fue que las membranas de UF recicladas demostraron una eficiencia en la remoción de PS comparable a las membranas comerciales, lo que sugiere su potencial como alternativa sostenible en aplicaciones de BRM.

En conclusión, esta investigación contribuye al modelo de economía circular en la tecnología de membranas, ofreciendo soluciones sostenibles para el tratamiento de agua y la recuperación de recursos. Los hallazgos proporcionan información sobre la selección de las membranas adecuadas a cada caso, así como el potencial de las membranas recicladas para enfrentar desafíos en la gestión del agua.

Abstract

Water scarcity is a growing global challenge, and by 2050, it is estimated that billions of people will reside in regions experiencing water stress. Factors such as climate change, population growth, and pollution intensify this problem, particularly affecting vulnerable areas like the Mediterranean. In response to this issue, various solutions have emerged, among which desalination and wastewater regeneration stand out.

Desalination is a widely used process for providing drinking and processing water in areas with significant water scarcity. Wastewater regeneration enables reuse and consequent reduction of the consumption of drinking water for activities such as crop irrigation while providing an alternative source of nutrients. Thus, the recovery of substances like nitrogen allows wastewater to be used not only as a water resource but also as a source of essential elements. However, this practice faces challenges, mainly due to issues as varied as salinity present in wastewater and the presence of emerging contaminants such as micronanoplastics (MNPs). In particular, smaller plastics (nanoplastics, NPs) present greater complexity for both their removal and analysis (detection and quantification), due to low concentrations in water bodies and limitations of current analytical techniques.

For developing and implementing both desalination and wastewater treatment, membrane-based technology maintains a central role in water management. The application of this technology also continues to advance, contributing to more sustainable approaches to water treatment. An example of the sustainable approach is recycling Reverse Osmosis (RO) membranes at the end of their useful life, through direct and indirect methods. These recycling processes not only extend the lifespan of membranes but also reduce waste generation in line with circular economy principles and promote more sustainable water management practices. Likewise, the versatility facilitated by using membranes has also enabled the introduction of this technology for the pretreatment and/or treatment of samples for subsequent analysis. One example is the use of membranes in the concentration of contaminants such as MNPs in environmental samples prior to their detection and quantification.

This thesis explores innovative approaches in water treatment using membrane technologies, employing recycled membranes, as well as addressing critical issues in water scarcity and environmental sustainability. The research focuses on three key areas. First, it addresses the issue of saline intrusion in wastewater facilities, which presents an additional challenge and requires the development of alternatives in wastewater treatment, especially when treated water is intended for agricultural irrigation. In this context, the feasibility of implementing recycled membranes to treat high-salinity wastewater was studied. For this, recycled nanofiltration membranes (rNF) and recycled anion exchange membranes (rAEM) were obtained from discarded RO membranes at the end of their useful life. These recycled membranes were used in the treatment of urban wastewater with high salt content for crop irrigation. The rNF membranes demonstrated high selective rejection of divalent ions, while the rAEM showed demineralization rates comparable to commercial membranes in electrodialysis systems. Both systems produced effluents suitable for irrigation, as validated in a lettuce cultivation study.

On the other hand, this thesis studies the emerging issue of NPs in wastewater, whose presence and behavior in treatment systems is a growing concern, addressing two complementary aspects. First, the potential use and behavior of different membranes in NP concentration were evaluated to identify the most suitable membrane for a sample pretreatment stage for subsequent detection and quantification. The behavior of different types of membranes was studied through the filtration of treated water-containing NPs. These plastics, such as polystyrene (PS), present a challenge for membranes in terms of fouling and efficiency reduction. Therefore, a study of the fouling behavior of polyethersulfone (PES), regenerated cellulose (RC), and recycled PES membranes was carried out during the filtration of wastewater containing PS nanoparticles and bovine serum albumin (BSA). To better understand these effects, optical coherence tomography (OCT) was used, a technique that allows real-time observation of fouling formation and particle accumulation on the membrane surface. The findings suggested that membrane properties influence the reversibility of fouling, highlighting RC membranes, which achieved total permeability recovery after physical cleaning. Consequently, this membrane material was selected as the most suitable membrane for the pretreatment of water samples containing polystyrene.

Finally, the study extended to the second aspect: NP removal. Therefore, the feasibility of implementing aerobic membrane bioreactors (MBR) for NP removal from wastewater was also studied at a laboratory scale. Commercial microfiltration (MF), ultrafiltration (UF), and recycled ultrafiltration membranes were used for this purpose. PS removal was monitored using pyrolysis gas-mass spectrometry (Pyr-GS-MS) in both matrices: mixed liquor and permeate. For the analysis of permeate samples by Pyr-GS-MS, a pre-concentration step using RC membranes was implemented. The CR membranes were selected for this pre-concentration step as they were found to be the most suitable membranes in the previous study due to their reversibility to fouling. The results of this work showed that all membranes studied in the MBR system achieved high organic matter removal. However, the presence of PS-NPs had an impact on membrane performance and microbial community composition. A notable finding was that recycled ultrafiltration membranes demonstrated PS removal efficiency comparable to commercial membranes, suggesting their potential as a sustainable alternative in MBR applications.

In conclusion, this research contributes to the circular economy approach in membrane technology, offering sustainable solutions for water treatment and resource recovery. The findings provide information on the selection of appropriate membranes for each case, as well as the potential of recycled membranes to address challenges in water management.

Publications

This thesis is a compendium of scientific articles, each addressing specific aspects of recycled membrane technology and its applications in water treatment. The following published scientific papers correspond to chapters of the current thesis:

Scientific Article I (Chapter 3):

Pompa-Pernia, A.; Molina, S.; Lejarazu-Larrañaga, A.; Landaburu-Aguirre, J.; García-Calvo, E. Validation of Recycled Nanofiltration and Anion-Exchange Membranes for the Treatment of Urban Wastewater for Crop Irrigation. *Membranes* **2022**, *12*, 746. https://doi.org/10.3390/membranes12080746.

Scientific Article II (Chapter 4):

Pompa-Pernía, A.; Aleman, A.; Kerst, K.; Molina, S.; Lerch, A.; Landaburu-Aguirre, J. Experimental evaluation of nanoplastics fouling behavior on ultrafiltration membranes using optical coherence tomography (OCT). *Separation and Purification Technology* **2024**, 354, 129520. https://doi.org/10.1016/j.seppur.2024.129520.

Scientific Article III (Chapter 5):

Pompa-Pernía, A.; Molina, S.; Cherta, L.; Martínez-García, L.; Landaburu-Aguirre, J. Treatment of Synthetic Wastewater Containing Polystyrene (PS) Nanoplastics by Membrane Bioreactor (MBR): Study of the Effects on Microbial Community and Membrane Fouling. Membranes 2024, 14, 174. https://doi.org/10.3390/membranes14080174.

Other Contributions:

Additionally, the following communications have been presented at Conferences:

Oral presentations:

Anamary Pompa-Pernia, Serena Molina, Junkal Landaburu-Aguirre. Polymeric Membranes Recycling. Oral Lecture presented in SEJIPOL 2022, ITCP-CSIC, Madrid, 2022.

Anamary Pompa- Pernía, Aleman, A., Kerst, K., Serena Molina, Lerch, A, Junkal Landaburu-Aguirre. Experimental evaluation of nanoplastics fouling behavior on ultrafiltration membranes using optical coherence tomography (OCT). Oral Lecture presented in Euromembrane Congress 2024, Prague, Czech Republic, 2024.

Posters:

Anamary Pompa-Pernía, Amaia Lejarazu-Larrañaga, Serena Molina, Junkal Landaburu-Aguirre, Eloy García-Calvo. Validation of recycled membranes in saline urban wastewater treatment. Poster presented in Summer School of European Membrane Society (37th edition) Alentejo, Portugal, 2022.

Anamary Pompa-Pernía, Serena Molina, Junkal Landaburu-Aguirre. Performance evaluation of MBR in treating plastic nanospheres of polystyrene. Poster presented in Euromembrane Congress 2022, Sorrento, Italy, **2022**.

Anamary Pompa-Pernía, Amaia Lejarazu-Larrañaga, Serena Molina, Junkal Landaburu-Aguirre, Eloy García- Calvo. Validation of recycled membranes in saline urban wastewater treatment. Poster presented in Euromembrane Congress 2022, Sorrento, Italy, 2022.

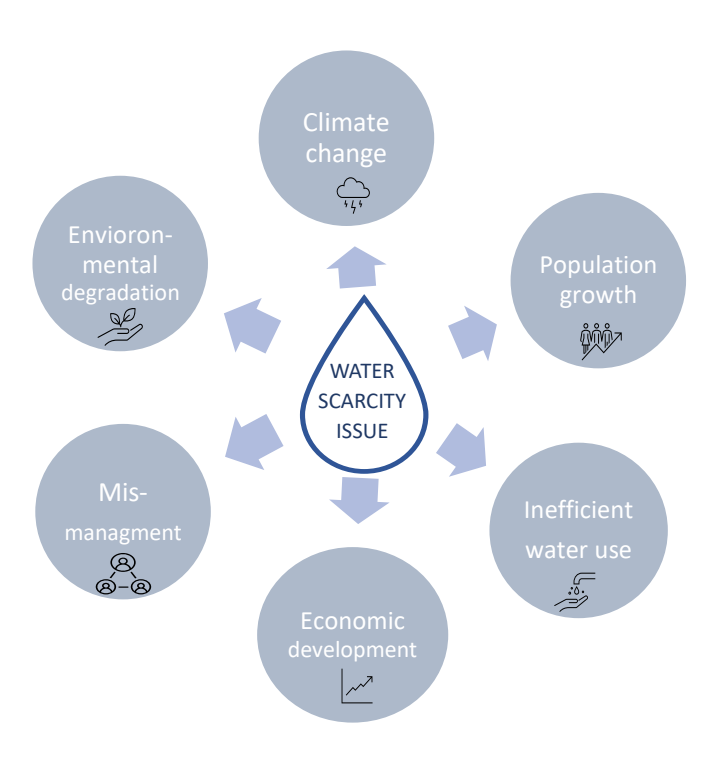
Anamary Pompa-Pernía, Serena Molina, Junkal Landaburu-Aguirre. Polystyrene Nanoplastics Removal from Urban Wastewater by Aerobic Membrane Bioreactor. Poster presented in SETAC Europe, Dublin, Ireland, 2023.

Research stay

The three-month research stay was conducted at the Hydro Science Department of the Technical University of Dresden, Germany (Technische Universität Dresden), under the supervision of Dr. Kristin Kerst and the guidance of the department head, Professor André Lerch.

The results of the experiments conducted during the stay led to the collaborative research article listed as number II above (Pompa-Pernía, A.; Aleman, A.; Kerst, K.; Molina, S.; Lerch, A.; Landaburu-Aguirre, J. "Experimental evaluation of nanoplastics fouling behavior on ultrafiltration membranes using optical coherence tomography (OCT)." *Separation and Purification Technology* 2024, 354, 129520. https://doi.org/10.1016/j.seppur.2024.129520).

CHAPTER I: General Introduction





CHAPTER I: General Introduction

1.1 Water scarcity

Water is the foundation of life and an integral part of human health, economic development, and ecological balance. Nevertheless, billions of people worldwide face the unrelenting challenges of water scarcity, where the demand for freshwater sharply exceeds the available supply within a region. Projections indicate that global urban water scarcity will exacerbate [1]. By 2050, it is estimated that 1.693–2.373 billion people, nearly half of the urban population worldwide, are expected to live in water-stressed regions [2].

Climate change disrupts precipitation patterns, intensifying droughts, particularly affecting arid and semi-arid regions [3]. Population growth and urbanization further strain resources, particularly in agriculture, which is a significant consumer of freshwater. Pollution compounds exacerbate the problem, degrading water quality and reducing usable freshwater supplies [4].

The Mediterranean region is a particularly vulnerable hotspot within the global water scarcity landscape. Its unique climate limits freshwater reserves, and growing demand makes it highly vulnerable. Southern and eastern Mediterranean countries face severe water stress, with several of them classified as 'water-poor,' including Algeria, Libya, Tunisia, Morocco, Israel, Jordan, Syria, Lebanon, and Palestine [5].

To address water scarcity, innovative solutions have emerged as key strategies including desalination and wastewater reclamation. Converting seawater into freshwater is a promising solution, particularly in coastal regions dealing with water shortages. Technological advancements are increasingly rendering desalination methods to be more energy-efficient and economically viable. Additionally, alternative approaches for treating wastewater aim to achieve safe levels of water quality, facilitate water reuse in various sectors, including irrigation, industrial processes, and in some instances, increasing drinking water reserves [6]. The subsequent section examines global wastewater regeneration and reuse processes, as well as desalination especially focusing on Reverse Osmosis (RO) technology.

1.2 Desalination and Wastewater Regeneration and Reuse

Traditional freshwater resources, such as lakes, rivers, and groundwater, are often overused or misused [7]. Consequently, these resources are either diminishing or becoming saline. In addition, emerging pollutants are increasingly threatening these vital water resources through multiple pathways. These contaminants enter water systems primarily through municipal sources, including domestic wastewater discharges, hospital effluents, and consumer product disposal. The number of substances that can be considered emerging is indeterminate and includes an extensive range of contaminants [8]. Typically, these compounds are not subject to specific regulations limiting their presence in water but could be regulated in the future if they pose a risk to or through the aquatic environment.

As countries continue to develop and consequently, many cities are continuously expanding, few new water resources are available to support daily freshwater needs. Solutions like desalination and water reuse have therefore emerged as essential alternatives for sustaining future generations globally [9].

As an example, in 2021, the global installed capacity for desalination plants was approximately 115 million cubic meters per day (m³/day) [10]. Further, wastewater reclamation facilities had a global capacity of around 126 million cubic meters per day (m³/day) in the same year. These figures highlight the significant role that desalination and wastewater reclamation already play in global water management.

Desalination Technology

Desalination is the process of removing salts and other minerals from seawater or brackish water [11] that has been around for centuries. However, large-scale desalination for municipal and industrial use is a relatively recent development. Early desalination plants predominantly implemented thermal technologies. Prior to the 1980s, 84% of all global desalinated water was produced by the two major thermal technologies such as multi-stage flash distillation (MSF) and multi-effect distillation (MED) [12]. Since then, technological advancements have transformed desalination into a vital tool for water-stressed regions.

Today, RO is the dominant desalination technology, accounting for roughly 60% of global desalination capacity [13]. RO is highly efficient and offers key advantages, such as improved energy efficiency, lower costs, and no phase-change requirement [12] compared to older thermal desalination methods like MSF and MED [11].

Wastewater Reclamation

Wastewater reclamation, i.e. the treatment or processing of wastewater to a quality level acceptable for reuse, has been identified as one of the most significant approaches to meet current and future water demands. Treated wastewater can be employed for various non-potable purposes, including irrigation, industrial processes, and even aquifer replenishment. According to the review by Jodar-Abellan et al. [14], the primary use of wastewater in Spain is in the agricultural sector, accounting for approximately 40–70% of the total reused water. This is followed by 36% used for irrigating parks and recreational areas. Industrial uses account for 10%, and 7% is used for various applications of reclaimed water, including urban and residential purposes, discharges from sanitary installations, and other related activities. Finally, 2% is utilized for cleaning sewage systems and/or street cleaning. However, a significant challenge arises within wastewater reclamation: the issue of salinity and hypersalinity [15]. High concentrations of salts in wastewater can pose a severe threat to soil health and crop yields when used for irrigation. To overcome this obstacle, further advancements in desalination processes and salt management strategies within wastewater treatment are imperative.

Projections suggest a robust growth trajectory for both desalination and wastewater reclamation technologies in the coming decades [16]. By 2050, wastewater reclamation

facilities are expected to experience substantial growth, with their global capacity projected to exceed 200 million cubic meters per day (m3/day) by 2050 [16]. These forecasts are driven by increasing water stress due to population growth, urbanization, and climate change, as well as ongoing technological advancements improving the efficiency and cost-effectiveness of desalination and wastewater treatment processes.

1.3 Microplastic and Nanoplastic Pollution: Emerging contaminants

Among the most concerning contributors to water body contamination are emerging contaminants. As presented previously, emerging pollutants are chemicals and compounds that have recently been identified as dangerous to the environment, and consequently to the health of human beings. They are called "emerging" because of the rising level of concern linked to them, and the fact that many are not yet regulated [17].

Examples of emerging pollutants include antibiotics, drugs, steroids, endocrine disruptors, hormones, industrial additives, chemicals, microbeads, and microplastics. These last group of pollutants are categorized as microplastics (MPs, ≤ 5 mm) and nanoplastics (NPs, 1-1000 nm), garnering particular concern [18]. MNPs are classified as primary, intentionally manufactured for use in personal care products (e.g., microbeads in exfoliants) and industrial applications. Additionally, MNPs often originate from the breakdown of larger plastic products like bottles, bags, and fishing gear, classified as secondary MPs. In January 2018, the European Union adopted a European strategy for plastics. As part of the strategy, the European Commission (EC) identified microplastic pollution as an issue warranting the development of innovative reduction solutions [19]. The Circular Economy Action Plan of the European Commission aims to restrict intentionally added microplastics and address unintentional releases, with a 30% reduction target for microplastic releases by 2030 [19].

The primary pathway for MNPs to enter the aquatic environment is through wastewater treatment plants (WWTPs) [20]. Although WWTPs can remove a significant proportion of MPs [8, 9], the sheer volume of effluent they discharge, coupled with the continuous generation of secondary NPs from the degradation of larger plastics, poses a significant environmental risk [23]. The percentage of MPs removal in WWTPs can vary widely depending on the specific technologies and processes used. However, studies generally estimate that WWTPs can remove approximately 90-99% of MNPs from wastewater [24].

Unlike MPs, the fate of plastic debris at the nanoscale remains largely unknown. Theoretically, a 2 mm polyvinyl chloride (PVC, a density of $\sim 1.4 \, \text{g/cm}^3$) bead is determined to settle in water at a rate of about 87 cm/s according to Stokes' law (for ideal conditions), while the settling rate of a 100 nm PVC bead would be $\sim 6.9 \, \text{cm/year}$. Thus, NPs and MPs would show distinct transport and fate behavior in urban waters, due to their different physicochemical properties [25]. NPs particles are too minuscule to be observed, characterized, or quantified using optical microscopy. Furthermore, they exhibit Brownian motion and do not readily settle, posing challenges to their efficient characterization and purification in real environmental samples. These obstacles have impeded the reliable assessment of the extent of the nanoplastic pollution issue [26]. Of

significant worry is the NPs potential introduction into the food chain, where they can accumulate within organisms and disrupt biological processes. This bioaccumulation poses a direct threat to the intricate balance of ecosystems, leading to potential harm across various species and a heightened risk of biodiversity loss [27]. The persistent nature and insidious effects of MNPs emphasize the urgent need for comprehensive research and mitigation strategies to address this emerging environmental crisis (Fig. 1).

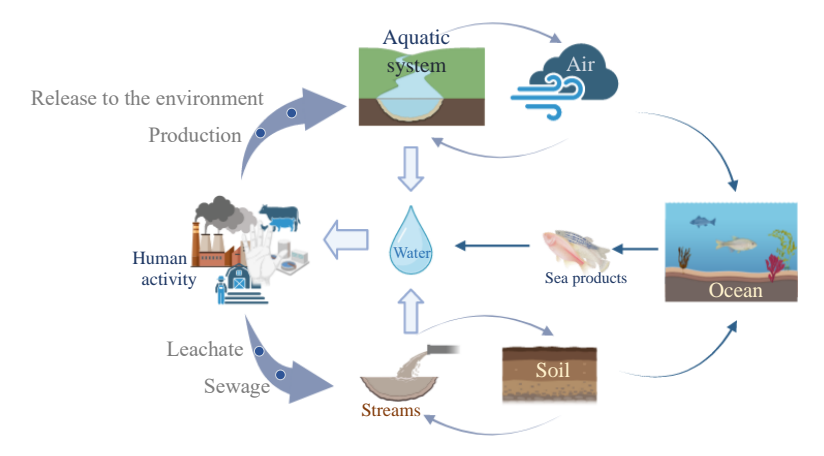


Figure 1. Schematic representation of micronanoplastics circulation in the environment.

While techniques such as microscopy, spectroscopy, and dynamic light scattering (DLS) are valuable for qualitative analysis, there remains a need for improved sensitivity and standardization of analytical methods [28]. Commonly used techniques for MPs include vibrational spectroscopic methods (FTIR or Raman spectroscopy) for identification and semi-quantification of MPs [29]. These methods can be used to collect appropriate parameters because of the availability of multi-analysis. However, they are limited since they do not detect particles smaller than 20 µm [30], which is a significant limitation for characterizing and semi-quantifying NPs. In this context, thermal degradation-based techniques such as Pyrolysis Gas Chromatography-Mass Spectrometry (Py-GC-MS) have shown promising results for MNPs analysis. This technique relies on pyrolysis for the identification and semi-quantification of polymers, effectively overcoming the size limitation.

The general workflow for the MNPs analysis involves laboratory preparation to separate MNPs from the sample matrix, simplifying the subsequent processes for identification and/or semi-quantification. These procedures vary depending on the complexity of the sample matrix. For instance, water samples require large volumes due to the relatively low concentration of NPs, needing previous preconcentration strategies such as the use of membranes to isolate and enrich NPs from environmental matrices [31]. Membrane technology is crucial in these preconcentration processes, as it allows the retention of smaller nanoparticles through the sieve effect. This selective separation leads to more accurate and reliable analysis [32].

Further, research is ongoing to better understand the full extent of the impacts of MNPs and to develop strategies for mitigating their risks. Some key areas of focus

include: (i) improving detection and monitoring [33], (ii) assessing health risks [34], and (iii) reducing plastic pollution [35].

The intersection of water scarcity, emerging contaminants, and the potential of advanced membrane technologies for water remediation presents both critical challenges and promising solutions.

1.4 Membrane-based technologies

Membrane-based technologies have become crucial in modern wastewater treatment and reclamation systems. These technologies use semi-permeable membranes to remove a wide range of pollutants [36]. According to Abdullah et. al [37], a complete definition of a membrane could be stated as a semi-permeable barrier which, under a certain driving force, permits preferential passage of one or more selected species or components (molecules, particles, or polymers) of a gaseous and/or liquid mixture or solution.

Membranes can be classified from various perspectives. One classification is based on their nature, distinguishing between natural and synthetic membranes. Synthetic membranes are further subdivided into organic (polymeric or liquid) and inorganic (ceramic or metallic) types [38]. This current work will focus exclusively on polymeric membranes.

On the other hand, in membrane processes, transport through the membranes takes place as a result of a driving force acting on the components in the feed. Driving forces can be gradients in pressure, concentration, electrical potential, or temperature [38]. An overview of various membrane processes divided by their driving forces is given in the following sub-sections.

1.4.1 Pressure – Driven membranes

Pressure-driven membranes are a type of membrane separation technology that uses pressure as the driving force to separate components in a fluid mixture. Fig. 2 represents the separation process of the four pressure-driven membranes and Table 1 summarizes their general characteristics. This section explores different types of polymeric membrane-based wastewater technologies, their mechanisms, advantages, and challenges.

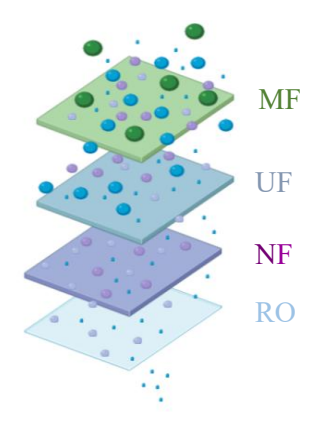


Figure 2. Illustration of the separation process of pressure-driven polymeric membranes.

Table 1. Summary of the general characteristics of pressure-driven membranes.

Membranes	Permeability (LMH bar)	Pore size (nm)	Pressure (bar)	Rejection matters
MF	>1000	100-10 000	0.1-2	Bacterias, suspended solids
UF	10-1000	2-100	1-10	Viruses, proteins, starches, colloids, silica
NF	1.5-30	0.5-2	5-20	Sugar, pesticides, herbicides, divalent ions
RO	0.05-1.5	< 0.5	10-80	Monovalent ions

Microfiltration (MF)

Microfiltration (MF) membranes are membranes that operate under low pressures (typically 0.1–2 bar) and are designed to allow water and small solutes to pass through while retaining particles, microorganisms, and larger suspended solids [39]. MF membranes are widely used for drinking water purification, wastewater treatment, and the clarification of beverages and pharmaceuticals.

The first MF membranes, developed in the mid-20th century, were made from cellulose acetate and similar early polymers. Today, the market is dominated by advanced materials such as polyethersulfone (PES), polyvinylidene fluoride (PVDF), and polypropylene (PP), known for their excellent chemical resistance and mechanical strength [40].

MF membranes typically have pore sizes ranging from 0.1 to 10 μ m [39]. The separation mechanism in MF membranes is primarily based on size exclusion or sieving, where particles larger than the membrane pores are retained on the surface or within the porous structure, while smaller particles pass through with the permeate stream.

Modern MF membranes are manufactured in various configurations, including hollow fiber, flat sheet, and tubular forms [39]. Hollow fiber modules consist of many thin, flexible fibers that provide a large surface area within a compact volume, allowing for high throughput and efficient backwashing. Flat sheet modules are used in plate-and-frame or cassette systems, offering easy replacement and maintenance.

Ultrafiltration (UF)

Ultrafiltration (UF) membranes work under moderate pressure, allowing water and low-molecular-weight solutes to pass through the membrane, whilst macromolecules, colloids, and microorganisms are retained. UF membranes are widely used for water purification, wastewater treatment, and the concentration of proteins and other large molecules in industrial processes.

The first UF membranes were developed in the mid-20th century [36] and they were primarily made of cellulose acetate and other early polymers. Nowadays, the market is dominated by membranes made from advanced polymeric materials such as PES, polysulfone (PSf), and PVDF [41]. These materials are preferred for their superior chemical resistance, thermal stability, and mechanical strength.

UF membranes typically have a pore size range of 1–100 nm, with the exact pore size tailored to the specific application. The separation mechanism in UF membranes is predominantly based on size exclusion or sieving [36]. Molecules larger than the membrane pores are retained on the surface or within the porous structure of the membrane, while smaller molecules pass through with the permeate stream.

Modern UF membranes are also often manufactured in hollow fiber or flat sheet configurations. Overall, UF is a powerful technology for removing impurities from a sample, separating large molecules of interest, or even concentrating them [42].

Nanofiltration (NF)

Nanofiltration (NF) membranes operate under moderate pressures (typically 5–20 bar) and are designed to selectively allow water and certain low-molecular-weight solutes to pass through the membrane, while retaining larger solutes such as divalent and multivalent ions, organic molecules, and some salts. NF membranes have been commercialized since 1980, and their properties are between RO and UF membranes [43].

NF membranes have pore sizes typically in the range of 0.1–1 nm. Their separation mechanism combines size exclusion with electrostatic interaction. Consequently, they can effectively remove solutes based on both size and charge [44]. For example, they reject divalent ions like calcium and magnesium more effectively than monovalent ions like sodium and chloride.

In industrial applications, NF membranes are commonly used in water softening, wastewater treatment, and the removal of specific contaminants in the food and beverage industry [44]. They are usually configured in spiral wound modules to maximize surface area and pressure resistance. The modules are designed for easy integration into existing water treatment systems and offer efficient contaminant removal with moderate energy requirements.

Reverse Osmosis (RO)

Reverse osmosis (RO) membranes are nonporous membranes designed to allow water to pass through the membrane, while retaining salts, dissolved organic matter, viruses, and other compounds under high pressure (40–50 bar for seawater and 20 bar for brackish water) [45]. They are highly effective at rejecting monovalent salts, such as NaCl, with rejection rates between 99 and 99.7%, making them ideal for desalination of seawater and brackish water [46].

The first RO membranes, developed in the 1960s, were made of cellulose acetate. Today, Thin Film Composite Polyamide (TFC-PA) membranes dominate the market [31, 32]. These membranes are composed of several polymer layers: an ultrathin (\sim 0.2 μ m) dense polyamide (PA) layer that serves as the selective barrier, a thicker (\sim 40 μ m) porous PSf layer, and much thicker (\sim 100 μ m) non-woven PET layer for mechanical support [48].

Unlike other pressure-driven membranes with a mechanism of permeation of solutes described by sieving through tiny pores, RO membranes use a solution-diffusion mechanism [49]. Solutes dissolve in the dense polyamide layer and diffuse through the membrane, moving against the concentration gradient. Industrial-scale RO membranes are typically produced in a spiral wound module configuration (Fig. 3). This design maximizes membrane surface area within a compact space and enhances pressure resistance [50].

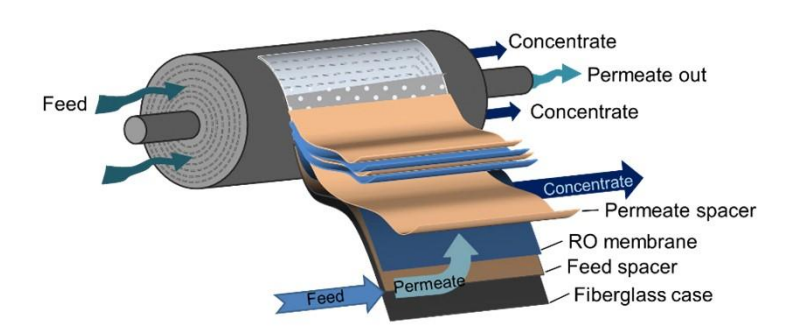


Figure 3. Scheme of a spiral wound module configuration. Taken from [50]

1.4.2 Membrane Bioreactors (MBR)

Membrane Bioreactor (MBR) systems combine biological wastewater treatment processes with membrane filtration, offering an advanced solution for municipal and industrial wastewater treatment [51]. Usually, wastewater is subjected to a three-step treatment process involving sedimentation of large solid particles in the influent, aerobic decomposition of organic substances, and a subsequent sedimentation stage to remove biomass. An MBR eliminates the two physical separation stages by filtering biomass through a membrane (Fig. 4), resulting in significantly higher water quality than conventional treatment methods and eliminating the need for additional tertiary

disinfection processes. In addition, integrating membrane separation with a bioreactor offers several distinct advantages, such as a smaller physical footprint, high-quality water with consistent properties, and a high concentration of microbes or solids within the bioreactor [52].

The first MBR systems were developed in the late 20th century, utilizing early polymeric membranes [53]. Today, MBR systems use advanced polymeric membranes made from materials such as PES, PVDF, and PP, valued for their chemical resistance, thermal stability, and mechanical strength.

The membranes used in MBR systems are typically MF or UF membranes, with pore sizes ranging from 0.01 to $1.0~\mu m$ [54]. These membranes act as a physical barrier, retaining biomass and suspended solids while allowing treated water to pass through. The separation mechanism in MBR membranes is primarily based on size exclusion, where particles and microorganisms larger than the membrane pores are retained.

MBR systems are available in two main configurations: submerged (immersed) and side-stream. In submerged MBR systems, the membranes are directly immersed in the biological reactor, and treated water is drawn through the membranes by suction [55]. This design minimizes energy consumption and simplifies system operation. In side-stream MBR systems, the membranes are located outside the reactor, and mixed liquor is pumped through the membranes under pressure. This configuration allows easier maintenance and membrane cleaning.

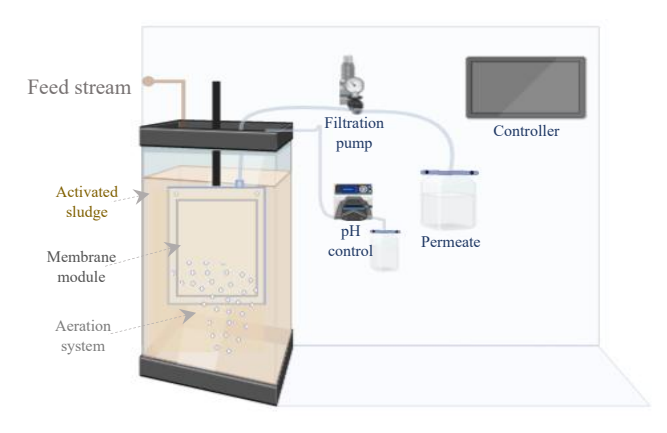


Figure 4. Representation of an automatized aerobic MBR of submerged flat-sheet membrane configuration.

Modern MBR systems incorporate additional components such as aeration systems for maintaining microbial activity and preventing membrane fouling, as well as pumps, valves, and automated controls for efficient system operation. The membranes themselves are often housed in modules that facilitate easy installation, cleaning, and replacement. These configurations include: (i) hollow fiber (the most common configuration, consisting of a bundle of tiny hollow fibers). Wastewater flows through the inside of the fibers, while cleaner water permeates through the fiber walls. (ii) flat sheet (typically arranged in a cassette-like configuration). Wastewater flows across the surface of the flat

sheets, and permeate water passes through channels between the sheets. (iii) tubular or multi-tubular (comprises two main parts, the membrane core equipped with tubes and the shroud).

1.4.3 Electrodialysis (ED)

ED technology is essentially different compared with pressure-driven processes since it is an electrically driven membrane process. ED uses an electric field to drive ions through selective ion-exchange membranes (IEM), separating them from the water [56].

Based on the charge of their fixed functional groups, the IEMs can be categorized into two principal groups such as Anion-Exchange Membranes (AEMs) and Cation-Exchange Membranes (CEMs) [57].

- AEMs contain positively charged groups, allowing negatively charged ions (anions) to pass through the membrane, while rejecting positively charged ions (cations).
- CEMs contain negatively charged groups, allowing positively charged ions (cations) to pass through the membrane, while rejecting negatively charged ions (anions).

CEMs and AEMs are alternately placed in a stack, achieving the separation of cations and anions, respectively. This selective permeability is due to the Donnan exclusion effect [58], where ions with the same charge as the membrane's functional groups are repelled (Fig. 5).

The IEMs can also be categorized based on the distribution of their functional groups into homogeneous and heterogeneous.

- Homogeneous IEMs have a uniform distribution of ion-exchange sites, facilitating ion transport and offering lower electrical resistance.
- Heterogeneous IEMs have an uneven distribution of ion-exchange sites, potentially leading to a more tortuous ion path and higher electrical resistance. However, they often exhibit better mechanical properties and can be produced at a lower cost.

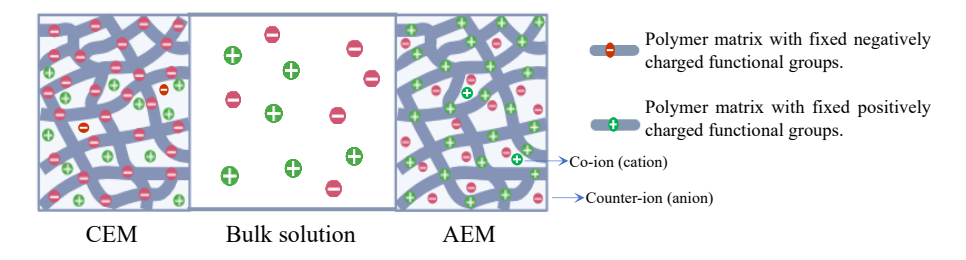


Figure 5. Scheme illustrating the distribution of the co- and counter-ions between the membranes and the bulk solution. Adapted from Strathmann, H, et al., [58].

The performance of ED systems is heavily influenced by the properties of the IEMs used. Ideal IEMs for ED should possess high perm-selectivity [59], which is the ability

to selectively transport desired ions while rejecting others; low electrical resistance that minimizes energy consumption during the ED process; good mechanical, chemical, and thermal resistance that ensures durability and longevity of the membranes under various operating conditions; and low production cost, which makes the technology more economically viable.

However, optimizing all these properties simultaneously is challenging, as they often have opposing effects. For example, increasing crosslinking can improve permselectivity but also leads to higher electrical resistance. Therefore, a compromise must be made based on the specific requirements of the ED application.

1.5 Membrane-based Technologies: advantages and drawbacks:

Membrane-based technology offers several key advantages, as summarized by Sánchez-Arévalo et al. [42]. These include a significant reduction of the energy and chemicals invested in the process compared to traditional separation methods such as distillation, centrifugation, extraction, and precipitation. Additionally, membranes can be tailored to selectively allow certain molecules to pass through the membrane while blocking others, providing precise control over separation processes. Furthermore, membrane-based technologies are easy to automate, scale up, and combine with other processes. These attributes make membrane technology suitable for a wide range of applications, including wastewater treatment, water reclamation, medicine, chemistry, food processing, concentration of high-added value compounds, and valorization of residues.

However, there are notable drawbacks to membrane-based technology, particularly membrane fouling, and limited lifespan [35]. These issues not only increase the operational cost of the technologies but also the generation of waste sources. Fouling, caused by the accumulation of suspended solids, microorganisms, and organic matter on the membrane surface, reduces efficiency and increases maintenance requirements. The fouling process is influenced by operational factors such as trans-membrane pressure [60], crossflow velocity, temperature [61], feed characteristics (including foulant form and size, foulant concentration, and feed pH), and membrane properties (such as hydrophilicity/hydrophobicity, roughness, pore size, and pore type) [40].

Fouling propensity is commonly assessed experimentally by monitoring permeate flux and transmembrane pressure (TMP) [62], as well as by using various models developed to study fouling. On the other hand, membrane surface characterization techniques such as scanning electron microscopy (SEM) and atomic force microscopy (AFM) are also used for fouling analysis. Still, they can only be applied after the membrane process is finalized. In that sense, Optical Coherence Tomography (OCT) has recently received increased attention as a novel approach for real-time analysis of membrane fouling [63]. OCT is a relatively quick, sensitive, non-invasive method that provides high-resolution images. It allows the observation of fouling structures on the millimeter scale under continuous operation, as shown in Fig. 6 (b), and generates 2D and 3D scans with short acquisition times of seconds to minutes. The system emits a low-coherence light source (near-infrared light) that reflects off different structures within the

sample as represented in Fig. 6 (a). The interference pattern formed by the reflected light waves is processed to produce cross-sectional images of the matter located in the sample arm. Hence, OCT devices are point scanners [63].

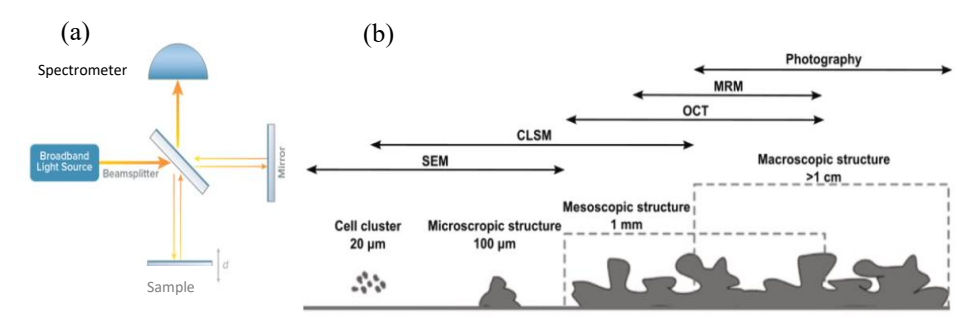


Figure 6. (a) Operating principle of OCT. (b) Comparison of techniques to investigate fouling structure at different scales, taken from [63].

Despite ongoing advancements in fouling-detection techniques and getting a deeper understanding of fouling mechanisms, membrane fouling remains unavoidable, leading to a reduced membrane lifespan. Specifically, in RO desalination, it is estimated that more than 840,000 end-of-life (EoL) RO modules (>14,000 tons of plastic waste) are discarded annually, according to Landaburu-Aguirre et al. [64]. Additionally, based on the growth rate of the desalination market, Senán-Salinas et al. [65] estimated that by 2025, more than 2,000,000 EoL RO modules might be discarded globally. Therefore, plastic waste generation and management represent a critical challenge for the sustainable growth of the RO desalination industry. In addition, although energy typically represents the largest operational expense (OPEX) for RO seawater desalination plants (over 50% of the total cost), chemicals and membrane replacement combined can contribute to 15-25% of the OPEX, depending on factors such as feedwater quality, operating conditions, and membrane lifespan [66]. Consequently, by reducing the frequency of membrane replacement, plants can lower their OPEX. Furthermore, extending the membrane lifespan not only decreases the demand for new production but also minimizes raw material use and waste generation. In this regard, the reuse and recycling of membranes may offer an advantage due to their lower cost and the reduced environmental impact associated with their production and discharge.

1.6 Membrane recycling:

EoL RO management

The management of the End-of-Life (EoL) membranes is still based on a linear model [67], which tends to discard the membranes once their overall performance declines (separation capacity, permeability, effluent quality, etc). These modules are commonly disposed of in landfills or, less frequently, incinerated for the recovery of energy [68]. Incineration is generally regarded as the final method for eliminating plastic waste, as it

ultimately converts polymers into CO₂ and mineral fractions [69]. However, the mentioned methods adversely affect the environmental impacts [70] such as, land occupation, generation of greenhouse emissions [69], the production of toxic leachates (which can contaminate groundwaters), odors and visual impact, the loss of valuable raw materials and energy, and emissions associated to the transport of EoL RO membranes to landfill facilities [71]. In this context, membrane technology could be integrated into a circular economy model, in concordance with the European Green Deal [72] and the priority order of waste management (prevention, reuse, recycling, recovery, and disposal) regulated in the European Directive 2008/98/EC.

The implementation of membrane reuse and recycling strategies presents a promising pathway for extending the lifespan of RO membranes and reducing waste. Continued research into innovative recycling and modification techniques will further expand the potential applications for EoL membranes, contributing to a more sustainable approach to membrane management.

Advance in recycled membranes: Transformation from EoL membranes

TFC-PA RO membranes have remained the gold standard technology for desalination and water purification for nearly half a century, as previously mentioned. Polyamide films offer excellent water permeability and salt rejection but suffer from poor chlorine resistance, high fouling propensity, and low boron rejection [73].

Under this framework, the Membrane Technology Group of IMDEA Water has sought alternatives to reuse, recycle, and recover discarded RO modules. Different approaches have been conducted, from the chemical transformation of the spiral wound module (direct recycling) to the management and recycling of the individual components by the deconstruction of them (indirect recycling) [74].

Direct Recycling

Direct recycling of EoL RO membranes involves intentional degradation of the PA layer using oxidizing agents (chemical agents), converting the membrane's functionality without altering the original spiral-wound configuration of the module. Rodríguez et al. [75] pioneered the concept of converting EoL RO membranes into ultrafiltration membranes for wastewater treatment, identifying K_7MnO_4 as the most effective chemical agent. Later, other researchers found sodium hypochlorite to be the best oxidizing agent [76]. Another research has focused on transforming EoL membranes into ultrafiltration or nanofiltration membranes by controlling chlorine exposure time [77]. Molina et al. [78] confirmed that an exposure level of 30,000 ppm·h effectively removed the PA layer, revealing the polysulfone substrate with nanopores around 13 nm in diameter. García-Pacheco et al. [79] explored the conditions defining the transition between RO, NF, and UF properties characterizing the membranes using a mixed solution of synthetic brackish water. The degree of degradation determines the resulting membrane properties, with lower exposure doses leading to NF-like properties and higher doses resulting in UF-like properties (Fig. 7).

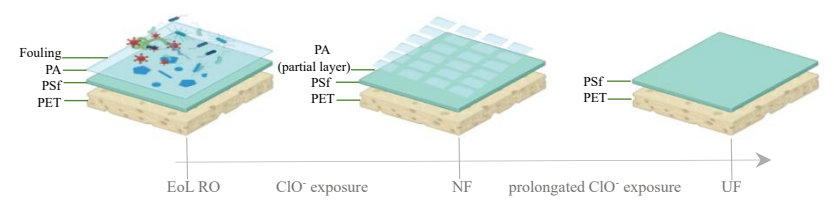


Figure 7. Schematic representation of EoL RO membrane transformation to NF and UF membranes.

These recycled UF and NF membranes have been successfully validated in brackish water desalination [80], RO pretreatment, tertiary wastewater treatment, and household water treatment systems.

However, while direct recycling of EoL RO membranes offers a promising approach, it may not always be feasible due to the degree of degradation or damage caused by chemical exposure, fouling, or physical wear. This can result in the membrane performance falling below acceptable levels for direct recycling applications. To address this challenge, indirect recycling has emerged as a complementary strategy.

Indirect Recycling

Indirect recycling involves deconstructing RO modules to separate their components for individual management. Plastic parts can be incorporated into existing recycling streams, while the recovered flat sheet membranes offer greater versatility for transformation [70].

Both nanofiltration- and ultrafiltration-like properties have been obtained from discarded RO membranes in flat sheet configurations by controlling the exposure time to the chemical agent [79]. Furthermore, several recycling routes of these transformed membranes have been explored, enhancing their applicability across various processes.

For instance, Contreras et al. [81] employed electrospinning to apply a polyvinylidene fluoride nanofibrous layer using recycled UF membranes as support. These membranes, used in Direct Contact Membrane Distillation (DCMD), achieved high salt rejection rates (99.99%). Further, Contreras et al. [82] tested recycled UF membranes for Forward Osmosis (FO) applications in wastewater treatment. These recycled membranes were modified by interfacial polymerization with polyamide or polyester layers. The recycled membranes exhibited similar characteristics to commercial FO membranes and achieved higher rejection rates of humic acids (HA) and NaCl compared to some commercial alternatives.

In other studies, Morón-López et al. developed biofilms on recycled UF and NF membranes to degrade microcystins (MC) [83,84]. These bioactive membranes were implemented in membrane biofilm reactors, successfully removing 2 ppm of MC within 24 hours. This method also proved to be economically competitive compared to conventional treatments.

Rodríguez-Sáez et al. [85] explored a new application for flat-sheet recycled UF membranes. Specifically, the authors conducted a proof-of-concept study regarding their

performance as submerged flat-sheet membranes in an aerobic MBR system, focusing on membrane permeability, permeate quality, and membrane fouling behavior [85]. As the first feasibility study of this kind, it demonstrated the potential application of recycled UF membranes submerged in aerobic MBR, highlighting their promise as a sustainable alternative in wastewater treatment. In a follow-up study, the same authors conducted long-term experiments to further validate the recycled UF membranes for MBR application. The results confirmed that recycled UF membranes can be successfully implemented in aerobic MBR systems for wastewater treatment, offering a sustainable and cost-effective alternative to commercial membranes while addressing common challenges such as membrane fouling and replacement needs [86].

Additionally, AEMs have been prepared from EoL RO membranes, focusing on their applications and recycling methodologies. A pioneering research study introduced a new recycling method using EoL RO membranes as support for AEMs [87]. This process involved casting a polymeric mixture containing a polymer binder and anion-exchange resin onto these recycled UF membranes. The AEMs obtained from recycled UF membranes were validated by comparison with commercial anion-exchange membranes (Ralex®). They have been studied in applications such as electrodialysis, selective electro-separation of nitrate [88], and nitrate removal from drinking water using Donnan Dialysis [89] and Ion-Exchange Membrane Bioreactor systems [90].

These advancements in modifying and applying recycled membranes through indirect recycling highlight their potential to effectively replace or complement conventional water treatment methods, underscoring their versatility and efficiency in various environmental and industrial processes. This innovative approach not only recycles waste materials but also contributes to the advancement of membrane technology and supports the transition toward a Circular Economy.

This doctoral thesis builds upon prior research efforts in the application of recycled membranes within ED and MBR systems, extending their use to address new environmental challenges and establishing a clear link between past work and this current investigation into sustainable, membrane-based water treatment technologies. The research aims to explore innovative solutions for water scarcity through advanced membrane technologies, focusing on wastewater treatment systems. Specifically, it seeks to recover valuable compounds, such as nitrate (NO₃-), present in wastewater and to remove emerging contaminants, such as nanoplastics. Each technology applied is based on the use of recycled membranes at a laboratory scale. The scope and outline of the thesis are further detailed in Chapter 2.

CHAPTER II: Scope and Outline of the Thesis



CHAPTER II: Scope and outline of the Thesis

2.1 Justification of the Thesis

This study builds upon extensive research into innovative recycling methods for endof-life RO membranes, previously developed by the Membrane Technology Research
Group at the IMDEA Water Foundation. Specifically, the thesis focuses on validating
recycled membranes obtained through indirect recycling processes. Indirect recycling
becomes particularly valuable when other management options, such as direct reuse or
direct recycling, are not feasible. This approach involves deconstructing discarded RO
membrane modules, enabling the individual management and transformation of their
components [70]. Overall, indirect recycling represents an innovative pathway that aligns
with the principles of the Circular Economy, supporting advancements in water and
wastewater treatment technologies.

The indirect recycling approach offers versatile applications from NF and UF systems to the creation of novel products, such as functional AEM. In this context, this thesis is a direct continuation of previous studies focused on:

- (i) The development of recycled AEM, produced by applying a polymeric mixture (comprising a binder and anion-exchange resin) onto recycled UF membranes [91].
- (ii) The use of recycled UF membranes as submerged flat-sheet configurations in membrane bioreactor (MBR) systems [85,86].

Further, building on the significant foundational contributions of prior research in indirect recycling of end-of-life RO membranes, and within the framework of two national projects (INREMEN 2.0 and nanoCLEAN), this thesis aims to validate the performance of newly developed recycled membranes in wastewater treatment applications. The primary focus is on integrating these membranes into existing wastewater treatment systems to tackle challenges such as water pollution and the recovery of valuable compounds. By doing so, this work contributes to the development of sustainable, cost-efficient, and environmentally friendly water treatment practices.

The objectives of this thesis will be further detailed in the following subchapter, which provides a structured breakdown of the research goals and methodologies.

2.2 Research objectives and Thesis outline

In light of the aforementioned, this thesis aims to further validate and enhance the performance of recycled membranes, contributing to more sustainable and efficient wastewater treatment solutions. Specifically, this work addresses two major water contamination challenges: high salt loads in wastewater systems and the presence of emerging contaminants in wastewater. The research framework is represented in Fig. 8.

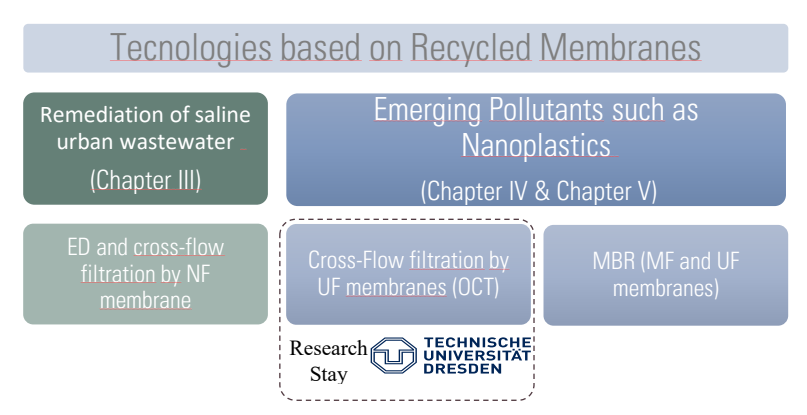


Figure 8. The research framework of the present thesis.

Chapter III (Scientific paper I): Nutrient recovery from urban wastewater: recycled membrane validations. This chapter evaluates the potential of recycled membranes for the remediation of saline urban wastewater, comparing their performance with commercial membranes. The main objectives of this study are:

- To validate the feasibility of NF and ED recycled membranes-based processes for the remediation of saline urban wastewater (UWW).
- To investigate the overall performance and application potential of studied recycled membranes compared to commercial ones.
- To assess the water quality of effluents from both NF and ED processes to determine suitability for water reuse for irrigation.

Chapter IV (Scientific paper II): Fouling study of Ultrafiltration Membranes by Optical Coherence Tomography for membrane selection. This study investigates fouling behaviors of polyethersulfone (PES), regenerated cellulose (RC), and recycled PES membranes during filtration of wastewater containing polystyrene nanoparticles and bovine serum albumin applying the OCT technique. The main objectives of this study are:

- To better understand the membrane fouling mechanism of polystyrene nanoparticles on ultrafiltration membrane surfaces through real-time, non-invasive OCT technique.
- To study the effect of membrane properties (membrane materials, surface charge, molecular weight cut-off) on membrane fouling and membrane filtration performance.

Chapter V (Scientific paper III): Emerging pollutants removal from urban wastewater: study of Membrane Bioreactor. Finally, this study investigates the removal of PS-NPs using microfiltration, commercial ultrafiltration, and recycled ultrafiltration membranes submerged in a lab-scale aerobic membrane bioreactor (aMBR). The main objectives of this study are:

- To study the efficacy of submerged MBR systems for the removal of nanoplastics from urban wastewater.
- To compare the performance of recycled UF membranes with commercial UF membranes.

CHAPTER III: Nutrient recovery from urban wastewater: recycled membrane validations.





Validation of Recycled Nanofiltration and Anion-Exchange Membranes for the Treatment of Urban Wastewater for **Crop Irrigation**

Anamary Pompa-Pernía 1,2,*, Serena Molina 10, Amaia Lejarazu-Larrañaga 10, Junkal Landaburu-Aguirre 1 and Eloy García-Calvo 1,2

- IMDEA Water Institute, Avenida Punto Com, 2, 28805 Alcalá de Henares, Madrid, Spain; serena.molina@imdea.org (S.M.); amaia.ortiz@imdea.org (A.L.-L.); junkal.landaburu@imdea.org (J.L.-A.); eloy.garcia@imdea.org (E.G.-C.)
- Chemical Engineering Department, University of Alcalá, Ctra. Madrid-Barcelona Km 33.600, 28871 Alcalá de Henares, Madrid, Spain

 * Correspondence: anamary.pompa@imdea.org





Article

Validation of Recycled Nanofiltration and Anion-Exchange Membranes for the Treatment of Urban Wastewater for Crop Irrigation

Anamary Pompa-Pernía 1,2,*, Serena Molina 1, Amaia Lejarazu-Larrañaga 1, Junkal Landaburu-Aguirre 1 and Eloy García-Calvo 1,2

Citation: Pompa-Pernía, A.; Molina, S.; Lejarazu-Larrañaga, A.; Landaburu-Aguirre, J.; García-Calvo, E. Validation of Recycled Nanofiltration and Anion-Exchange Membranes for the Treatment of Urban Wastewater for Crop Irrigation. *Membranes* 2022, 12, 746. https://doi.org/10.3390/membranes1 2080746

Academic Editor(s): Alessandra Criscuoli

Received: 11 July 2022 Accepted: 26 July 2022 Published: 29 July 2022

Publisher's Note: MDPI stays neutral with regard to jurisdictional claims in published maps and institutional affiliations.



Copyright: © 2022 by the authors. Submitted for possible open access publication under the terms and conditions of the Creative Commons Attribution (CC BY) license (https://creativecommons.org/license s/by/4.0/).

- ¹ IMDEA Water Institute, Avenida Punto Com, 2, Alcalá de Henares, 28805 Madrid, Spain;
 - serena.molina@imdea.org (S.M.); amaia.ortiz@imdea.org (A.L.-L.); junkal.landaburu@imdea.org (J.L.-A.); eloy.garcia@imdea.org (E.G.-C.)
- ² Chemical Engineering Department, University of Alcalá, Ctra. Madrid-Barcelona Km 33.600, Alcalá de Henares, 28871 Madrid, Spain
- * Correspondence: anamary.pompa@imdea.org

Abstract: One of the alternative sources to tackle the problem of water shortage is the use of reclaimed water from wastewater treatment plants for irrigation purposes. However, when the wastewater has a high conductivity value, it becomes unusable for crop irrigation and needs a more specific treatment. In this work, recycled nanofiltration (rNF) membranes and anion-exchange membranes (rAEMs) obtained from end-of-life RO membranes were validated to evaluate their application capability in saline wastewater treatment. The use of recycled membranes may represent an advantage due to their lower cost and reduced environmental impact associated with their production, which integrates membrane-based technology into a circular economy model. Both recycled membranes were tested in crossflow filtration and electrodialysis (ED) systems. The results of the rNF membrane showed a high selective rejection of divalent ions (SO₄²⁻ (>96 %) and Ca²⁺ and Mg²⁺ (>93 %)). In the case of the ED process, the comparison between rAEMs and commercial membranes showed an appropriate demineralization rate without compromising the power consumption. Finally, the quality of both system effluents was suitable for irrigation, which was compared to the WHO guideline and validated by the 7week lettuce crop study.

Keywords: circular economy; membrane recycling; nanofiltration membranes; nanofiltration; anion-exchange membranes; electrodialysis; wastewater treatment

1. Introduction

Water scarcity is a big problem because the demand for the available water exceeds the conventional water resources due to population growth, climate changes, and ongoing industrialization. Under this context, the use of reclaimed water from wastewater treatment plants (WWTPs) as a source of irrigation water is an important strategy to ensure water security in many regions experiencing water scarcity issues [92]. The advantage of water reuse is directly connected to the avoidance of using drinking water for irrigation, reducing the over-extraction of surface and groundwater, and decreasing its dependence on climate change by using sustainable water resources [93]. However, it is estimated that around 5 % of the total worldwide influent of WWTPs comprises saline and hypersaline wastewater quality [94]. In agriculture and water studies, electrical conductivity (EC) is used as an indicator of soil and water salinity. The EC values above 3000 µScm⁻¹ are considered high values in water for irrigation purposes, representing a high risk for the yield of crops and for the structure and permeability of the soil [95]. Very high values of EC (hardness of water) in WWTPS effluents are commonly provided by various sources such as seawater intrusion, aquaculture, agriculture, and saline wastewater dischargement of various industries (i.e., petroleum and gas extraction, leather manufacturing) [96]. If water with high conductivity is applied to soil, it could have negative consequences such as reduced plant productivity, crop failure, and in extreme cases, death of vegetation [97,98]. Therefore, reclaimed water for agriculture, particularly for irrigation, should obey water quality guidelines and requires the development of a proper water management strategy. Consequently, to improve the quality of the WWTP secondarytreated wastewater effluents, advanced technologies must be applied.

Among the different technologies, membrane-based technologies are especially attractive for saline wastewater regeneration due to their intrinsic desalination capability, flexibility, and high permeate quality. Nor Naimah et al. [96] summarized the different applications of membrane-based processes in saline wastewater treatment. Within membrane processes operated under pressure-driven mode, there is microfiltration (MF), ultrafiltration (UF), nanofiltration (NF), and reverse osmosis (RO). MF and UF membranes are normally used to remove high-molecular-weight compounds (e.g., particulate matter and bacteria) from the water as the sole treatment process or pre-treatment for other processes due to the larger pore size [99,100], which implies that they fail to remove dissolved ions. On the contrary, NF and RO membranes with a tighter pore size are compelling for the separation of inorganic salts and small organic molecules. RO has been known for its capability to reject almost all impurities in the water, which leads to the use of RO to desalinate seawater and brackish water to produce drinking water. Compared to RO, the property of the charged surface of NF allows reducing hazardous electroconductivity values in wastewater treatment by exerting electrostatic repulsion toward multivalent ions [101]. Those characteristics of NF membranes have led to the implementation of NF

as a tertiary treatment for olive oil mill wastewater, for removing dyes in the textile industry, and as a treatment to recover useful resources from the wastewater (e.g., fractional process of humic substances, sulphates from tannery wastewater) [96]. Nor Naimah et al. [96] also highlighted electrodialysis (ED) as another promising membrane-based separation that can be used in saline wastewater treatment. The ED technology is essentially different compared with pressure-driven processes since it is an electrically driven membrane process, where cation- and anion-exchange membranes are alternately placed in a stack, achieving the separation of cations and anions, respectively [56]. However, its application in wastewater treatment such as oil and gas effluent, leachate, textile, and tannery wastewater has also been reported.

Despite the promising performance of membrane technologies, they still deal with drawbacks such as fouling issues and limited lifespan, which increase not only the operational cost of the technologies but also the generation of waste sources. In this regard, the use of recycled membranes may represent an advantage due to their lower cost and the reduced environmental impact associated with their production. In this sense, membrane technology could be integrated into a circular economy model, in concordance with the European Green Deal [72] and the priority order of waste management (prevention, reuse, recycling, recovery, and disposal) regulated in the European Directive 2008/98/EC.

An innovative approach in membrane recycling was proposed since the introduction of the concept of transformation of end-of-life membranes into ultrafiltration membrane in 2002 [102]. Different studies have given a second life to discarded RO membranes by the transformation of spiral wound module configuration into recycled NF- and UF-like membranes [103–105]. Those recycled UF membranes were tested to treat wastewater [103] and gray water reclamation [106], while recycled NF membranes were tested for brackish water treatment [107]. In addition, other studies proposed the deconstruction of the spiral wound configuration to enable the individual management and valorization of the membranes and other plastic components of the RO module (e.g., polypropylene feed spacers). Under this last approach, anion-exchange membranes (AEMs) have been prepared by upcycling discarded RO membranes and have been validated as proof of concept in the ED process [108,109]. In that sense, the technical viability of the recycled AEM was shown to be viable in brackish water desalination experiments with a synthetic solution of NaCl, obtaining 84.5 % of salt removal [108].

Even though there is a recognized potential of the recycled membranes, it is still required to investigate whether the recycled membranes have overall performance characteristics and application capabilities comparable with the performance of commercial membranes. In addition, wastewater regeneration is perfectly integrated within the circular economy definition, and hence, it is in very good alignment with the membrane recycling approach. Therefore, the present work aimed to make one further step in evaluating the implementation of recycled membranes previously developed by our research group (i.e., recycled NF membrane and recycled AEM) in

NF and ED processes for saline urban wastewater (UWW) remediation to obtain water for crop irrigation. The quality of both system effluents was evaluated by comparing the quality of the water reused for irrigation, which is based on the guideline of the World Health Organization (WHO) [93]. To further validate the quality of the effluents, the obtained regenerated waters using recycled membranes were studied for the first time for lettuce cultivation.

2. Materials and Methods

2.1. Wastewater Sample

The feed used in this work was synthetic saline wastewater. The recipe was prepared based on the data analysis from an urban WWTP on the Levante coast in Spain, which confronted a salinity intrusion issue. The real UWW samples were collected every month over three years from the secondary clarifier tank of the plant, where wastewater is biologically treated by the conventional activated sludge. The UWW in this study contained Cl⁻ (1220 mg L⁻¹), NO₃⁻ (57.22 mg L⁻¹), SO₄²⁻ (263 mg L⁻¹), Na⁺ (694 mg L⁻¹), K⁺ (40 mg L⁻¹), Ca²⁺ (204 mg L⁻¹), and Mg²⁺ (99.9 mg L⁻¹) with a pH of 7.16–7.85 and electrical conductivity (EC) of 4830–5237 μS cm⁻¹.

2.2. Chemical Reagents

Sodium hypochlorite (NaClO, 14 %), sodium hydrogen phosphate (NaH₂PO₄), sodium chloride (NaCl), calcium chloride dihydrate (CaCl₂·2H₂O), magnesium sulfate heptahydrate (MgSO₄·7H₂O), sodium hydrogen carbonate (NaHCO₃), potassium nitrate (KNO₃), sodium nitrate (NaNO₃), calcium carbonate (CaCO₃), magnesium chloride hexahydrate (MgCl₂·6H₂O), potassium sulfate (K₂SO₄), sodium sulfate (Na₂SO₄), calcium sulfate dihydrate (CaSO₄·2H₂O), boric acid (H₃BO₃, 0.5%), hydrogen peroxide (H₂O₂, 30%), and chloride acid (HCl, 0.1 M) were purchased from Scharlab S.L., Barcelona, Spain. The ultrapure water (Milli-Q) used in the experiments was obtained from Millipore, Molsheim, France, equipment (conductivity less than 0.055 μ S cm⁻¹).

Polyvinyl chloride (PVC, Mw 112,000 g mol⁻¹) was supplied by ATOCHEM, Madrid, Spain. Tetrahydrofuran (THF) was purchased from Scharlab S.L. Amberlite[®] IRA-402 (Cl⁻ form, total exchange capacity ≥ 1.0 mol L⁻¹) was supplied by Merck Life Science, Darmstadt, Germany, S.L.U.

2.3. Preparation of Membranes

Following the protocols previously reported in [88,110], recycled nanofiltration membranes (rNF) and recycled anion-exchange membranes (rAEMs) were prepared [104,108]. For this purpose, the membrane coupons (~315 cm²) were extracted from discarded 8" diameter RO membrane spiral wound module (TM720-400, Toray Industries, Inc., Osaka, Japan) by membrane autopsy explained elsewhere [104]. Then, the passive transformation protocol was followed [104] at different exposure doses (detailed below) to obtain rNF and recycled ultrafiltration (rUF) membranes (see Figure 9).

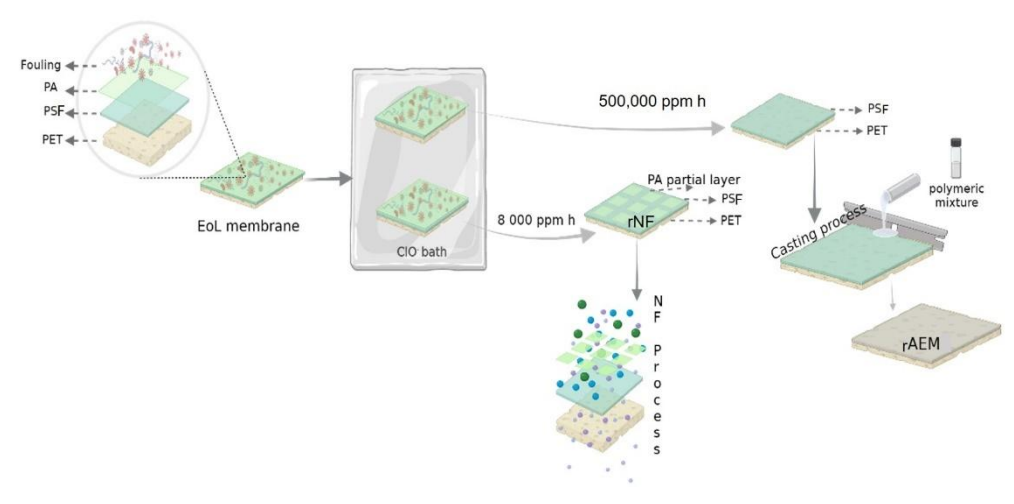


Figure 9. Schematic representation of membrane preparations (rNF and rAEM membranes). PA, polyamide; PSF, polysulfone; PET, polyester.

The oxidizing agent for membrane transformation was NaClO (14%), and the free chlorine concentration was analyzed using a Pharo 100 Spectroquant spectrophotometer before membrane exposure. The feed and permeate spacers from the end-of-life RO module were also reused for the NF and ED processes, as is specified in Sections 2.4.1 and 2.4.2.

2.3.1. Recycled Nanofiltration Membranes

The rNF membrane transformation was conducted using an exposure dose of 8000 ppm h of NaClO solution at room temperature (~21 °C). This exposure dose ensured the total elimination of the fouling and the partial elimination of the polyamide thin film layer of the discarded RO (Figure 9), as it has been widely investigated previously by our research group [111,112]. To ensure partial removal of the polyamide layer (PA) and check the achievement of rNF membrane properties, attenuate total reflectance Fourier transform infrared (ATR-FTIR) spectroscopy was used (Perkin-Elmer RX1 spectrometer) (Perkin-Elmer, Waltham, MA, USA) (Figure S1), and some characterizations tests were carried out (see the Supplementary file, Section S1).

2.3.2. Recycled Anion-Exchange Membranes

The preparation of the rAEM was conducted following the procedure previously reported by Lejarazu-Larrañaga et al. [108]. Briefly, the first step was to obtain the rUF membranes for their use as mechanical support. The transformation into rUF membranes was conducted with an exposure dose of 500,000 ppm h NaClO solution at room temperature (~21 °C). It was verified that the thin film PA layer was completely removed by employing the ATR-FTIR technique (Figure S1). The polymeric mixture employed was prepared using the following chemicals: (i) PVC as a polymer blinder, (ii) THF as the solvent, and (iii) Amberlite® IRA-402 as anionexchange resin. Then, the membranes were prepared using a casting knife and extending an 800 µm thick polymeric mixture on the surface of the rUF membrane. Subsequently, the solvent was evaporated for 60 min at room temperature, and the membranes were finally immersed in a water bath at 20 °C. The performance of the rAEM was compared with a commercial AEM, in this case, Ralex® AMH-PES from Mega a.s., Czech Republic. This membrane (Ralex® AMH-PES) was selected as a reference as long as it had a heterogeneous structure, like the prepared rAEM, which included conducting and non-conducting regions [113]. Indeed, the type of the structure (heterogenous membrane) of the prepared membrane was observed by SEM and compared with a heterogenous Ralex® AHM-PES membrane, which was reported previously and can be found in [108].

2.4. Membrane Performance in UWW Treatment

2.4.1. Nanofiltration Experiments

Crossflow flat-sheet membrane system (from IBERLACT S.L., Alcalá de Henares, Spain) used to perform the NF tests for the filtration of the synthetic UWW is represented in Figure 10a. The system has a high-pressure pump, a 25 L feed reservoir, and a tubular heat exchanger with a temperature controller. The NF membrane with an effective membrane filtration surface of 84 cm² was placed into a flat-sheet stainless steel RO test cell, arranging the permeate and feed spacers from the discarded RO module in the same position as in the original module. The UWW feed and permeate conductivity were measured every 10 min as described in Section 2.6.

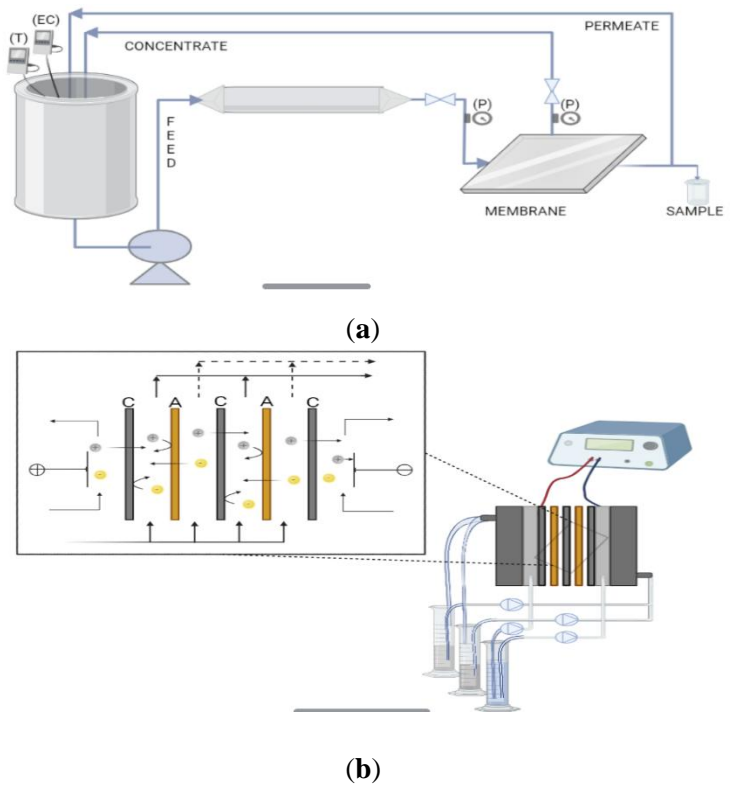


Figure 10. Diagram of (a) NF system (T, temperature; EC, electric conductivity; P, pressure) and (b) ED system (C, cation-exchange membranes; A, anion-exchange membranes).

For the NF assays (based on recycled membranes), the coupon was compacted with a total UWW feed volume of 5 L, a flow rate of 3.9 L min⁻¹, a temperature of 25 °C, and 10 bar transmembrane pressure (TMP). The permeate samples were returned to the feed tank to hold the feed solute concentration. Then, when the steady state was reached (after the first 60 min), feed and permeate samples were taken every 10 min for analysis. Individual ion concentration was measured as it is described in Section 2.6. The permeance of the membrane (*P*, L m⁻² h⁻¹ bar⁻¹) was calculated from the solution flux and the applied pressure [114].

$$P = \frac{\binom{m/\rho}{\rho}}{S \cdot t \cdot n} \tag{1}$$

where m is the sample weight (g), ρ is the density value of the solution at room temperature (g L⁻¹), S is the effective surface of the membrane (m²), p is the pressure applied during the crossflow filtration (bar), and t is the experimental time (h).

Salt rejection was calculated by measuring the conductivity of the feed (C_f) and the permeate (C_p) as is indicated in the following equation [104]:

$$\%R = \left(1 - \frac{C_p}{C_f}\right) \cdot 100\tag{2}$$

Both (permeance and salt rejection) were calculated with an average of at least six measurements (relative error <5 %), and by repeating the experiments 3 times with 3 different membrane coupons.

2.4.2. Electrodialysis Experiments

The ED schematic diagram and the stack configuration are represented in Figure 10b. Therein, 5 cation-exchange commercial membranes and 4 anion-exchange membranes (thus, 4 cell pairs) were alternatively arranged between two electrodes. Two different stack configurations were tested, the first one using a commercial cation-exchange membrane (Ralex® CMH-PES, from Mega a.s., Czech Republic) and rAEM, and a second one assembled using only commercial membranes (CMH-PES and AMH-PES). The electrodes were a dimensionally stable electrode (DSE, titanium coated with iridium oxide) for the anode (Inagasa S.A., Barcelona, Spain) and a stainless-steel electrode for the cathode (Tamesanz®, Madrid, Spain). The effective area of each membrane was 16 cm². To ensure a tortuous configuration for the solutions path and separate the membranes, allowing complete mixing and air removal in the ED stack [115], the reused polypropylene spacers (0.8 mm thick, 3 mm mesh size) from the end-of-life RO membrane were arranged between the membranes in all the experiments.

In this study, the experiments were carried out at constant voltage in a batch mode at room temperature (~21 °C). The synthetic UWW solution was used as feed for the diluted compartment. Na₂SO₄ solution (with a conductivity similar to the diluted solution) was fed in the concentrated chamber. The relation of volume concentrate: dilute (Vc:Vd) was 500:500 mL. A 4 g L⁻¹ Na₂SO₄ solution was used for both electrode compartments, connected to the same reservoir to avoid pH changes and the potential drop in the ED system. A peristaltic pump HEIDOLPH PD 5206 with a multichannel head circulated the solutions throughout the membranes and anolyte/catholyte chambers, maintaining a uniform flow rate of 20 mL min⁻¹. The power supply was an EA-PS 5080-10 A (0-80 V) from EA Elektro-Automatik, Viersen, Germany. The voltage value applied and current variation values were recorded from an Amprobe AM-540-EUR and an Amprobe AM-500-EUR multimeter, respectively. In order to determine the applied operational voltage and the limiting current density (LCD), the same feed solutions were passed through the system. The initial voltage was 0 V and it was increased stepwise up to 30 V, and the resulting current was recorded for each voltage.

In all ED assays, the membranes inside the ED stack were previously equilibrated with the synthetic UWW solution for 24 h. Before the experiments, the working solutions were replaced with new ones and circulated throughout the system for 30 min without an applied electrical current for the homogenization of the solutions.

Then, samples were taken from dilute and concentrate reservoirs, analyzed, and recorded as the initial value. Throughout the experiments, samples of concentrate and dilute solutions were taken periodically without exceeding 10 % of the total dilute volume variation in each test. Elemental parameters (pH and EC) and concentration of individual ions (Cl⁻, NO₃⁻, SO₄²⁻, Na⁺, K⁺, Ca²⁺, and Mg²⁺) were measured for each sample, following the methodology specified in Section 2.6.

The specific energy consumption ($E_{consumption}$, kW h m⁻³) of the process was calculated as [116]:

$$E_{consumption} = \frac{U}{V_d} \int_0^t I \, dt \tag{3}$$

where U is the potential applied to the ED cells (V), I is current (A), V_d is the initial volume of the dilute solution (m³), and t is the ED operation time (h). In this case, the integration (which is defined as Riemann integral) was solved as the calculation of the area under the curve (plotted I vs. t) as follows: $I(t) \approx \sum_{0}^{t} \left[\frac{I(t_f)+I(t_i)}{2}(t_f-t_i)\right]$, where I(t) is a function defined over the positive interval between 0 and the experimental time and (t_f-t_i) is the difference in the time of the evaluated range. It should be mentioned that the energy consumption only included the operational energy consumed by the demineralization process evaluated.

The demineralization rate (%DR) indicates the total amount of salt removed, and it was calculated according to the following equation [117]:

$$\%DR = \left[1 - \frac{\kappa_t}{\kappa_0}\right] \cdot 100\tag{4}$$

where κ_o and κ_t are the initial conductivity and conductivity over time of the dilute chamber, respectively.

To observe and compare the surface morphologies of the rAEM and their stability in the implementation in ED to treat UWW, scanning electron microscopy (SEM) was employed (details in Supplementary Material).

2.5. Irrigation of Lettuce

Lettuce (*Lactuca sativa* L. var. longifolia) plants, belonging to a Romaine type (Chatelaine), were grown for 7 weeks in a controlled climate growth cabinet (1 m³ size). Lettuce seedlings were selected and transplanted when they presented 4 to 5 definitive leaves, between 9 to 15 cm maximum heights. The soil used was standard soil 5M (from Lufa Speyer), and the main characteristics are summarized in Table 2. Standard soils are frequently used for pot experiments in the laboratory and the field. The low level of available N was suitable for the sake of comparison of the treatments. Each pot contained 1750 ± 0.19 g of soil and 374 ± 0.22 g of gravel placed at the

bottom as a filter bed. The pots were arranged in a completely randomized design; see Figure S3 in the supplementary file.

Table 2. Chemical and physical characteristics of standard soil 5 M ¹.

Parameters	Standard Soil 5M
Soil type	Sandy loam
Sampling date	20/07/2021
pH value (0.01 M CaCl ₂)	7.4 ± 0.1
Organic carbon (% C)	0.88 ± 0.18
Nitrogen (% N)	0.11 ± 0.03
Max. water-holding capacity (g/100 g)	41.8 ± 5.3
Weight per volume (g/1000 mL)	1219 ± 88
Cation-exchange capacity (meq/100 g)	8.5 ± 0.25

Particle size distribution (mm) according to USDA (%)

<0.002	0.002-0.05	0.05-2.0
11.9 ± 1	31.6 ± 3.2	56.5 ± 3.3

¹ Data taken from the supplier (Lufa Speyer) [118].

Three different treatments were established with four replicates (plants) each: (i) irrigation with fresh water (tap water, TW), (ii) irrigation with reclaimed water by rNF membrane (IRR), and (iii) irrigation with reclaimed water by ED using rAEM (fertigation, FRT). Throughout the experiment, the temperature (23 \pm 1 $^{\circ}$ C), a photoperiod of 16/8 h (light/darkness), and photosynthetically active radiation (280 $\mu mol\ m^{-2}\ s^{-1}$) were recorded. Each lettuce was irrigated using the drip system installed 0.05 m from the lettuce plant.

After a cultivation period of 49 days, shoots were cut from each plant at the soil level (this can be observed in Figure S4). The growth and yield of the lettuce plants were evaluated through the measurement of head diameter, fresh and dry biomass, and uptake of macroelements.

2.5.1. Statistical Analysis

Data were analyzed statistically using a statistical significance level of 0.05 by ANOVA for the main treatments. The comparison between the treatments was evaluated through analysis of means (Tukey–Kramer test; p < 0.05) to identify the differences [119].

2.6. Analytical Methods

The main parameters for wastewater analysis were measured in the initial synthetic UWW and samples collected from the effluents of NF and ED assays, according to Standard Methods [120], which included EC, pH, anions (Cl $^-$, NO $_3^-$, and SO $_4^{2-}$), cations (Na $^+$, K $^+$, Ca $_2^{2+}$, and Mg $_2^{2+}$), and sodium adsorption ratio (SAR). The conductivity values of solutions were measured by a conductivity meter CM 35 (Crison Instrument, Barcelona, Spain) and the individual ion concentrations by a 930 advanced compact IC Metrohm Ionic Chromatograph.

Prior to the determination of macroelement uptake by the lettuce, the harvested plants were frozen and then freeze-dried using a LyoMicron -80 °C freeze-dryer in order to remove the water present in the lettuce. Hereafter, 100 mg of plant dry mass was taken in a quartz digestion vessel to which 1 mL of boric acid (0.5 %), 2 mL of H₂O₂ (30 %), 0.2 mL of HCl (0.1 M), and 6.8 mL of MilliQ water were added. Subsequently, the samples were digested in the microwave oven (ETHOS One de Milestone) at 190 °C.

The *SAR* equation is used to predict irrigation water sodium hazards. *SAR* is the ratio of sodium to calcium and magnesium concentration (meq L^{-1}) and is calculated as [121]:

$$SAR = \frac{[Na^{+}]}{\sqrt{0.5([Ca^{2+}] + [Mg^{2+}])}}$$
(5)

However, the *SAR* parameter is not of significant value itself to predict the impact of irrigation water on soil. Either EC or *SAR* affects water infiltration in soil; hence, both must be considered in evaluating water quality for irrigation (Table S2). In general, sodium hazard increases as *SAR* increases and EC decreases [121].

3. Results

3.1. UWW Treatment by rNF Membranes

To study the rNF membrane performance in tertiary treatment of UWW (composition detailed in Table 3), the quality of the treated effluent in terms of salinity was evaluated. Figure 11 shows the rNF membrane permeance over the experiment and the total salt rejection (in terms of solution conductivity).

Table 3. Characteristics of the synthetic solution and the effluents of NF and ED technologies.

Water Source	Conductivity (dS m ⁻¹)—	Ionic Compound (ppm)						
water source		Cl ⁻	NO ₃ ⁻	Na ⁺	K ⁺	Ca ²⁺	Mg^{2+}	
Synthetic UWW	4.90 (±0.1)	1224.8	68.21	694	47.20	209	102	
Permeate of rNF	0.98 (±0.02)	249	24.20	153	14.50	14.10	6.86	
Product of ED (<i>rAEM–CMH-PES</i>)	1.93 (±0.1)	390	22.90	320	23.60	52.90	29.20	

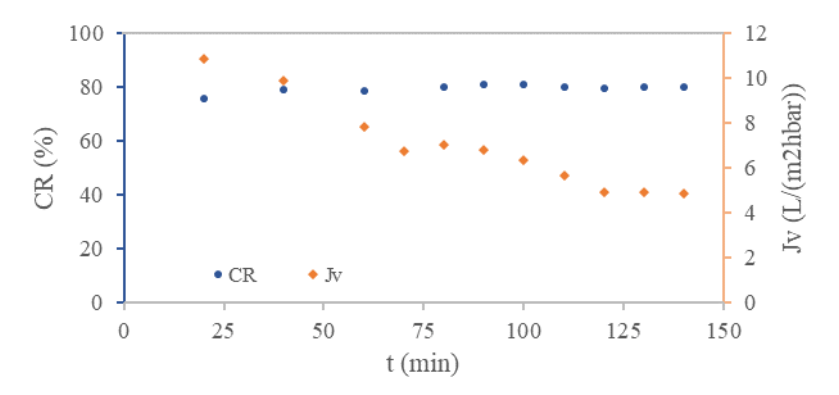


Figure 11. Conductivity rejection (CR) and permeance (Jv) in the function of time (t) for the recycled NF membrane.

Regarding permeance, we could see two different trends in the curve (Figure 11). The linear trend with a surge over the first 60 min (from 10.8 to $7.8 \text{ L m}^{-2} \text{ h}^{-1} \text{ bar}^{-1}$) was due to the compaction of the membrane after its transformation. Then, the region where the steady state was achieved (after 60 min) reached the permeance value of $4.89 \text{ L m}^{-2} \text{ h}^{-1} \text{ bar}^{-1}$ (with an error <1 %) after 120 min. In addition, as it is represented in Figure 11, the total salt rejection was maintained at around 80 % (decrease in electrical conductivity) during the experiment. This result is comparable with a commercial NF membrane performance [4,33].

At 140 min of crossflow filtration, samples were taken and analyzed. The rNF membrane showed a high selective rejection of SO_4^{2-} ions (>96 %) and very high calcium and magnesium separation coefficients (>93 %), in concordance with preliminary characterization tests presented by García-Pacheco et al. [104]. Regarding the rejection of monovalent ions, it showed more significant monovalent separation coefficients: 80.02 % for Cl^- , 66.44 % for NO_3^- , and 74.54 % for Na^+ .

3.2. UWW Treatment by ED Applying rAEM

3.2.1. Determination of the Operating Voltage and LCD

LCD is a critical operating parameter that controls, among other parameters, the optimal demineralization efficiency [122]. The current–voltage curve was experimentally measured in the stack configuration assembled with CMH-PES and the prepared rAEM to determine the LCD, using the UWW as feed solution (Figure 12a). Typically, the current increases linearly at low voltage (Ohmic's region), then the increase rate reduces to reach a "plateau" (LCD region), and finally, the current density increases again (over-LCD region). However, measurements in a multi-cell stack often do not show a clear indication of the slope-changing point. Therefore, the Cowan–Brown method was also applied to verify the LCD value by plotting the overall resistance versus the reciprocal current density (Figure 12b) [123].

Based on the intersection points in Figure 12a, the LCD was identified as equal to 1.90 mA cm⁻¹ at the voltage of 8.77 V (2.19 V/cell pair). The same LCD value was defined by the resistance –1/I graph, in which the LCD was considered as the lowest point on the curve as shown in Figure 12b (show up with the arrow). The boundary layer resistance drastically increases in the LCD region because of the complete depletion of the salt at the membrane surface facing the dilute solution [124]. Above LCD, a non-desired phenomenon of water-splitting occurs, which affects drastically the efficiency of the process and can provoke irreversible damage to ion-exchange membranes due to pH changes [125].

Therefore, in this study, the experiments were carried out below the LCD to maximize current efficiency, minimize the boundary layer effect caused by the concentration gradient, and compare testing results. The literature considers the range between 60 and 80 % of the limiting voltage the safer operating voltage [125,126]. Thus, the experiments were run at around 80 % of the limiting voltage (1.7 V/cell pair).

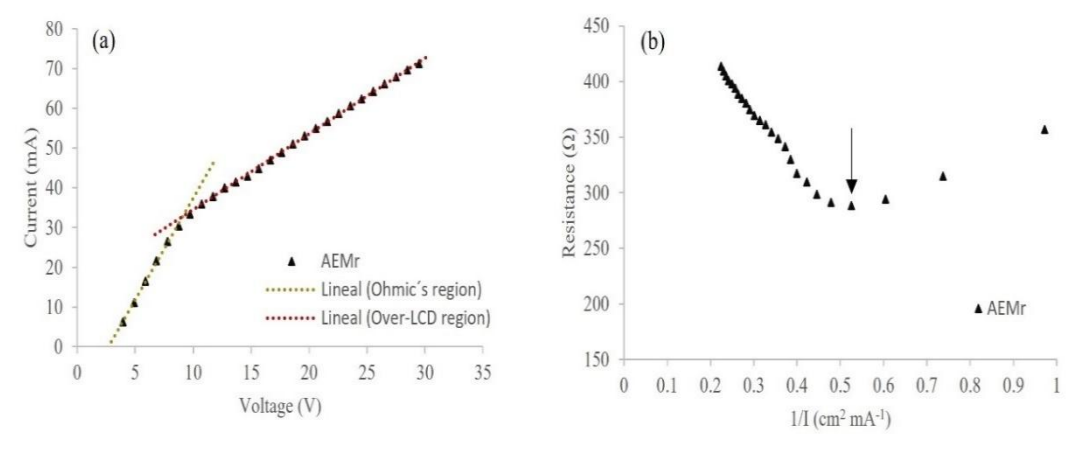


Figure 12. (a) Current-voltage and (b) Cowan-Brown method for the determination of LCD with recycled anion-exchange membranes (rAEMs) (flow rate of 20 mL min-1 and 4 cell pairs).

3.2.2. rAEM Evaluation

To study the performance of rAEM in UWW remediation, the stack was assembled by 5 CMH-PES and 4 rAEM (thus, 4 cell pairs) at a working voltage of 1.7 V/cell pair. The DR percentages were calculated based on the measured dilute conductivity. The relationship between DR and energy consumption is shown in Figure 13. Additionally, the performance of the rAEM in the ED system to demineralize the synthetic UWW was compared with the AMH-PES testing under the

same conditions (i.e., the stack assembled with 4 cell pairs, a working voltage of 1.7 V/cell pair, and Vc: Vd of 500: 500 mL).

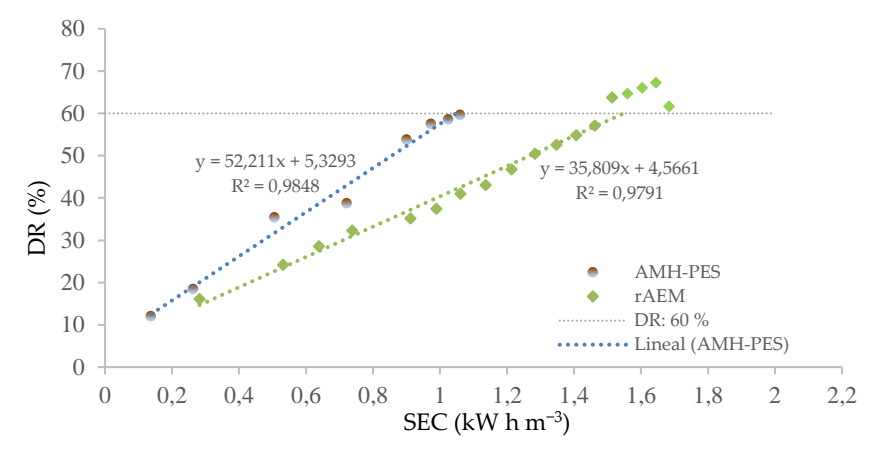


Figure 13. Comparison of demineralization rate (DR, %) of AMH-PES and rAEM based on specific energy consumption (SEC, kW h m-3) by electrodialysis treatment.

As can be seen in Figure 13, a linear tendency of consecutive DR rise by increasing the energy consumption of the system was observed. In the case of the rAEM, an increase in the energy consumption needed for the demineralization process above 60 % of the DR was noticed. The evolution of the demineralization process is correlated with the system resistance (SR). The SR arises from the intrinsic resistance of the membranes inside the ED stack and the resistance of the treated solutions [127]. Thus, the latter hindering ion migration can be attributed to the ion depletion attained for the dilute solution. In this case, the good balance of the macronutrients (corresponding with the water quality for irrigation regulated by WHO) was achieved at 60 % of the DR for both systems (stack assembled by rAEM and the stack assembled by AMH-PES), which is further discussed in the corresponding section (Section 3.3). Therefore, 60 % of DR was set as the completion of the ED experiments.

Additionally, the energy consumption of the stack assembled with rAEMs was less than 1.5 kW h m⁻³ to reach 60 % of DR. Under the same conditions, the stack assembled using only commercial membranes consumed 1.06 kW h m⁻³ to reach the same desalination rate. The slightly higher energy consumption of the rAEMs can be attributed to their higher electrical resistance in comparison with the commercial Ralex membranes. It can be considered that the rAEMs operated with a good level of permselectivity, considering the small difference in the energy consumption between both systems. Furthermore, the slightly higher energy consumption of recycled membranes could be balanced by a lower economic cost associated with the production of such membranes [128]. Surface SEM micrographs were employed to observe the rAEM stability after the experiment. No significant differences could be noticed from the images in Figure S2. Further, pinhole and crack formation were not detected by the SEM analysis.

Overall, membrane recycling is a more sustainable approach than landfill disposal of end-of-life membranes, and it has been demonstrated that the production of recycled membranes results in a lower water and carbon footprint than the production of new membranes [67,129].

3.3. Water Quality for Crop Irrigation.

Conductivity is a very important water quality factor for crop production as a high conductivity causes the inability of plants to compete with ions in the soil solution and water [130]. In addition to conductivity, sodium imbalance in irrigation water can have a substantial impact on crop production. When irrigation water has high sodium content relative to the calcium and magnesium contents (i.e., a high SAR value), water infiltration decreases [131]. Thus, the main parameter compared in this study was the SAR value along with the EC of the treated effluents.

The initial conductivity of UWW was higher than the limits for use in agriculture without severe restrictions (>3 dS m⁻¹, [95]). After the rNF treatment, as expected, the conductivity dropped from 4.90 to 0.98 dS m⁻¹ (Table 3) since the NF membranes usually provide good retention of inorganic salts, especially if multivalent ions are involved [10]. According to WHO guidelines (Table S2), which are connected to the crop sensibility and the content of salts, the rNF effluent falls in the category of "Slight to moderate" concerning the water infiltration, as the calculated SAR value was 6.85 and EC < 1 dS m⁻¹.

On the other hand, the ED process using $16~cm^2$ of rAEM area ($64~cm^2$ of rAEM in total) to treat 0.5~L of the UWW was carried out in a mean time of 8~h. The effluent quality obtained at that time, corresponding with a 60~% value of DR, could be considered in the category of "Slight to moderate" concerning the water infiltration because the SAR value was 6.01 (in the 6-12 range) and EC was $<2~dS~m^{-1}$ ($500-1900~\mu S~cm^{-1}$). Eventually, the ED treatment showed a reasonable extraction for all ions in the solution without compromising the balance ratios and ensuring adequate-quality water for reuse (Table 3).

As a result, both tested recycled membranes showed adequate potential in wastewater treatment for crop irrigation purposes in terms of conductivity and SAR value.

3.4. Lettuce Yield and Macronutrient Uptake in Dry Weight

Lettuce is a vegetable crop that has high nutritional and health value and is best consumed fresh. Fresh lettuce leaves contain about 91–96 % water [132]. Figure 14 shows the average values of the analyzed lettuce fresh wight samples (**a**) and water content for each treatment, (**b**) using the different water qualities obtained.

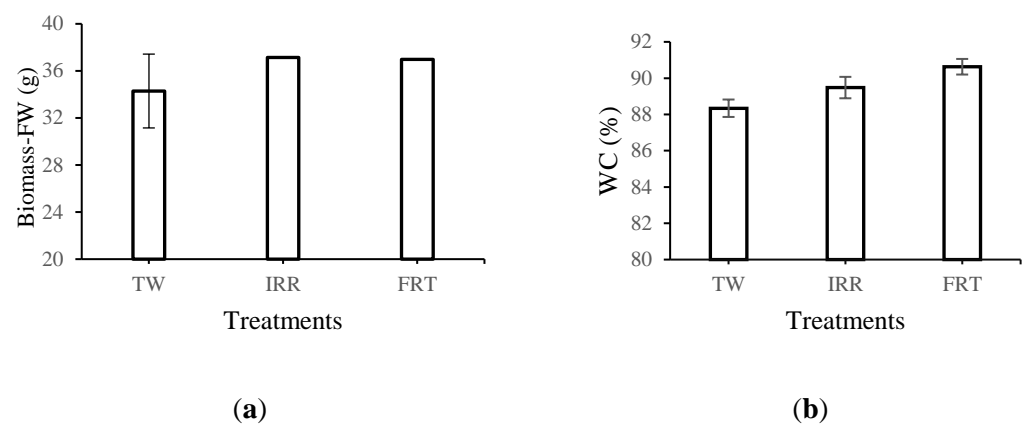


Figure 14. Comparison of the different treatments (TW: tap water; IRR: treated wastewater by NF; FRT: treated wastewater by ED) (a) according to the average biomass fresh weight (FW) and (b) water content (WC, %) in lettuce leaves. Error bars are reported.

No statistically significant differences were found in the biomass-fresh weight according to the treatments TW, IRR, and FRT, which ranged from 34 to 37 g. However, the water content (WC) percent was altered between TW and FRT treatments, showing a statistically significant difference (p < 0.05). Although the WC was not drastically affected by the different nutrient solution concentrations (IRR and FRT), the WC value for lettuces irrigated by IRR water was below the normal range for this crop (i.e., 91-96 %). This effect might be attributed to the influence of the nutrient balance of the different effluents, applied as treatments, on water uptake by plants [132].

Individual macronutrients such as total nitrogen, potassium, calcium, and magnesium of leaves of the lettuce were chemically analyzed (Table 4). In addition to the different nutrient availability of each treatment studied, no significant differences in nutrient absorption were observed between them.

Table 4. Macron	utrient concentrat	ions of leave	in dry weight.
------------------------	--------------------	---------------	----------------

	NTK	IN	K	Ca	Mg
	(%)	(%)	(%)	(%)	(%)
TW	1.03	0.11	4.10	1.71	0.25
IRR	1.20	0.12	4.42	1.48	0.28
FRT	1.24	0.11	4.91	1.68	0.29
CV (%)	0.22	0.22	1.16	0.48	0.10

CV%: coefficient of variation; NTK: total nitrogen Kjeldhal; IN: inorganic nitrogen $(NO_3^- + NO_2^-)$; TW: tap water; IRR: treated wastewater by NF; FRT: treated wastewater by ED.

Vegetables, especially leafy ones, represent the major sources of dietary nitrate intake, owing to their nitrate accumulation capacity. Nitrate and nitrite (which can be formed as an intermediate product of nitrate reduction) are toxic to human health. Therefore, it is essential to keep a low nitrate concentration in the edible parts of crop plants [133]. For the reused wastewater treatments, proper values of nitrogen uptake by lettuce leaves (shown in Table 4) were achieved in compliance with the literature data (range from 1.13 to 5.02 % N in dry weight), which was summarized by M. Petek et al. [132]. Potassium content in lettuce dry weight in the three treatments ranged from 4.09 to 4.91 %. The highest potassium content was determined in FRT treatment, which is almost twice higher than that the reported by M. Petek et al. [132] but in agreement with M. R. Broadley et al. [134] who reported 4.5 % K DW in lettuce. Calcium content in lettuce dry weight in treatments ranged from 1.48 to 1.71 % Ca. The highest calcium content was found in TW treatment, which is in concordance with the results reported by M. Petek et al. [132] (i.e., the highest calcium content (1.42 % Ca) in the treatment with no fertilization applied). Behavior could be explained by the different concentrations of ammonium-N. High doses of ammonium-N cause impairment of other nutrient absorption (e.g., Ca) due to competition between NH₄ and Ca²⁺ cations [135]. The average magnesium content in lettuce dry matter was 0.27 % Mg, which is lower than the 0.52 % Mg DW value obtained in Ref. [132] but falls within the range of 0.15 to 0.35 % Mg DW reported in the literature [132].

4. Conclusions

Different membrane processes can be integrated into wastewater treatment systems, considering the challenging properties of saline wastewater. To make membrane processes an economically attractive and viable alternative, especially in the context of sustainability, two different recycled membranes in treating saline wastewater from an urban WWTP were validated in this work.

- The rNF membrane showed a high selective rejection of divalent ions (i.e., $SO4^{2-}$ (>96 %); Ca^{2+} and Mg^{2+} (>93 %)).
- Comparison between rAEM and commercial anion-exchange membranes (Ralex®) showed a suitable demineralization rate for irrigation of crops without compromising the power consumption.
- Both tested recycled membranes showed adequate potential in wastewater treatment for crop irrigation purposes in terms of conductivity and SAR value. No significant differences in individual macronutrients such as total N, P, Ca, and Mg of leaves of the lettuce of each treatment studied were observed.

Overall, this research showed, for the first time, the successful performance of recycled membranes for treating saline urban wastewater and its application for crop irrigation. In addition, this study showed that membrane recycling is a technically viable process that increases the sustainability of water separation processes and enables the valorization of wastewater for irrigation purposes, which conveys the strategy of the European Commission regarding the transition to a circular economy.

5. Supplementary Materials

S1. Attenuate total reflectance-Fourier transform infrared

Membranes exposed to NaOCl were characterized by ATR-FTIR spectroscopy using a Perkin-Elmer RX1 spectrometer equipped with an internal reflection element of a diamond at an incident angle of 45° . An adequate pressure was applied to the membrane placed on the crystal surface. The spectra were recorded at a resolution of 2.0 cm-1 in the frequency region of $4\ 000\ - 650\ \text{cm}\text{-}1$, with an average of $4\ \text{scans}$ per sample. Previously the samples were dried at $100\ ^{\circ}\text{C}$ to remove moisture for two days.

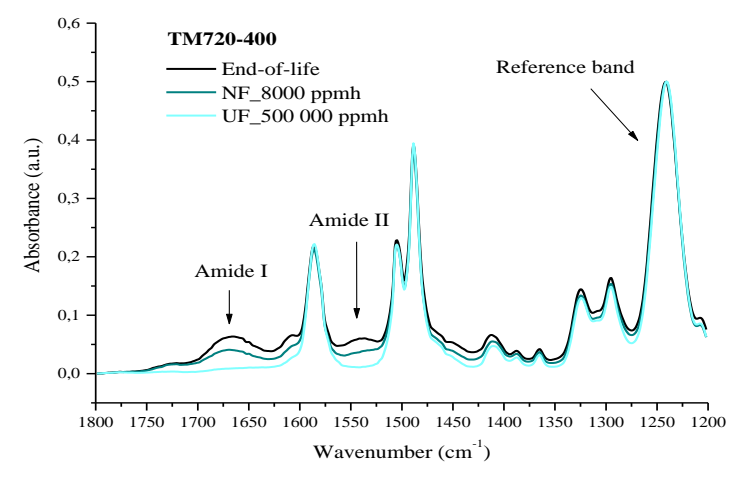


Figure S 1. Attenuated total reflectance-Fourier transform infrared comparison images to verify the end-of-life transformation.

It can be observed in Fig. S1 that the ATR-FTIR spectra of the membranes after being exposed to the NaOCl solution changed with respect to the pristine state (end-of-life membrane). These results indicate that these treatments were successfully achieved. For the transformation to nanofiltration membranes (dark green) the signals equivalent to the Amide I and Amide II groups can be detected with lower intensity compared with the end-of-life RO membranes. In contrast, for the transformation to ultrafiltration membranes (light green) no signals equivalent to the Amide I and Amide II groups can be detected, which means that the thin polyamide layer was completely removed.

S2. Scanning electron microscopy

Scanning Electron microscopy (SEM) using the S-8000 Model (Hitachi) image device was employed to observe the surface morphologies of the membranes and their stability in the implementation in ED to treat UWW. Preceding the microscopy analysis, the membrane samples were dried by heating at 50 °C for 48 hours and later were gold-sputtered with a Sputter Coater Polaron SC7640 model to achieve 13–15 nm thickness prior to the SEM analysis. Surface SEM microphotographs of rAEM samples in the pristine state and after ED treatment are presented in Fig. S2. The nature of this recycled membranes manufacturing technique results in heterogeneous

anion-exchange membranes, obtaining a dense and rough surface, with a considerably homogeneous distribution of ion-exchange resin particles.

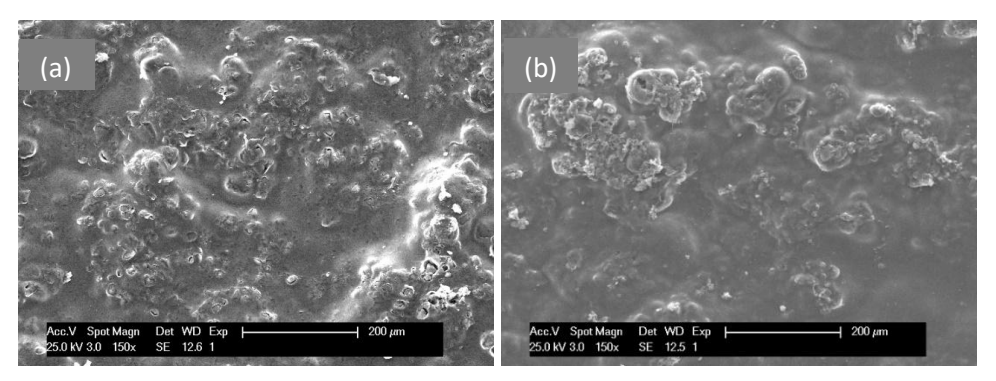


Figure S 2. SEM images of the rAEM membranes (a) pristine rAEM, and (b) tested rAEM.

As can be observed in Fig. S2, the membrane after being used in UWW treatment did not present a salt deposition on its surface. Although, the long-term stability of the rAEMs in UWW treatment by ED should be addressed in future studies.

S3. Guideline of the water quality for irrigation

Table S1 summarizes the main parameters of the quality of reclaimed water for irrigation purposes regulated by the World Health Organization (WHO).

Table S 1. WHO guidelines of wastewater reuse for irrigation.

Parameter		Unit	De	egree of restriction on	use
			None	Slight to moderate	Severe
SAR	=0-3	EC =	>700	700 – 200	<200
	=3-6	EC =	>1200	1200 - 300	<300
	=6-12	EC =	>1900	1900 – 500	< 500
	=12 - 20	EC =	>2900	2900 – 1300	<1300
	=20 - 40	EC =	>5000	5000 – 2900	<2900
Na^+	Surface irrigation	mg L ⁻¹	<69	69 - 207	>207
	Sprinkler irrigation	mg L ⁻¹	<69	>69	
Cl ⁻	Surface irrigation	mg L ⁻¹	<142	142 – 354	>354
	Sprinkler irrigation	mg L ⁻¹	<106.5	>106.5	
Total Nitrogen (TN)		mg L ⁻¹	<5	5 – 30	>30
Nitrogen (NO ₃ -N)		mg L ⁻¹	<5	5 – 30	>30
pН		-		6.5 – 8 (8.5)	
Anions and cati	ions				
NO ₂ -		mg L ⁻¹ (meq L ⁻¹)		-	
SO4 ²⁻		mg L ⁻¹ (meq L ⁻¹)		960 (20)	
${\bf Mg^{2+}}$		mg L ⁻¹ (meq L ⁻¹)		61 (5)	
Ca ²⁺		mg L ⁻¹ (meq L ⁻¹)		400 (20)	
Nutrients					
NO ₃ -		mg L ⁻¹ (meq L ⁻¹)		140 (10)	
NH_4^+		mg L ⁻¹ (meq L ⁻¹)		90 (5)	
PO ₄ ³ -		$mg~L^{\text{-}1}~(meq~L^{\text{-}1})$		194 (2)	
\mathbf{K}^{+}		mg L ⁻¹ (meq L ⁻¹)		78 (2)	

CHAPTER IV: Fouling study of Ultrafiltration Membranes by Optical Coherence Tomography for membrane selection.

Separation and Purification Technology 354 (2025) 129520



Contents lists available at ScienceDirect

Separation and Purification Technology





Experimental evaluation of nanoplastics fouling behavior on ultrafiltration membranes using optical coherence tomography (OCT)

Anamary Pompa-Pernía a,b,* , Ana Aleman c , Kristin Kerst c , Serena Molina a , André Lerch c , Junkal Landaburu-Aguirre a

IMDEA Water Institute, Avenida Punto Com, 2, Alcalá de Henares, 28805 Madrid, Spain
 Chemical Engineering Department, University of Alcalá, Ctra. Madrid-Barselona Km 33.600, Alcalá de Henares, 28871 Madrid, Spain
 Chair of Process Engineering in Hydro Systems, TUD Dresden University of Technology, 01069 Dresden, Germany



Contents lists available at ScienceDirect

Separation and Purification Technology

journal homepage: www.elsevier.com/locate/seppur



Experimental evaluation of nanoplastics fouling behavior on ultrafiltration membranes using optical coherence tomography (OCT)

Anamary Pompa-Pernía^{a,b,*}, Ana Aleman c, Kristin Kerst c, Serena Molina a, André Lerch c, Junkal Landaburu-Aguirre

- ^a IMDEA Water Institute, Avenida Punto Com, 2, Alcala' de Henares, 28805 Madrid, Spain ^b Chemical Engineering Department, University of Alcala', Ctra. Madrid-Barcelona Km 33.600, Alcala' de Henares, 28871 Madrid, Spain
- ^c Chair of Process Engineering in Hydro Systems, TUD Dresden University of Technology, 01069 Dresden, Germany

ARTICLEINFO

ABSTRACT

Keywords:

UF membranes Membrane fouling Optical coherence tomography Recycled membrane Cross-flow filtration Nanoplastics

Ultrafiltration membranes find widespread use in water treatment but suffer from performance losses due to fouling. This study investigates the fouling behaviors of commercial polyethersulfone (PES), regenerated cellu- lose (RC), and recycled PES membranes during the filtration of wastewater containing polystyrene (PS) nano- particles and a mixture of PS and bovine serum albumin (BSA). Optical coherence tomography (OCT) is used for real-time, in-situ examination of fouling, providing unique insights into nanoplastics-induced fouling formation. Membrane performance was evaluated through flux decline and permeability recovery measurements. Results indicate that nanoparticles form a uniform cake layer, with membrane characteristics such as zeta potential and hydrophobicity influencing fouling reversibility. The RC membrane showed complete permeability recovery after physical cleaning, while hydrophobic interactions hindered recovery for PES membranes. Notably, flux reduction was greater for PES membranes (particularly with a 150 kDa MWCO) during PS filtration and wors- ened with the combined PS and BSA solution. Using the OCT technique, we observed two distinct types of fouling and their resulting structures: (i) a loose or fluffy-like formation; and (ii) flocs or particle agglomerates. This study also combined OCT with conventional techniques like SEM and CLSM. This knowledge offers guidance for choosing the proper membrane material in water treatment applications.

Abbreviations: PES, polyethersulfone: RC, regenerated cellulose: OCT, Optical Coherence Tomography: RI, Refractive Index: MNPs, micro-nano plastics; MPs, microplastics; NPs, nanoplastics; PS, polystyrene; UF, Ultrafiltration; RO, Reverse Osmosis; WWTPs, Wastewater Treatment Plants; DO, direct observations; SEM, Scanning Electron Microscopy; AFM, Atomic Force Microscopy; CLSM, Confocal Laser Scanning Microscopy; SEC, Size Exclusion Chromatography; MWCO, Molecular Weight Cut Off; WCA, Water Contact Angle; NaOCl, Sodium Hypochlorite; BSA, Bovine Serum Albumin; NOM, Natural Organic Matter; COD, Chemical Oxygen Demand; D, particle diameter; PR, Permeability Recovery; Po, Initial hydraulic permeability; Pc, Hydraulic permeability after the cleaning process; DI, Deionized water; $\lambda(ex.)$, Excitation wavelength; $\lambda(em.)$, Emission wavelength.

Received 17 July 2024; Received in revised form 22 August 2024; Accepted 2 September 2024 Available online 4 September 2024

1383-5866/© 2024 Elsevier B.V. All rights are reserved, including those for text and data mining, AI training, and similar technologies.

^{*} Corresponding author at: IMDEA Water Institute, Avenida Punto Com, 2, Alcalá de Henares, 28805 Madrid, Spain. E-mail address: anamary.pompa@(A. Pompa-Pernía).

1. Introduction

Water pollution, a widespread environmental challenge, poses a significant threat to the delicate balance of aquatic ecosystems. Plastics, with their indispensable role in modern life, have become one of the most persistent pollutants in water bodies, presenting a multifaceted challenge with ecological consequences. Among the various pollutants, micro-nano plastics (MNPs), involving microplastics (MPs, \leq 5 mm) [136] and nanoplastics (NPs, from 1 to 1000 nm) [137], have emerged from both intentional production and the breakdown of larger plastic items. The possible introduction of these MNPs into the food chain is worrying because it could harm the organisms in it, increasing the risk of damage to the ecosystem and loss of biodiversity [24].

Wastewater treatment plants (WWTPs) have been identified as the predominant route for MPs to infiltrate the aquatic environment [138,139]. Even though WWTPs exhibit a retention rate ranging from 98% to 99% of MPs [139], this is mainly attributable to the massive volume of effluent discharges by WWTPs. Moreover, it is expected that weathering of macroplastics and MPs will generate secondary NPs, although there is no available data on the environmental loads of NPs [140].

In that sense, membrane-based advanced technologies for wastewater treatment, such as pressure-driven porous membranes like ultrafiltration (UF), could be effectively implemented as a tertiary treatment for MNPs removal since the small pore sizes of UF membranes allow successfully retaining MNPs through size exclusion mechanism [141]. Indeed, Elsaid et al. [142] summarized the UF removal capacity of nanomaterials studied such as 78 nm SiO₂ and 30 – 60 nm Ag, demonstrating high separation efficiency (i.e. a separation of > 98% and 80%, respectively). Furthermore, membrane filtration poses advantages such as its wide market availability and easy retrofitting with minimal cost. Concerning the implementation of UF membranes for the removal of MNPs, particularly NPs, limited studies are focused on the membrane-based separation of nano-sized particles [143]. For instance, Wan et al. [144] explored nanofibrous membranes by a gravity-driven membrane filtration process to assess their efficacy in removing polystyrene NPs with sizes ranging from 107 to 1450 nm, achieving a 92% removal efficiency. On the other hand, Molina et al. [32] evaluated the separation efficiency of MF and UF flat-sheet membranes for different NP sizes (polystyrene of 120 and 500 nm, respectively) in dead-end configuration. They also introduced a different approach, emphasizing the use of pressure-driven membrane technology not only for tertiary wastewater treatment but also as a sample pretreatment method [32].

Nevertheless, during the filtration process, fouling remains a significant challenge due to its adverse effects on membrane performance [145]. While the presence of micro-nano plastics (MNPs) in water is anticipated to contribute to membrane fouling during water treatment, the actual impact of MNPs on membrane filtration performance remains still unclear [146]. Various studies have explored the influence of fouling mechanisms on UF membranes caused by MNPs [146], the combined fouling effects of MNPs and natural organic matter (NOM) on UF membranes [147], and the separation efficiency of different NPs sizes and mixed solutions containing NPs and Bovine Serum Albumin (BSA) by MF and UF membranes [32]. However, contradictory findings have been reported regarding the deposition of MNPs on polymeric membranes. While Markazi et al. [147] observed a higher amount of MNPs deposited on the membrane during combined foulants filtration

(i.e., MNPs and BSA), forming the cake layer at earlier stages, Molina et al. [32] concluded that BSA could also act as a stabilizer, leading to better dispersion of NPs and hindering pore blocking and cake layer formation. This discrepancy may be attributed to variations in the concentration ratio of MNPs and BSA, as well as differences in the operational conditions of the filtration system (dead-end and crossflow mode). Therefore, research on mixed solutions of MNPs and other compounds, such as NOM, is still in its early stages, and further studies in this area are required [32]. This observation has also been shared by Sharma et al. [148], who after conducting a comprehensive review on the relevant literature, particularly with a focus on membrane technologies for plastic particle removal, concluded that the existing body of research indicates that the removal of microplastics through membrane technology is still insufficient.

Fouling propensity is commonly assessed experimentally by monitoring permeate flux and transmembrane pressure (TMP) [62] as well as by using various models developed to study fouling (which can be classified into empirical, theoretical, or semiempirical models). Among all the existing models, Hermia models are the most used to fit experimental data in UF processes [149]. On the other hand, the use of membrane surface characterization techniques such as scanning electron microscopy (SEM) and atomic force microscopy (AFM) for fouling analysis are valuable, but they can only be applied after the membrane process is finalized. Although these "autopsy" approaches are still useful, it is necessary to monitor membrane fouling in real time during intermittent operation [150]. Accordingly, several direct observations (DO) through non-invasive techniques have been investigated [151]. Despite their utility, DO techniques encounter limitations such as the inability to measure the thickness of the fouling layer [62]. In that sense, Optical Coherence Tomography (OCT) has recently received increased attention as a novel approach for real-time analysis of membrane fouling [63]. Since 2006, OCT has been used to investigate biofilm structures in water and membrane filtration systems, in capillary flow cells [152], and in crossflow filtration systems under laminar, transient, and turbulent flow conditions [153,154]. OCT is a relatively quick, sensitive, noninvasive method that provides high-resolution images [155]. OCT has been also used for studying internal particulate fouling during dead-end microfiltration, focusing on the effects of particle surface charge, size, and composition [156]. Han et al. [157] investigated the influence of particle size on cake layer formation using monodispersed and bi-dispersed feed solutions containing latex particles. OCT images demonstrated that: high concentrations (11.6 mg/L) of large particles led to heterogeneous cake layers and low concentrations (2.5 mg/L) of large particles resulted in homogeneous cake layers. Lay et al. [158] examined membrane fouling caused by mixtures of oppositely charged latex particles. Surprisingly, mixtures with less positive charge than purely aminated latex particles resulted in worse flux declines. OCT analysis showed that these mixtures created taller buildups on the membrane and heterogeneous internal cakes. On the other hand, Park et al. [159] evaluated an ultrafiltration membrane fouling behavior using various model foulants, including humic acid, sodium alginate, and BSA. OCT measurements of fouling thickness revealed that while there is a correlation between resistance in series (RIS) and actual fouling thickness, the latter may be lower than estimated when pore blocking, and adsorption is significant.

In the present work, fouling behaviors of polystyrene (PS) nanoparticles across commercial polyether(sulfone) (PES), recycled PES, and regenerated cellulose (RC) UF membranes were investigated. The consequence of fouling on the membrane filtration performance regarding the different membrane materials, membrane surface charge, and molecular weight cut-off as well as the properties of the polymer were examined, alongside observations made by OCT. Furthermore, conventional techniques such as SEM and confocal microscopy were employed to characterize the membranes after cleaning. This study aims to evaluate the fouling behavior of UF membranes by filtering synthetic treated wastewater containing NPs and the combination of NPs with BSA.

2. Materials and Methods

2.1 Membranes and plastic foulants

Four flat-sheet ultrafiltration (UF) membranes were employed in the study. UF membranes were chosen due to their potential usage in water treatment processes, particularly in advanced filtration units that are already in operation. The RC membrane, MWCO 30 kDa was supplied by Millipore, USA. Among the PES membrane studied PES, MWCO 30 kDa (supplied by MANN+HUMMEL Water & Fluid Solutions, Germany), PES, MWCO 150 kDa, (supplied by Millipore, USA), and a recycled UF membrane were implemented. The characteristics of the recycled membrane have been reported in previous works [79]. Briefly, the membrane coupons were extracted from discarded 8" diameter RO membrane spiral wound module (TM720-400, Toray Industries, Inc., Osaka, Japan) by membrane autopsy explained in [79,85,110,160]. Then, the passive transformation protocol was followed, where the polyamide layer of the RO membrane is totally oxidized using sodium hypochlorite at the exposure doses of 500,000 ppm·h, obtaining recycled UF membranes [79]. Using recycled PES membranes aligns with the principles of the circular economy [161], promoting resource efficiency and reduced waste. While not directly addressed in the technical data, recycled membranes may offer a cost advantage over virgin membranes. Furthermore, previous studies indicated that recycled membranes can surprisingly demonstrate even lower fouling tendencies than their virgin counterparts [83]. This potential fouling reduction, combined with advantages in cost, makes them an attractive option for cost-sensitive applications. Thus, the decision to study and compare the recycled membrane alongside commercial ones was motivated by its potential advantages in sustainability, cost-effectiveness, and performance [70,83,162]. The nanoparticles used were polystyrene (PS) fluorescent carboxylate of 116 \pm 2 nm size and $\lambda_{ex.}$ / $\lambda_{em.}$: 576 nm / 596 nm (purchased from IKERLAT Polymers, Spain). Bovine Serum Albumin (BSA) protein was purchased from Sigma-Aldrich, Spain. Table 5 summarizes the membrane properties as provided by the manufacturer and as measured in the current study. The measurements were conducted to establish comparative results. The volumetric particle diameter (D) and ζ-potential of both individual foulants and combined compounds are also summarized in Table 5. Chemicals used for the preparation of synthetic treated wastewater were Urea (Urea reagent grade ACS), Sodium Chloride (NaCl reagent grade, ACS, ISO, Reag. Ph Eur), Sodium bicarbonate (NaHCO₃, extra pure, Pharmpure®, Ph Eur, BP, USP), di-Potassium

hydrogen phosphate anhydrous (K₂HPO₄ for analysis, ExpertQ®, ACS, Reag. Ph Eur), Calcium chloride dihydrate (CaCl₂.2H₂O powder, for analysis, ExpertQ®, ACS), and Potassium nitrate (KNO₃) supplied by Merck Life Science, Darmstadt, Germany, S.L.U.

Table 5. Technical data, MWCO, and ζ -Potential of the analyzed membranes and volumetric particle diameter (D) and ζ -potential of the foulants measured in the working solution (synthetic wastewater).

	Material	Nominal Size (nm)	Nominal MWCO ^a (Da)	ζ-Potential ^b (mV)	Water Contact Angle (°)
	M	embranes	(Du)		()
PES 150 kDa	Polyethersulfone	< 30	90,000	-28.01	49.9 ± 2.6
PES 30 kDa	Polyethersulfone	< 15	30,000	-23.24	$67.6 \pm 3.0 [146]$
RC 30 kDa	Regenerated Cellulose	< 15	50,000	-20.17	26.0 ± 3.0 [163]
Recycled membrane	Polyethersulfone		30,000	-26.78	65.2 ± 0.4 [160]
	Fou	ılants			
BSA (0.1 g L ⁻¹)	Bovine Serum	6.6 ± 2.9		-20.0 ± 0.12	
PS	Albumin	118 ± 31		-28.1 ± 0.07	
PS + BSA	Polystyrene	133 ± 43		-24.0 ± 0.10	

^aValues measured by Size Exclusion Chromatography (SEC). ^bValues measured at pH 8.7.

The Molecular Weight Cut Off (MWCO) is defined as the corresponding molecular weight with a retention coefficient of 90%. To ensure direct comparisons between the studied membranes, the MWCO of the membranes were determined under consistent conditions. The MWCO was determined from Size Exclusion Chromatography (SEC). For this purpose, an Agilent Technologies 1260 Infinity GPC/SEC System with a column from Polymer Labs (PL MIXED aqua gel-OH) of nominal pore size 8 μm was used. Milli-Q water was used as the eluent with 1 mL min⁻¹ of flow rate. The calibration was carried out with narrow standards of PEOs with molecular weights between 194 and 490,000 Da. The feed solution contained PEOs ranging from 103 to 105 g mol⁻¹, keeping the total concentration of 1 g L⁻¹ following the composition reported in previous studies [78,164].

Particle size and ζ -potential of both NPs and BSA were characterized by Dynamic Light Scattering (Mastersizer 3000 Malvern Panalytical, UK) and the ζ -potential analyzer (Zetasizer Nano ZSE, Malvern Paranalytical, UK), respectively. A wet laser diffraction technique, employing the Hydro SM dispersion unit with water as the dispersant, was used for particle-size analysis. The parameters included RI of 1.33, obscuration between 5 – 15%, recirculation speed of 2 500 rpm, and a measurement time of 30 seconds. The final DLS spectra were based on five measurements.

For the ζ -potential measurements, the following conditions were employed: analysis probe DTS 1070, RI of 1.59 and 1.50 for PS and PE, respectively, absorbance of 0.01, temperature of 25 °C, and 90 seconds of measure time. All the samples were analyzed without previous treatment.

The ζ -Potential of the membrane samples were analyzed using the Zeta Potential Analyzer ZPA 20 with the streaming potential method supplied by DataPhysics Instruments GmbH. To ensure the cleanliness of the measuring device and samples measuring cell, the equipment was thoroughly cleaned with ultra-pure water before preparing the measuring cell with the flat-sheet membrane samples. From the streaming potential vs. pressure ramps obtained in several oscillations, the zeta potential was calculated for the given pH values. An automatic titration function of the LDU 25 liquid dosing unit from DataPhysics Instruments determined the zeta potential automatically in the pH range from 2.6 to 9.6 approximately. As titrants HCl (0.1 mol L⁻¹) and KOH (0.1 mol L⁻¹) were used.

2.2 Crossflow filtration experiments

UF membranes with a surface area of $30.2~\rm cm^2$ were used for all experiments to filter solutions containing PS nanoplastics in synthetic wastewater through a crossflow filtration system. The experiments were run using constant pressure mode at 1 bar. The concentration of the nanoplastic foulant in the feed solution was $3.3~\rm mg~L^{-1}$ and the feed (total volume of 3 L) was constantly stirred to ensure the nanoplastics dispersion. The choice of the NP concentration was based on the literature, ranging from 1 mg L⁻¹ [158] to $10~\rm mg~L^{-1}$ [32,146]. Permeate streams were collected for measurements and discharged to keep a continuous filtration mode.

The feed solution was circulated through the cell using a Peristaltic pump ISMATEC: MCP-Z Process IP65. The crossflow rate was controlled at a constant value of \sim 200 mL min⁻¹ with a duration of each fouling experiment of 150 min. The filtration cell employed was round-shaped, with a length of 5.8 cm and a weight of 1.6 cm, as depicted in Fig. 15.

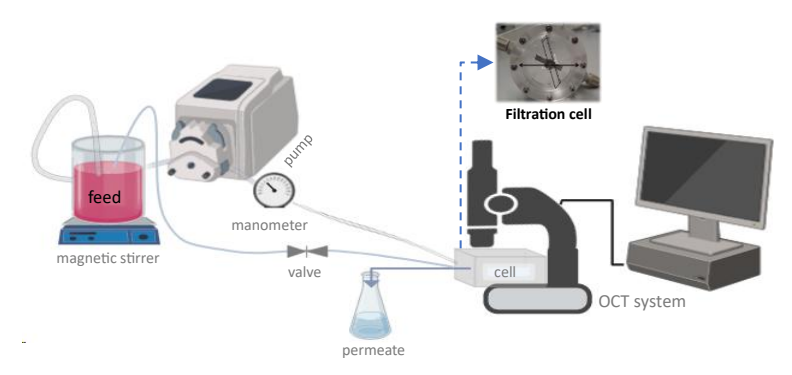


Figure 15. Schematic diagram of the filtration and monitoring.

In a real environment, NPs may interact with various constituents present in the water, like other pollutants, organic matter, and minerals. For that reason, in the present study, a synthetic wastewater feed was employed to mimic the complexities of the actual environment where the technology could be applied as tertiary treatment. The synthetic wastewater feed simulated an MBR permeate with a chemical oxygen demand (COD) of 22 mg L⁻¹ and 30 mg L⁻¹ of urea as organic matter. Furthermore, BSA was added and

chosen as a foulant, which is commonly used as a model compound for membrane fouling studies, being a natural organic matter (NOM).

Membranes were compacted and cleaned up prior to each filtration experiment to remove any residual protective layer. After the end of each filtration test, a cleaning step was performed by rinsing the membranes with deionized (DI) water out of the cells. Permeability recovery rate PR (%) was calculated based on the initial hydraulic permeability (P_0) and the one after the cleaning process conducted by rinsing the membrane with DI water (P_c) , Equation (6):

$$PR(\%) = \frac{P_C}{P_0} * 100 \tag{6}$$

For each type of foulant, the fouling and cleaning experiments were repeated at least twice.

2.3 Real-time observations of fouling formation

2.3.1 Optical Coherence Tomography (OCT)

Membrane fouling-layer evolution was investigated using a spectral domain system OCT (SD-OCT) (Thorlabs Ganymede 611). The system used acquired images with a central light source wavelength of 930 nm with an axial resolution of 4.1 μm and an imaging depth of 2.2 mm in water. Volumetric scanning (or C-scans, 3D) was performed using the Thorlabs software (ThorImage OCT version 5.5.1) with a field of view of 2.50 x 1.00 mm and a refractive index (RI) of 1.33. The C-scans consisted of 207 B-scans (2D) with a resolution of 530 x 595 pixels, corresponding to a physical profile of 2.50 x 1.27 mm and a pixel resolution in "x" of 4.72 μm/pixel and in "y" of 2.14 μm/pixel.

Even though the OCT technique employs a light beam with a diameter of approximately 4 μ m [165], which is significantly larger than the individual PS plastics (116 nm), significant signals were detected within the regions where the nanoparticles were concentrated or formed a cake layer. The optical device was positioned adjacent to the filtration system so that fouling could be observed in real time. A measurement window (size 3 mm x 3 mm) was defined on the lid of the filtration cell. Every 30 minutes, the cell was manually moved to the OCT base, and the images were acquired for the same position, as schematically represented in Fig. 15.

2.3.2 Images processing

Processing of images from OCT was developed using ImageJ, a Java-based software (version 1.54f). To enable automated processing of the images, a multi-step method was applied using ImageJ macros. An image processing workflow composed of three macros was created to estimate the thickness of the fouling layer at each filtration time (Fig. S3). An example of the tomographic imaging process used to determine the cake thickness is shown in Fig. S4. A total of 265 measurements of the fouling layer thickness were taken per image.

2.4 Membrane characterization

2.4.1Scanning Electron Microscopy (SEM)

Scanning Electron Microscopy (SEM) using the S-8000 Model (Hitachi) image device was employed to observe the morphology of the membrane surfaces and the fouling degree of the studied membranes after the physical cleaning at the end of each assessment. Preceding the microscopy analysis, the membrane samples were dried by heating at 50 °C for 48 hours.

2.4.2 Confocal laser scanning microscopy (CLSM)

Confocal laser scanning microscope (CLSM Leica SP5, Leica Microsystems) technique was chosen due to the fluorescent properties of the PS standard and as a supplementary approach to investigate the reversibility of the fouling layer. Notably, the observations were conducted post-physical cleaning. Each membrane was cut into 5 mm x 5 mm pieces, and three different areas were examined. The resulting images were analyzed by the ImageJ software (Version 1.51n). The 3D projection images of the particles were constructed by the ImageJ 3Dviewer plugin.

Results and discussions

3.1 Membranes and Foulants properties

The properties of the studied membranes are summarized in Table 5. The hydrophilic character of the RC membrane could be confirmed, with an average water contact angle (WCA) of $26.0 \pm 3.0^{\circ}$. In contrast, the PES membranes exhibited a relatively hydrophobic nature (Table 5). ζ -Potential measurements of the membrane surfaces revealed that all four membranes had a similar negative charge at the pH of the working solution. A direct comparison is feasible between the recycled membrane and the commercial PES 30 kDa membrane, as both exhibit similarities in nominal molecular weight cut-off (MWCO), ζ -potential, and hydrophobicity.

The average size of the particles and the ζ -potential of solutions containing individual and combined foulants were measured in the same dispersion medium as the working solution, as previously mentioned (Table 5). This investigation aimed to explore the real interactions between foulants and the membrane over the experimental period. The reported results indicate that the working solution had no influence on the average size of the model protein used (BSA), which remained similar to that measured in MQ water (6.3 \pm 1.7 nm). Likewise, the average measurements of the PS nanoparticles and the combination of PS and BSA were unaffected by the medium compared to those in MQ water, as previously reported in [32] (PS: 122.6 ± 0.7 nm; PS + BSA: 128.1 ± 1.1 nm). However, the comparison between the size of the single PS particles and PS in the presence of BSA showed an increase. This result is consistent with the observed variation in the ζ -potential of PS, which became less negative. This consistent finding implies an interaction between the functionalized carboxyl PS beads and BSA, resulting in a less negative charge in both solutions (i.e., MQ water and working solution). It appears that

the foulant combination (i.e., PS+BSA) may behave similarly to a protein corona [166], potentially leading to alterations in the size of individual PS particles.

3.2 Evolution of the permeate flux for single foulant and combined foulants

3.2.1 Fouling phenomena of single PS foulant

Fig. 16 shows the normalized flux decline of the four membranes under study in the present work and the calculated fouling layer thickness from the post-processing of the images while filtering a solution containing PS. It is important to highlight that the permeability values of all the pristine membranes measured with MQ water were similar between each other. Results reveal a consistent pattern, indicating that all normalized membrane fluxes experienced a significant decline. For the three UF membranes sharing similar properties such as MWCO value and surface charge (between -26 and -20 mV), the normalized fluxes exhibited a decline of 43.2%, 45.4 % and 45.3% for PES 30 kDa, RC, and recycled membranes, respectively. This decline can be attributed to the deposition of PS nanoparticles on the membrane surface, blocking the pores and creating a fouling layer that impeded water flux, ultimately reducing it [167]. A previous study by Enfrin et al. [146] examined how NP particles of various sizes interact with a commercial PES-UF membrane. The experimental results showed that the particles adhered to the membrane surface, reducing the water flow through the membrane by up to 38% compared to pure water filtration. The decline in flow was analyzed and found to follow intermediate and complete blocking models. The study identified the membrane-surface properties and surface repulsion as crucial factors affecting its performance during the filtration of NPs [146]. Notably, the performance of the recycled membrane is comparable to that of the commercial ones with the close values of MWCO. In the case of PES 150 kDa, the decline in normalized flux was slightly less, correspondingly to the lowest thickness of the layer observed by OCT (i.e. less deposition of the PS on the membrane surface).

Molina et al. [32] reported the less cake layer formation during filtration experiments in the case of RC membranes, based on post-analysis by SEM and Confocal. The phenomenon was explained based on the hydrophilic characters of the studied membranes (RC and PES). In the current study, real -time observations through OCT reveal that same PS deposition on both RC and PES membranes were obtained (Fig. S5), calculating high thickness values for PS fouling ($28.35 \pm 0.57 \mu m$) on the RC membrane surface. Indeed, the increase of the thickness of the fouling layer formed on the membranes are in concordance with the similar flux decline as shown in Fig. 16 ((a), (b), and (d)). The sequence of the OCT images in Fig. S5 shows the development of the fouling layer obtained on the surface of the studied membranes for 150 minutes.

Since NPs and PES membranes are hydrophobic and negatively charged, attractive polar forces are expected to counterbalance the repulsive electrostatic forces induced by the particles and membrane surface charge [146]. However, upon individual analysis of the cake layer formation observed through OCT, the PES 150 kDa membrane exhibited the lowest thickness values, when compared to the other two PES membranes, the cake layer formed on PES 150 kDa membrane is more than 50% thinner than PES 30 kDa and

Recycled membranes. Interestingly, the ζ-Potential value of PES 150 kDa is the most negative compared to the other membranes (Table 5), suggesting that repulsive electrostatic forces may play a key role in forming a thinner fouling layer on the surfaces of the PES 150 kDa membrane. Similarly, the observable behavior suggests that repulsive electrostatic forces are predominant in forming the thickest fouling layer on the RC membrane surfaces, as it exhibits the least negative zeta potential (Table 5), thus weakening the repulsive electrostatic forces.

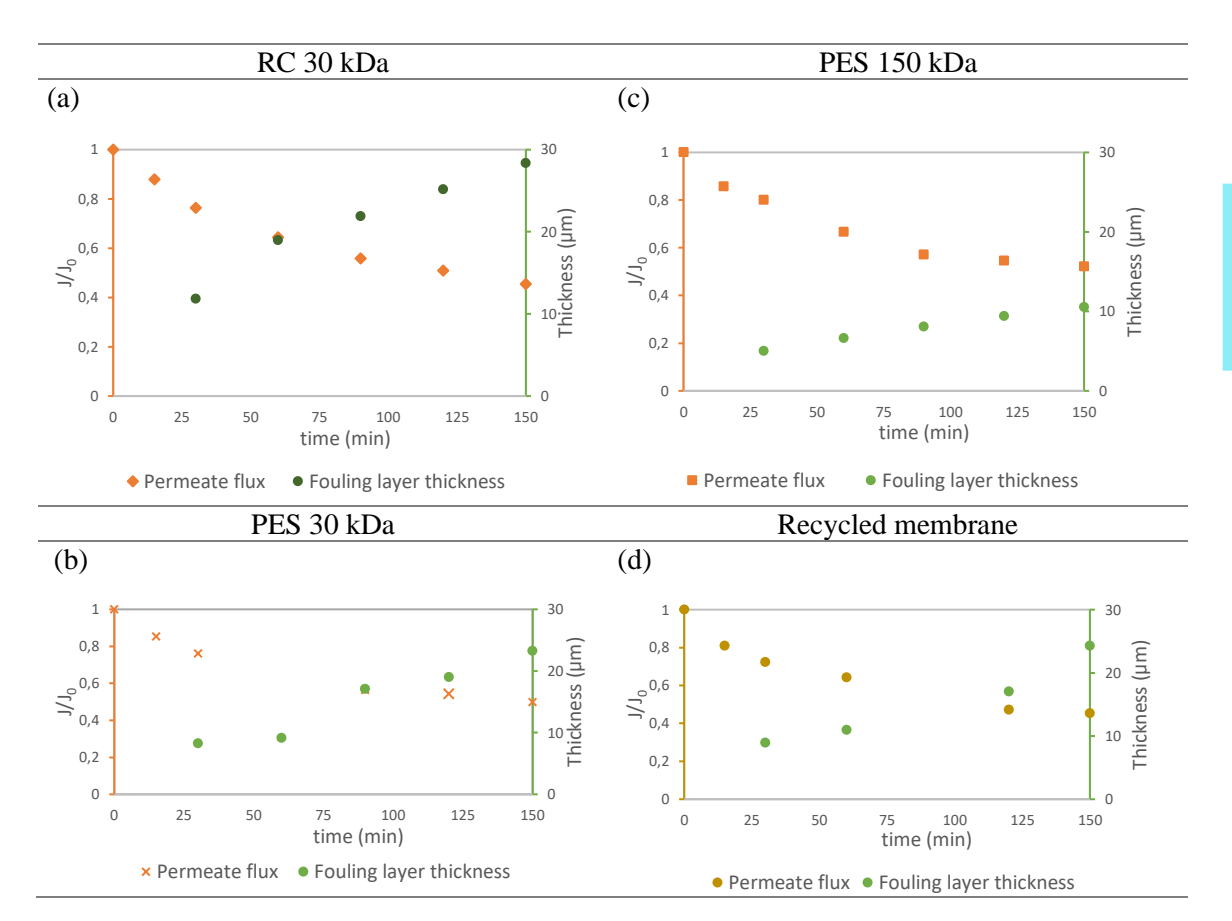


Figure 16. Normalized flux decline behavior of the permeate and fouling layer thickness of (a) RC 30 kDa, (b) PES 30 kDa, (c) PES 150 kDa, and (d) recycled membranes used to treat the solution containing PS.

3.2.2 Fouling phenomena of combined foulants PS and BSA

Fig. 17 shows the normalized flux decline of the four membranes under study in the present work and the calculated fouling layer thickness from the post-processing of the images while filtering a solution containing the combination of PS and BSA.

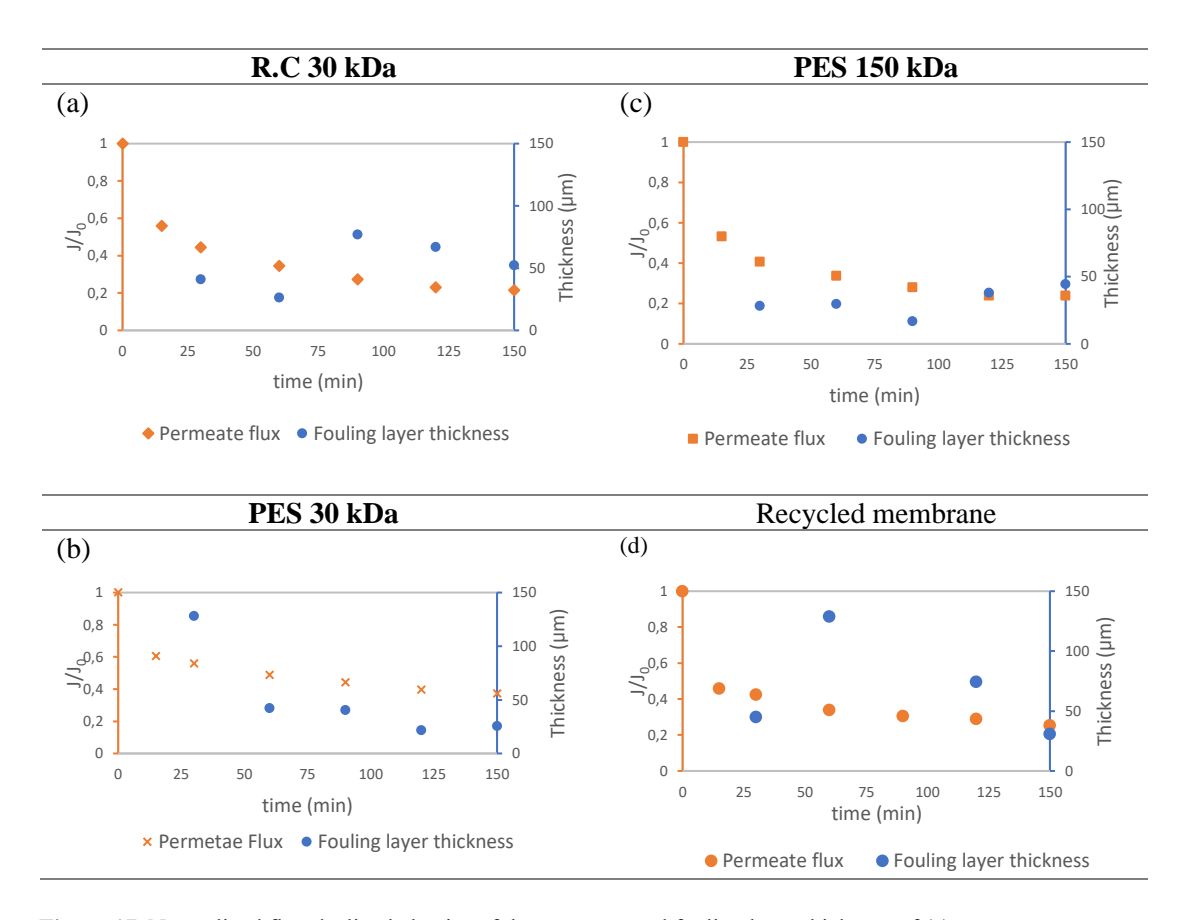


Figure 17. Normalized flux decline behavior of the permeate and fouling layer thickness of (a) RC 30 kDa, (b) PES 30 kDa, (c) PES 150 kDa, and (d) Recycled membrane used to treat the solution containing PS and BSA.

As it can be observed in the images of Fig. 17 and Fig. S6, the presence of BSA caused different fouling formation. Indeed, the characteristics of the fouling layer of the membranes using combined foulants (i.e., PS + BSA) were completely different from characteristics found when having single foulants. Specifically, the combined foulants exhibit both a loose or fluffy-like structure and the formation of flocs or particle agglomerates on the membrane surfaces. Consequently, throughout our discussion, we will reference the observable fouling thickness on the membrane surface. However, it is important to note that a direct correlation between thickness measurements and membrane operation cannot be established.

The loose and unstable cake layer formation observed with the combined foulants (PS + BSA), suggests the interactions between BSA and PS plastics. These interactions alter the NPs surface properties and colloidal stability, consequently obtaining the different type of fouling layer. The flocs and fluffy-like structures could indicate areas with different ratios of PS to BSA. The denser flocs might have a higher concentration of PS particles, while the BSA forms a matrix around them.

Indeed, the interaction mechanisms between PS and BSA were investigated using FTIR spectra, fluorescence spectra, and CD spectra by Guo et al. [166]. They observed and indicated the adsorption and covering of BSA on PS surface to form protein-corona. Furthermore, since BSA is a soluble substance, deposited BSA causes a homogeneous fouling layer with a lower permeability [147]. Consequently, the detrimental effect of the mixed solution of PS and BSA on the normalized flux decline increased.

Fig. 18 represents the summary of the normalized permeate flux declines from the cross-flow filtration of each experiment, including BSA, PS, and the combination of PS and BSA Fig. 18a illustrates that during single BSA filtration, there was a rapid decline in flux at the initial filtration stage. This rapid decline can be attributed to hydrophobic interactions between BSA and the membrane, facilitating rapid binding and attachment of BSA to the PES UF membrane. Consequently, the rapid deposition of BSA on the membrane surface led to pore blockage and a sharp decline in flux at the beginning of filtration, as was explained in [147]. Additionally, BSA molecules displayed a lower negative surface charge in comparison to PS (Fig. 18b), leading to diminished electrostatic repulsion both among BSA molecules themselves and between BSA and the membrane. Consequently, this facilitated the development of a denser BSA layer on the membrane surface, intensifying flux decline and fouling resistance.

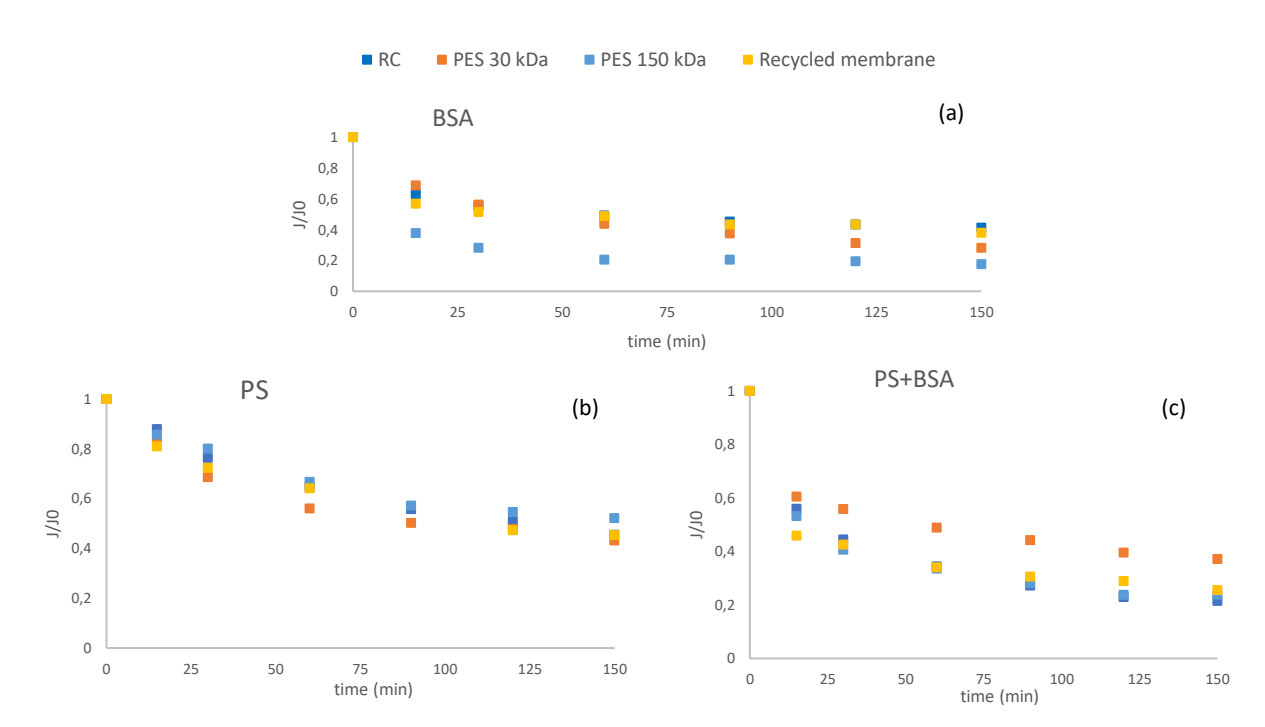


Figure 18. Normalized permeate flux (J/J0) declines from the cross-flow filtration experiments. (a) BSA protein, (b) polystyrene (PS), and (c) combination of PS and BSA.

It can be seen from Fig. 18c that when filtering the combined PS and BSA solution, the flux declined quickly during the initial filtration stage, mirroring the behavior

observed during the filtration of BSA alone. Also, the initial sharp behavior of the flux curve exhibited a pattern similar to that observed with colloidal silica (ranging from 40 to 60 nm) in the study conducted by Contreras et al. [168]. Initially, the flux decreases rapidly due to the effects of concentration polarization, progressing to a slower decrease as a consequence of fouling. This is the usual behavior in UF processes with protein solutions reported in literature [169]. Also, Ayoubian Markazi et. al. [147], suggested that BSA molecules in the combined fouling layer could fill in the macrovoids between the PS, reduce the particle fouling layer porosity, ultimately reducing the normalized flux. However, as it was mentioned earlier, unlike to the case of PS filtration as a single foulant, for the combined PS and BSA solution, no correlation between flux decline and thickness measurements from the OCT scans could be established. This lack of correlation may be attributed to the complex interactions between the foulants (PS and BSA) and the resulting fouling morphology, as described earlier.

3.2.3 Comparison of fouling behavior

In summary, the OCT technique allowed for the observation of the differences in layer formation between two types of foulant. For NPs as a single foulant (PS), the growth of the cake layer along the membrane surface was uniform. As shown in Fig. S5. and Fig. 19, fouling particles were deposited on the membrane surface with equal probability, resulting in a consistent cake layer formation at all points on the membrane surface. The in-situ observations agreed with modeled behaviors of the formation of the membrane fouling layer in presence of PS nanoparticles (mean hydrodynamic diameter 218 ± 12.2 nm) reported by Ayoubian Markazi et al. [147]. The PS particles, due to their larger size than the membrane pores, were entirely rejected, leading to deposition on the membrane surface, pore blockage, and eventual cake layer formation attributed to hydrophobic interactions between PS MNPs and the membrane.

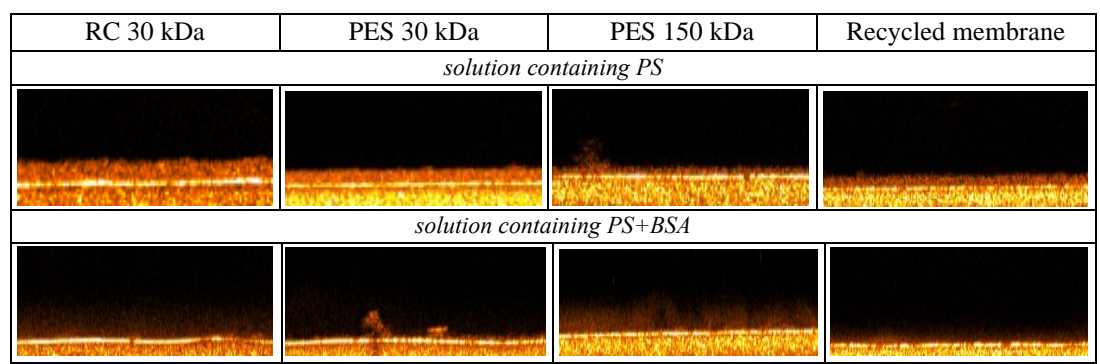


Figure 19. B-scans depicting the fouling on each membrane surface at the end of the experiment (150 minutes). RC 30 kDa, PES 30 kDa, PES 150 kDa, and Recycled membrane, during the filtration of the solution containing PS and PS+BSA, respectively.

In contrast, the PS + BSA fouling exhibited different behavior. Notably, two types of the combined fouling behavior were identified from the OCT scans based on changes in morphology. The first one is characterized by a layer with a loose or fluffy-like structure, while the second type, observed mainly in UF-PES 30 kDa and UF-PES 150

kDa, showed deposition characterized by the appearance of flocs or agglomeration of particles. As depicted in in Fig. 19 and supported by thickness measurements in Fig. 17, the fouling formation in the PS + BSA experiments did not occur in a homogeneous or stable manner.

3.3 Permeability Recovery

Table 6 summarizes the hydraulic permeability recovery after the physical cleaning of studied membranes. The measurements of the permeability after the physical cleaning were conducted with DI water. Since BSA was employed as a model NOM but it is also considered a foulant [170], synthetic solution with BSA was considered as the blank solution to study the interaction between BSA and NPs.

Table 6. Hydraulic permeability recovery (PR) of the UF membranes evaluated with different foulants in the synthetic solution.

Membranes	Solutions	PR (%)	SD
	BSA	79.6	± 6.63
PES 30 kDa	PS	55.38	± 0.18
	PS + BSA	80.86	\pm 13.65
	BSA	70.90	± 3.13
PES 150 kDa	PS	69.54	± 9.94
	PS + BSA	90.33	± 3.21
	BSA	60.72	
Recycled membrane	PS	69.68	± 9.46
	PS + BSA	78.38	± 9.25
	BSA	100	± 8.32
RC 30 kDa	PS	98.80	\pm 18.28
	PS + BSA	114.32	± 11.31

In terms of permeability recovery, there was a loss between 20 to 40% of the initial hydraulic permeability after filtration of 0.1 g L⁻¹ BSA solution trough UF-PES membranes, as it reported in Table 6. It is known that BSA protein has a relatively low free energy of cohesion (i.e., strong BSA-BSA interactions) and adhesion (strong BSA-membrane interactions), which led to aggregation and deposition [171]. In contrast, the hydraulic permeability recovery of RC was 100%. In the case of the RC membranes, the BSA-membrane hydrophobic interaction was weak, which means that the fouling layer deposited on the membrane was reversible. Accordingly, the fouling behavior observed aligns with the finding by Molina et. al. [32], who reported that the fouling layer deposited on the RC membrane was reversible.

On the other hand, Table 6 shows that the permeability recovery was substantially improved for all the studied membranes when PS nanoplastics were mixed with BSA. Therefore, the results show that the combination of NPs and BSA leads to the improvement of the reversibility of the cake layer formation. As it was described above, OCT scans show changes in the morphology of the fouling layer. The presence of BSA

characterized the layer with a fluffy-like structure and with the appearance of flocs, respectively, which enabled the cake layer removal. These results are aligned with the findings reported by Ma et al. [172] and are also in concordance with the results obtained by Molina et al. [32], who reported that the synergetic effect of BSA and PS allows a better dispersion of the nanospheres on the bulk solution, hindering the accumulation of the NPs on the membrane surface. This lack of interaction when only the PS particles were filtered might explain the compacted layer formed (observed by OCT scans) on the membrane surface when the PS nanoplastics were the only foulant present in the solution.

Experimental permeate flux recovery values are further supported by surface characterization through SEM and CLSM. Fig. 20 displays the SEM micrographs and the 3D projections of the studied membranes after conducting the physical cleaning with MilliQ water at the end of the experiments.

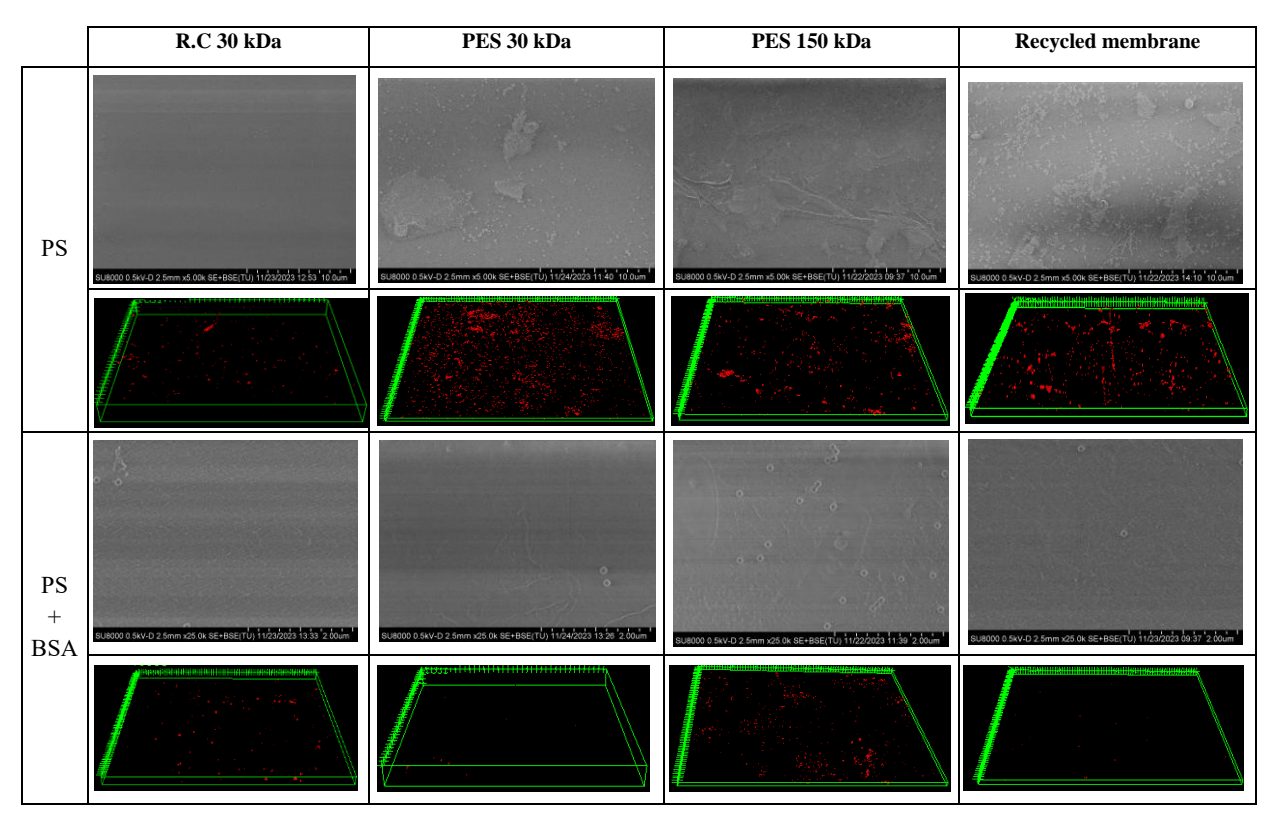


Figure 20. SEM and 3D-projection CLSM images of studied membranes after the physical cleaning of their surfaces with MilliQ Water. The red color in the 3D projections represents the fluorescent PS nanospheres.

In Fig. 20, SEM micrographs and CLSM images reveal that the PS nanoparticles were deposited on the membrane surfaces after the cleaning protocol with Milli Q water. Fig. S7 depicts the SEM micrographs of the pristine surfaces of the studied membranes. Conversely, membranes used to filter the mixture of PS and BSA exhibited a significantly lower deposition of PS nanospheres on their surfaces after the physical cleaning protocol

was conducted. This is in concordance with the higher permeability recovery values obtained in all the studied membranes when PS nanoplastics were mixed with BSA (Table 6).

The impact of PS-induced fouling becomes more noticeable when comparing the membrane materials of regenerated cellulose and polyethersulfone. Specifically, the PS particles remained as a substantial cake layer on the PES membrane surface after the physical cleaning, while the RC membrane showed considerably less PS deposition, aligning with the hydraulic permeability recovery results presented in Table 6. Consequently, the hydrophilic nature of the RC membrane might be the predominant surface characteristic involved in the fouling reversibility.

As previously explained, PES membranes are more hydrophobic than RC membranes, resulting in a stronger interaction with hydrophobic foulants. In the case of the mixed solution containing PS and BSA (Fig. 20, third row), the accumulation of PS nanospheres on the membrane surface of the UF membranes was not highly pronounced. This observation aligns with the OCT images taken during the experimental period, where the possible protein-corona formed by the presence of BSA could lead to the formation of a loose, fluffy-like structure and agglomerates due to the increased steric repulsion between the BSA-coated PS. The complex interaction between BSA and NPs and their deposition on the membrane surface are influenced by factors such as the protein-to-NP ratio, solution composition, and membrane properties [173].

4. Conclusion

The present study aimed to evaluate the fouling behaviors of commercial- and recycled-UF membranes of two different materials (i.e., PES and RC) by filtering synthetic wastewater containing a predefined concentration of PS nanoparticles and the combination of NPs with BSA. OCT was employed to observe fouling layer formation and particle accumulation in situ. While PS created a consistent layer on the membrane, when combining PS and BSA as mixed foulants, OCT observations revealed both types of fouling a loose or fluffy-like structure and flocs or particle agglomeration.

SEM and CLSM microscopy, performed after physical cleaning, corroborated the OCT observations, revealing a thick cake layer remaining from PS particles on membrane surfaces. In contrast, significantly lower PS nanosphere deposition was observed on membranes filtering the PS and BSA mixture, further supporting the hydraulic permeability recovery results.

The importance of membrane material in fouling behavior is highlighted. For our experiments with predefined synthetic water, a combination of PS with BSA mitigated PS deposition. Additionally, the performance of recycled membranes was comparable to commercial ones with similar MWCO, indicating their potential use for preconcentration of nanoparticle-containing samples for subsequent analytic measurements. This practical application offers a cost-effective alternative without compromising treatment efficacy. Further investigations with various concentrations of chemicals are outstanding to substantiate these statements and will be the subject of future studies.

5. Supplementary Materials

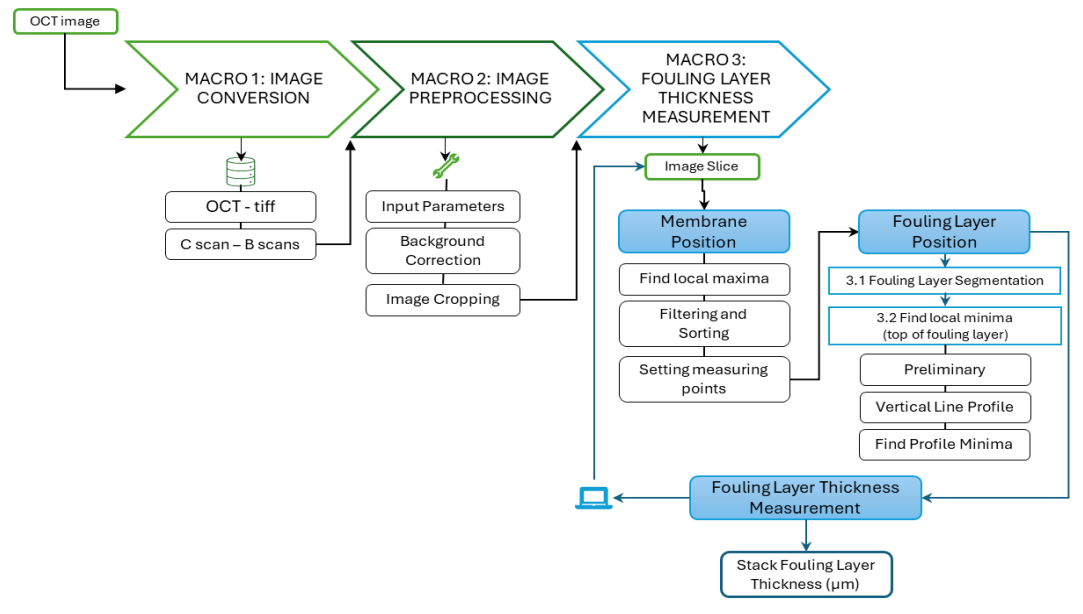


Figure S 3. Fouling Layer Thickness processing workflow in ImageJ software.

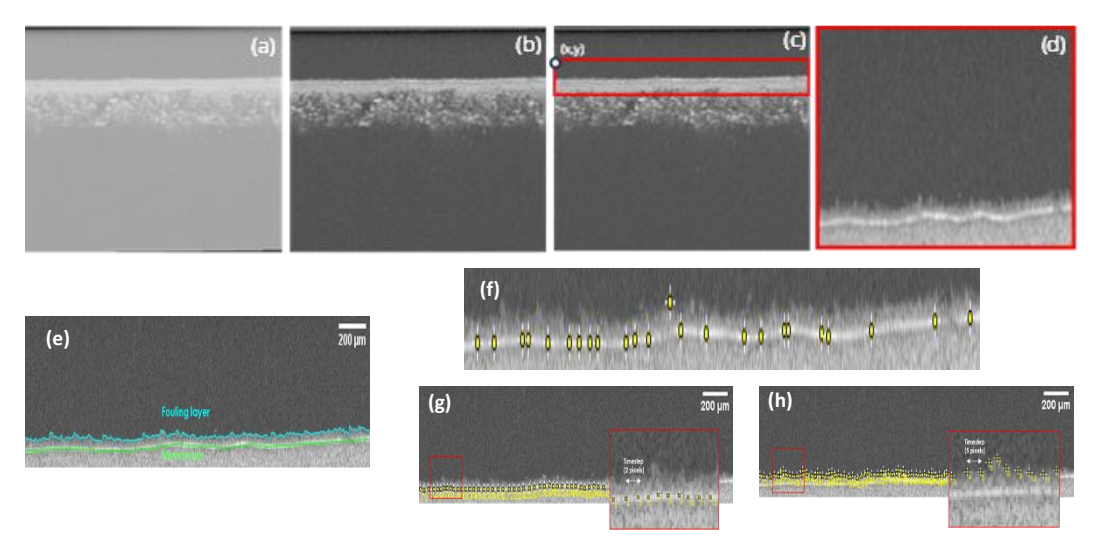
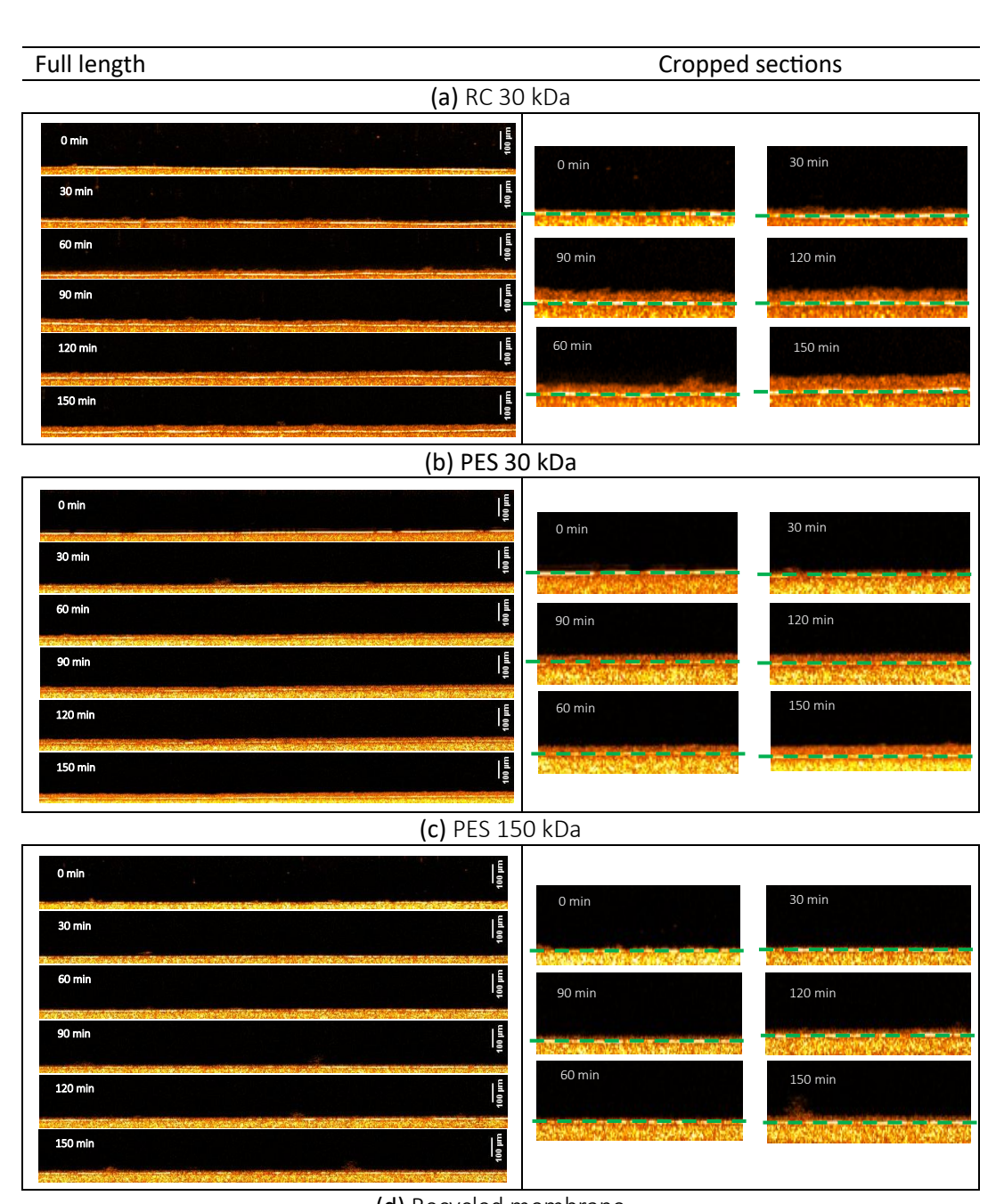


Figure S 4. Image preprocessing steps: Macro 2: (a) Unprocessed OCT image, (b) Background correction, (c) Image cropping, and (d) Final image. Macro 3: (e) Fouling layer (top) and membrane layer (bottom), (f) Local maxima, (g) Membrane measuring and location point with a 2-pixel timestep, and (h) Fouling layer measuring points using local minima with a 2-pixel timestep.



(d) Recycled membrane

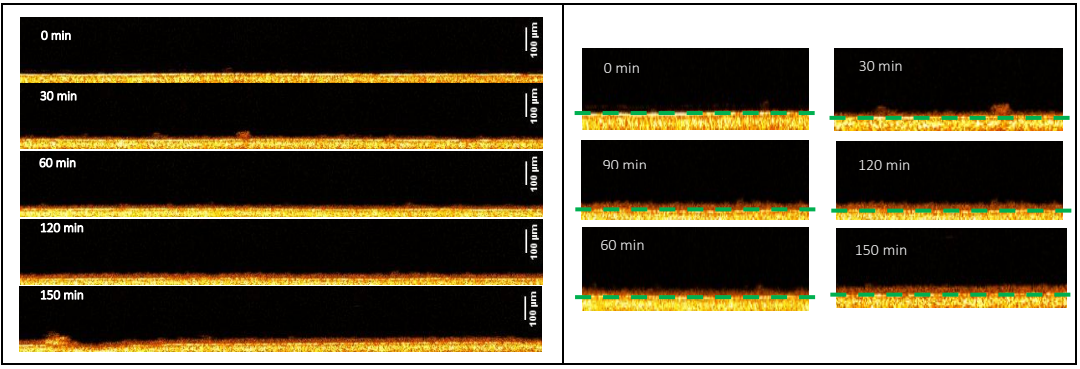
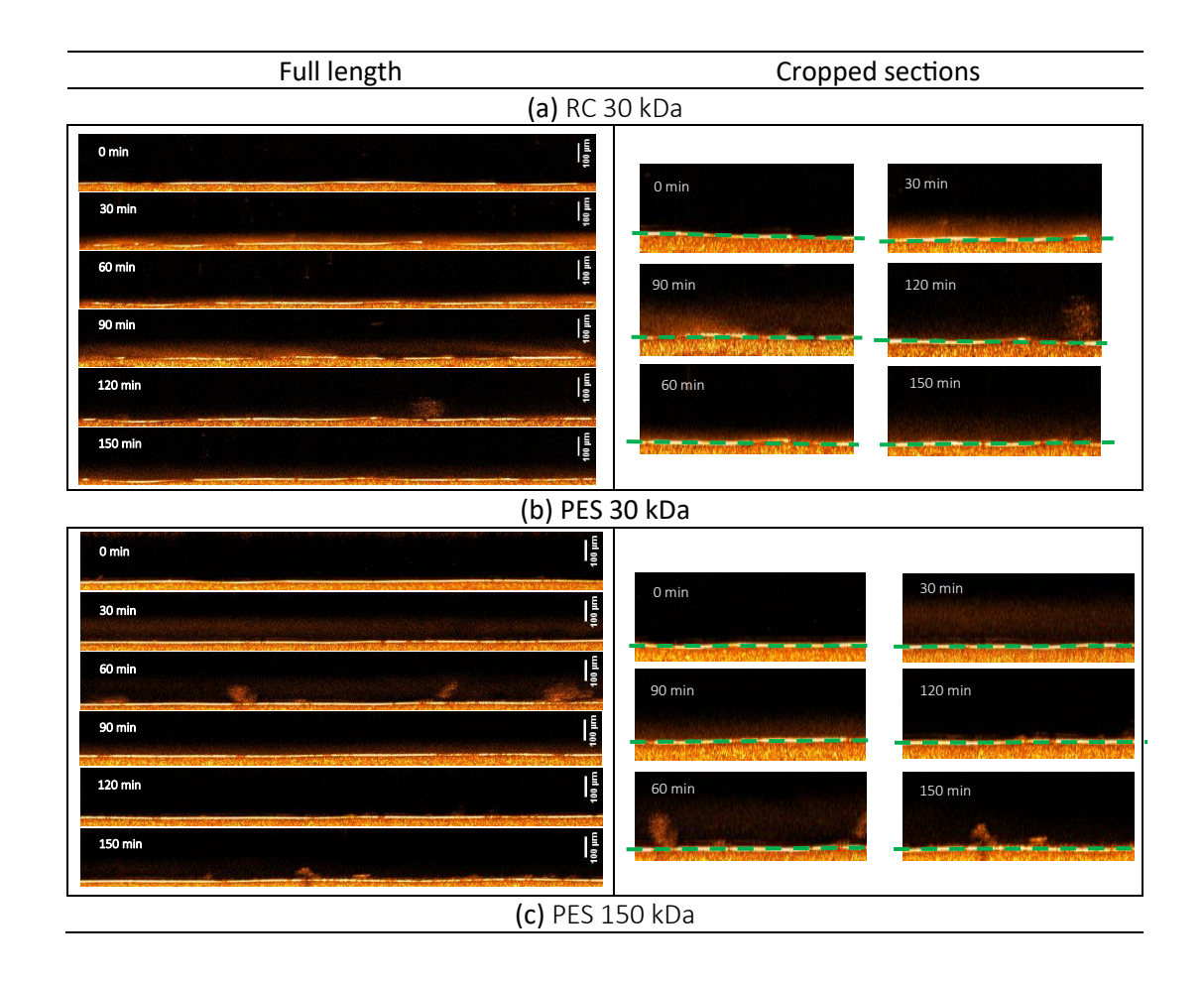


Figure S 5. B-scans depicting the growth of layers on each membrane surface at different time points throughout the experiment. (a) RC 30 kDa, (b) PES 30 kDa, (c) PES 150 kDa, and (d) Recycled membrane, during the filtration of the solution containing PS. The cropped images contain a straight green discontinuous line representing the membrane surface.



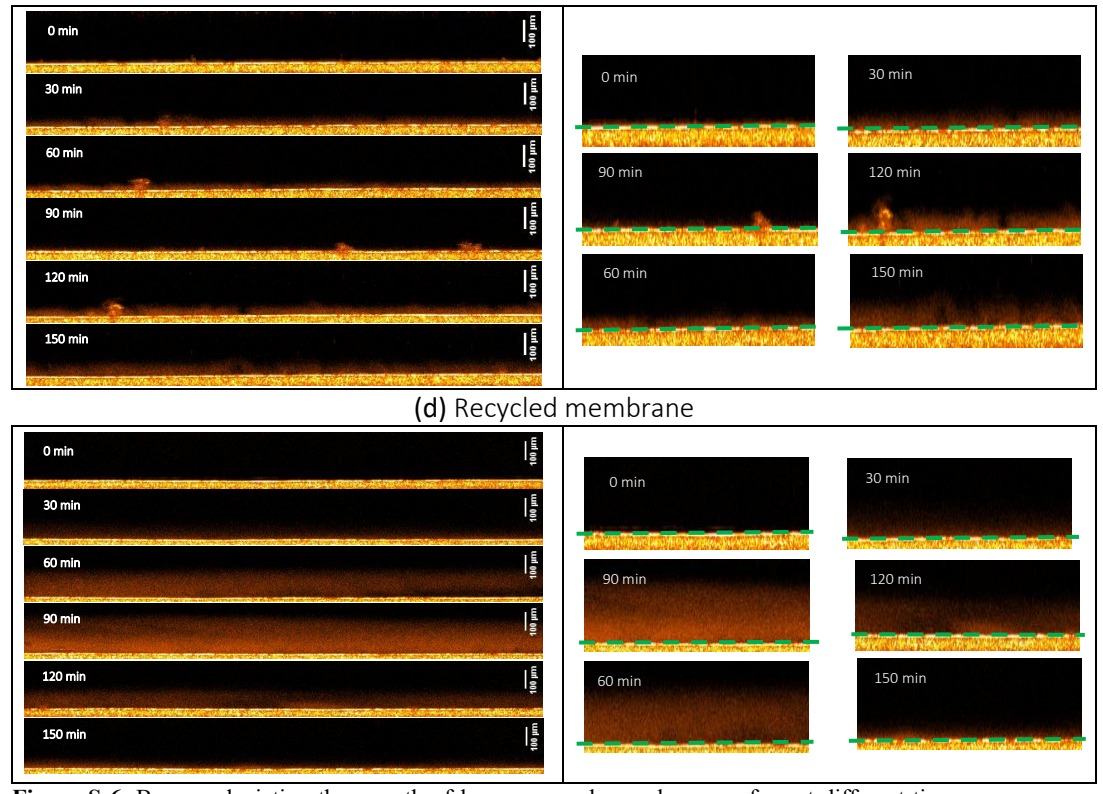


Figure S 6. B-scans depicting the growth of layers on each membrane surface at different time points throughout the experiment. (a) RC 30 kDa, (b) PES 30 kDa, (c) PES 150 kDa, and (d) Recycled membrane, during the filtration of the solution containing PS and BSA. The cropped images contain a straight green discontinuous line representing the membrane surface.

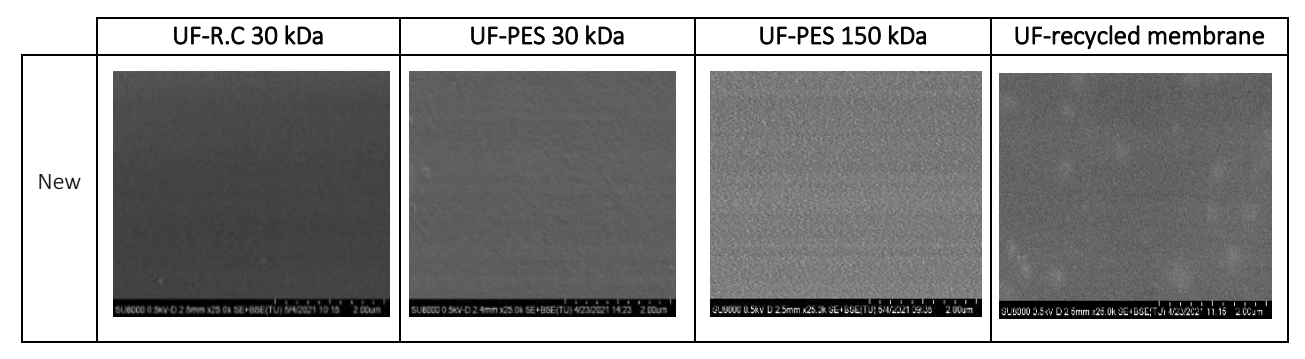


Figure S 7. SEM images of pristine membranes. SEM image of PES 30 kDa was taken from [13].





Treatment of Synthetic Wastewater Containing Polystyrene (PS) Nanoplastics by Membrane Bioreactor (MBR): Study of the Effects on Microbial Community and Membrane Fouling

Anamary Pompa-Pernía 1,2,*, Serena Molina 10, Laura Cherta 1, Lorena Martínez-García 1 and Junkal Landaburu-Aguirre 100

- IMDEA Water Institute, Avenida Punto Com, 2, Alcalá de Henares, 28805 Madrid, Spain; serena.molin@indea.org (S.M.); laura.cherta@imdea.org (L.C.); lorena.martinez@imdea.org (L.M.-G.); junkal.landaburu@imdea.org (J.L.-A.)
 Chemical Engineering Department, University of Alcalá, Ctra. Madrid-Barcelona Km 33.600,
- Alcalá de Henares, 28871 Madrid, Spain

 * Correspondence: anamary.pompa@imdea.org

CHAPTER V: Emerging pollutants removal from urban wastewater: study of Membrane Bioreactor.







Article

Treatment of Synthetic Wastewater Containing Polystyrene (PS) Nanoplastics by Membrane Bioreactor (MBR): Study of the Effects on Microbial Community and Membrane Fouling

Anamary Pompa-Pernía 1,2,*, Serena Molina 1, Laura Cherta 1, Lorena Martínez-García 1 and Junkal Landaburu-Aguirre 1

- ¹ IMDEA Water Institute, Avenida Punto Com, 2, Alcalá de Henares, 28805 Madrid, Spain;
- ² Chemical Engineering Department, University of Alcalá, Ctra. Madrid-Barcelona Km 33.600, Alcalá de Henares, 28871 Madrid, Spain

*Correspondence: anamary.pompa@imdea.org

Citation: Pompa-Pernía, A.;
Molina, S.; Cherta, L.; Martínez-García, L.; Landaburu-Aguirre, J.
Treatment of Synthetic
Wastewater Containing
Polystyrene (PS) Nanoplastics by
Membrane Bioreactor (MBR):
Study of the Effects on Microbial
Community and Membrane
Fouling. Membranes 2024, 14, 174.
https://doi.org/10.3390/membran
es14080174

Academic Editor(s): Silvia Álvarez Blanco, Carmen M. Sánchez-Arévalo and José Antonio Mendoza-Roca

Received: 8 July 2024 Revised: 2 August 2024 Accepted: 3 August 2024 Published: 9 August 2024



Copyright: © 2024 by the authors. Submitted for possible open access publication under the terms and conditions of the Creative Commons Attribution (CC BY) license (https://creativecommons.org/licenses/by/4.0/).

Abstract: The persistent presence of micro- and nanoplastics (MNPs) in aquatic environments, particularly via effluents from wastewater treatment plants (WWTPs), poses significant ecological risks. This study investigated the removal efficiency of polystyrene nanoplastics (PS-NPs) using a lab-scale aerobic membrane bioreactor (aMBR) equipped with different membrane types: microfiltration (MF), commercial ultrafiltration (c-UF), and recycled ultrafiltration (r-UF) membranes. Performance was assessed using synthetic urban wastewater spiked with PS-NPs, focusing on membrane efficiency, fouling behavior, and microbial community shifts. All aMBR systems achieved high organic matter removal, exceeding a 97% COD reduction in both the control and PS-exposed reactors. While low concentrations of PS-NPs did not significantly impact the sludge settleability or soluble microbial products initially, a higher accumulation increased the carbohydrate concentrations, indicating a protective bacterial response. The microbial community composition also adapted over time under polystyrene stress. All membrane types exhibited substantial NP removal; however, the presence of nanosized PS particles negatively affected the membrane performance, enhancing the fouling phenomena and increasing transmembrane pressure. Despite this, the r-UF membrane demonstrated comparable efficiency to c-UF, suggesting its potential for sustainable applications. Advanced characterization techniques including pyrolysis gas chromatography/mass spectrometry (Py-GC/MS) were employed for NP detection and quantification.

Keywords: activated sludge; membrane bioreactor; membrane fouling; microfiltration; microbial community; nanoplastics; Py-GC-MS; ultrafiltration recycled membrane

1. Introduction

The widespread use of plastics has led to a global pollution crisis, with detrimental impacts on ecosystems. Of particular concern are micronanoplastics (MNPs), raising questions about their effects on aquatic environments and the need for effective mitigation strategies [174]. MNPs are classified as primary (intentionally manufactured) or secondary (formed from the breakdown of larger plastics). Regarding their sizes, MPs are fragments smaller than 5 mm, and nanoplastics (NPs) are particles with a size ranging from 1 to 1000 nm [175].

Even though WWTPs exhibit a notable capacity to eliminate a significant proportion of MPs, with a retention rate ranging from 98% to 99% [20–22], they persist as the primary pathway through which MPs reach the environment. This is largely attributable to the massive volume of effluent discharged by WWTPs [23]. Moreover, it is expected that the weathering of macroplastics and MPs will generate secondary NPs, although there is no available data on the environmental loads of NPs [140]. This lack of information regarding the presence of NPs in the environment is especially concerning because studies have reported that nanosized particles primarily induce more toxicity in aquatic and terrestrial animals compared to larger particles [27]. Additionally, investigations show that NPs in urban waters differ from MPs in terms of their analytical challenges, transport properties, interactions with pollutants, bio-effects, and removal behavior [176].

In the search for more effective wastewater treatment solutions, membrane-based advanced technologies for wastewater treatment, such as membrane bioreactors (MBRs), have emerged as promising competitors. Along with the removal of advanced levels of organic and suspended solid particles, MBRs are also effective in the removal of MPs. MBRs have been demonstrated to reach a removal capacity of 99.9 % of MPs (> 20 μ m) [177]. While MBR systems were neither initially designed for the removal of MPs, their remarkable efficiency in removing them can be attributed to the synergy between the entrapment of MPs in the suspended sludge flocs and the sieving action of the membrane within the reactor [177,178].

With the demonstrated effectiveness of MBRs in removing MPs, it is highly important to take one further step in the implementation and assessment of MBR for the removal of NPs from wastewaters. Previous studies have shown that 99% of NPs were retained in the sludge during the activated sludge process of a municipal WWTP, highlighting that NPs form aggregates with the suspended solids found in the system [179]. Since MBRs also work with activated sludge, it is reasonable to hypothesize that MBR systems could effectively remove NPs. However, to the knowledge of the authors, no research has been conducted on the impact of NPs in MBR systems thus far.

Interestingly, the review articles focused on studies on MBR for MNPs removal, exclusively cited literature related to MPs [20,180,181]. In the work by Sutrisna et al. [180], a section is dedicated to reviewing studies on the effects of MPs and NPs on MBR. However, a closer look reveals that all the listed references concentrate solely on the potential use of MBR for the removal of MPs from water and wastewater. Concerning NPs, the review only briefly touches on their biodegradability without

addressing MBR efficiency. In fact, Sutrisna et al. [180] concluded that it is crucial to investigate the effects of NPs within the MBR unit, as the presence of these particles could potentially have both positive and negative impacts on MBR operation. On the other hand, MNPs can induce oxidative damage to microbes, disrupt cell membrane integrity, inhibit sludge activity, and reduce the abundance of crucial microbes. This can alter the composition and distribution of extracellular polymeric substances (EPS) and hindering sludge dewatering, according to the authors of reference [182]. Alvim et al. [183] studied the influence of 100 nm PS-NPs (10 μ g L $^{-1}$) on microbial community composition and activity of activated sludge and the quality of the final effluent at a sequencing batch reactor (SBR) over 63 days. The authors reported no damage of the activated sludge process under the proposed experimental conditions, meaning that NPs did not modify the global process. However, Zhou et al. [184] found that a high concentration (1000 μ g/L) of NPs decreased nitrogen removal efficiency by activated sludge in the SBR.

The evaluation of the removal capacity of NPs by advanced water treatment technologies has been limited due to the lack of standardized methods for sampling, identification, and quantification of NPs from wastewater [182]. The detection and quantification of NPs presents unique challenges due to their extremely small size. While techniques such as microscopy, spectroscopy, and dynamic light scattering (DLS) are valuable for qualitative analysis, there remains a need for improved sensitivity and standardization of methods [28]. Commonly used techniques for MPs include vibrational spectroscopic methods (FTIR or Raman spectroscopy) for identification and semi-quantification of MPs [29]. These methods can be used to collect appropriate parameters because of the availability of multi-analysis. However, they are limited in that they do not detect particles smaller than 20 μ m [30], which is a significant limitation for characterizing and semi-quantifying NPs.

To overcome these limitations, researchers are exploring the potential of thermal degradation-based technique such as Pyrolysis Gas Chromatography-Mass Spectrometry (Py-GC-MS), combined with preconcentration strategies that leverage membranes to isolate and enrich NPs from environmental matrices [31]. Membrane technology plays a crucial role in these preconcentration processes by selectively filtering out larger particles and concentrating the smaller NPs, making subsequent analysis more accurate and reliable [32].

In the context outlined above, the present research seeks to enrich the understanding of the treatment of wastewater containing PS-NPs using a lab-scale MBR. This study will examine the shift in microbial community composition and the behavior of membrane fouling in an aerobic MBR. The operational behavior of a microfiltration membrane and two ultrafiltration membranes, including a recycled one, will be compared in the presence of NPs. Finally, the semi-quantification of the PS-NPs in both permeates and activated sludge samples will be analyzed by Py-GC-MS after their chemical pretreatment. By addressing this critical research gap, our investigation aspires to offer insights into the challenges posed by NPs, contributing to strategies for minimizing their environmental impact.

2. Materials and Methods

2.1. Chemicals

Chemicals used for the preparation of synthetic urban wastewater were glucose $((C_6H_{12}O_6)D(+))$ glucose anhydrous, extra pure, Ph Eur, BP, USP), meat peptone, urea (urea reagent grade ACS, sodium chloride (NaCl reagent grade, ACS, ISO, Reag. Ph Eur), sodium bicarbonate (NaHCO₃, extra pure, Pharmpure®, Ph Eur, BP, USP), dipotassium hydrogen phosphate anhydrous (K_2HPO_4 for analysis, ExpertQ®, ACS, Reag. Ph Eur), calcium chloride dihydrate ($CaCl_2.2H_2O$ powder, for analysis, ExpertQ®, ACS), and magnesium sulfate heptahydrate ($MgSO_4.7H_2O$ for analysis, ExpertQ®, ACS, Reag. Ph Eur) supplied by Sigma-Aldrich, Spain. The chemical used for membrane transformation and membrane cleaning was sodium hypochlorite (NaClO~10%~w/v).

The nanoparticles used were PS fluorescent carboxylate with a 116 ± 2 nm size and $\lambda_{ex.} / \lambda_{em.}$: 576 nm/596 nm. These nanoparticles, purchased from IKERLAT Polymers, Spain, are standard, perfectly dispersed, and stable in water.

2.2. Membranes

Three flat sheet membranes were investigated in the current study: (i) a microfiltration (MF) membrane (nominal pore size of 0.4 μ m), (ii) commercial ultrafiltration membrane UF-PES 150 kDa-Microdyn (c-UF), and (iii) recycled ultrafiltration (r-UF) membrane. It should be noted that all the membrane tests only related to a single run. The membrane characteristics are summarized in Table 7. The nominal molecular weight cut-off (MWCO) values were measured by size exclusion chromatography. The MWCO was defined as the corresponding molecular weight with a retention coefficient of 90%. An Agilent Technologies 1260 Infinity GPC/SEC System with a column from Polymer Labs (PL MIXED aqua gel-OH) with a nominal pore size of 8 μ m was used. Milli-Q water was used as the eluent with a 1 mL min⁻¹ flow rate. The calibration was carried out with narrow standards of PEOs with molecular weights between 194 and 490,000 Da. The feed solution contained PEOs ranging from 103 to 105 g mol⁻¹, keeping the total concentration of 1 g L⁻¹ following the composition reported elsewhere [78,164].

Table 7. Technical data of the studied membranes.

Manufacturer					
Membranes	Material	Nominal Pore Size	Nominal MWCO (Da)	Nominal MWCO (Da)	
MF	Chlorinated polyethylene	0.4 μm			
r-UF	Polyethersulfone	12 nm [25]		30,000	
c-UF	Polyethersulfone	<30 nm	150,000	90,000	

The r-UF membranes were obtained by eliminating the polyamide layer of the End-of-Life (EoL) reverse osmosis (RO) membranes through exposure to a NaClO dose of 500,000 ppm·h at a pilot scale, following the procedure proposed by García-Pacheco et al. [79]. Furthermore, aligning with the principles of the circular economy [161], the study will explore the potential of recycled membranes in MBRs – a field supported by existing research that demonstrates their feasibility and even suggests potential advantages in fouling reduction [83].

2.3. Aerobic Membrane Bioreactor (aMBR) System

Two systems of submerged-membrane configuration were employed in parallel. The experiments were carried out on a lab scale aMBR at continuous flow. Each aMBR tank had a working volume of 30 L and an effective membrane area (flat sheet membrane module) of 0.11 m². One MBR was used as the control (aMBR-Control) (i.e., without the addition of PS nanospheres), and the other with spiked PS nanospheres (aMBR-PS) (Figure 21). The feed stream used was synthetic wastewater simulating urban wastewater (0.4–0.5 g/L COD), as reported elsewhere [85]. The aMBR feeding was performed by a peristaltic pump (type PPR, SEKO SpA, Barcelona, Spain), and a piston pump FMI (Fluid Metering Inc., Syosset, NY, USA) was used for constant flux operation, whereas a pressure transducer recorded the temporal evolution of the TMP. The reactors were automatically controlled. A pH meter with an integrated temperature sensor (713-type pH meter, Metrohm Ltd., Herisau, Switzerland) was used to monitor the pH and temperature of the bioreactor. The oxygen was supplied by air diffusers positioned at the bottom of the tanks to supply the oxygen required by the biomass and avoid the formation of dead zones by acting like the stirrer system.

The laboratory-scale aMBR unit was operated at a hydraulic retention time (HRT) of 15 h and the sludge retention time (SRT) was considered infinite since no purge was conducted during the experimental time. Regular measurements of pH, EC, and DO were performed to ascertain that the aMBRs operated under the same conditions. The activated sludge used was taken from the urban WWTP Guadalagua, located in Guadalajara, Spain. Specifically, the samples were collected from the recirculation stream to ensure higher total suspended solid (TSS) concentration values than those from the biological reactor. Prior to starting the experiment, the microbial community was acclimatized for almost 80 days, which ensured that pseudo-steadystate conditions were achieved. The average values remained at 7.86 ± 0.21 pH and $501 \pm 0.12 \,\mu\text{S/cm}$ in the case of EC. DO concentration in the bioreactor was measured by an oxygen probe (Z921, Consort). A steady-flux value of 18 LMH was employed, whereas the membrane operation was set on cycles of 8 min of suction followed by 2 min of relaxation. The aMBR permeate was analyzed twice a week (i.e., BOD₅, COD, TN, and TOC) as described in Section 2.4. With the same frequency, the characterization of the mixed liquor properties was conducted (i.e., floc macroscopy by V-30 test, floc microscopy by an optic microscope, and MLSS determination).

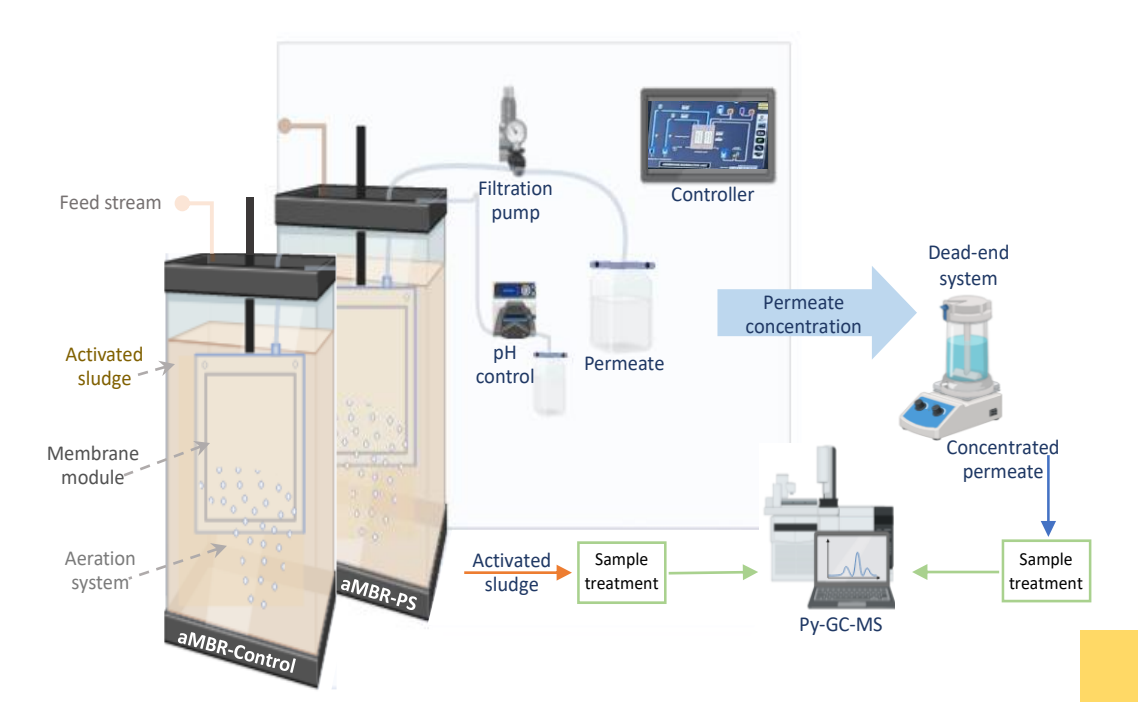


Figure 21. Representation of the experimental setup.

The PS nanoparticle (116 \pm 2 nm) was chosen as PS has been identified as one of the predominant plastic polymers found in marine environments [140]. Moreover, it is often chosen as a representative for studying the absorption and biotoxicity of MNPs in marine organisms [185]. Thus, the standard (20 g/L) of PS was added directly to the mixed liquor (i.e., NPs were added manually to the reactor to prevent their loss through the pump and tubing system). The addition was conducted daily during the first two weeks to reach a 20 mg/L concentration in the reactor (stage I). Thereafter, the addition was stopped for one week. Later, from day 21., the concentration of spiked PS was increased for the following week (stage II) to assess the eventual effects of an abrupt increase in NP concentration (up to 60 mg/L) on the MBR system. Finally, the MBR was operated under the total accumulated concentration from the two spiked stages for 5 more weeks without any other PS addition to evaluate the performance of different membranes under the same concentration of NPs. The MF membrane was used for the initial 39-day experiment. Following this, UF membranes (i.e., c-UF and r-UF) were tested individually for two weeks each.

2.4. Permeate and Sludge Characterization

2.4.1. Analytical Methods for Wastewater Parameters

The main parameters for wastewater analysis were measured according to standard methods [186] that included EC, pH, BOD₅, COD, TOC, TN, and MLSS. The conductivity values of the solutions were measured by a CM 35 conductivity meter

(Crison Instrument, Barcelona, Spain). TOC was measured by a TOC analyzer (TOC-5000A, Shimadzu Co., Japan). TN was determined colorimetrically (UV-1700 Spectrophotometer, Shimadzu Co.) after sample digestion using sulfuric acid/peroxodisulfate and alkaline potassium persulfate, respectively. MLSS was measured by filtration on a Whatman GF/A microfiber glass filter (1.6 µm nominal pore size). The sludge volumetric index (SVI) was calculated following Equation (7).

$$SVI = \frac{V_{30} \left[\frac{ml}{L}\right] * 2^{(n)}}{MLSS \left[\frac{g}{L}\right]}$$
 (7)

where V_{30} is the volume of settled mixed liquor measured at 30 min and n is the dilution number of the mixed liquor.

Data were analyzed statistically using a statistical significance level of 0.05 by T-test analysis.

2.4.2. Microbial Community Analysis and SMP

DNA from the MBR samples was extracted using a FastDNA SPIN® Kit for soil (MP Biomedicals,Madrid, Spain), according to the protocol from the manufacturer (FastDNATM Spin Kit for Soil DNA Extraction | MP Biomedicals, n.d.). DNA from all samples was extracted twice, obtaining 100 µL as the final volume. Inhibitors in the sample were removed by employing a One-Step PCR Inhibitor Removal Kit (Zymo Research, Irvine, CA, USA). DNA concentration was measured using the Qubit® dsDNA BR Assay Kit (Molecular probes, Eugene, OR, USA), and the absorbance rate (260/280 nm) was measured with a NanoDrop ND-1000 UV/Vis spectrophotometer (Thermo Fisher Scientific, DE, Waltham, USA). DNA samples were sequenced for V4 16S rRNA gene amplification using the primers 515F–806R. The subsequent amplicon sequencing was conducted on the Illumina Miseq platform.

To obtain the SMP in terms of carbohydrates and proteins, the mixed liquor samples were centrifuged at 15,000 rpm for 10 min at 4 °C. Later, the liquid part was filtered with a $0.45~\mu m$ filter size of cellulose acetate to obtain the soluble portion. To determine the carbohydrate concentration, the anthrone method [187] was employed. Protein concentrations were determined following the bicinchoninic acid (BCA) method [188].

2.4.3. Semi-Quantification of PS Nanoplastics by Pyrolysis Gas Chromatography-Mass Spectrometry (Py-GC-MS)

Sampling and Sampling Treatment

Activated sludge samples were collected once per week. To ensure representative sampling of the activated sludge, a sampler was utilized to take samples from the middle of the reactors. A volume of 10 mL of mixed liquor was treated prior to the analysis by applying a peroxidation process. The peroxidation reaction was

conducted with 10 mL of the sample (mixed liquor) and 20 mL of peroxide (H_2O_2 , 30% wt) for 4 h at a temperature of 60 °C, following the methodology outlined in a previous study by Bretas Alvim et al. [189]. Subsequently, the digested sample was vacuum filtered using alumina filters (AnodiscTM 47 mm, 0.02 μ m), and the filter was then dried at 50 °C in a laboratory oven for 1 h. Finally, the dried filter was milled in a ball mill for two minutes at 30 Hz and an aliquot of 1 mg was taken for Py-GC-MS analysis.

Permeate samples were also collected once per week. The analyzed volume of the different permeate samples ranged from 100 to 500 mL, which had been preconcentrated from an initial volume of 5 to 8 L. The pre-concentration process was carried out in a dead-end system with regenerated cellulose (RC, 30 kDa) membranes, as shown in Figure 21. The RC membrane was chosen due to the results obtained in previous studies [32] that showed fouling remotion and permeability recovery values up to 100%. The pre-concentrated permeate samples were also chemically digested by peroxidation reactions in a ratio of 100:1 (permeate sample: H₂O₂, 30% wt) for 2 h at a temperature of 60 °C following the same methodology by Bretas Alvim et al. [189]. The subsequent steps after digesting the sample were identical to those described for the mixed liquor (vacuum filtering, drying, and milling).

Identification and Semi-Quantification

A pyrolyzer 6200 (CDS Analytical) coupled to a gas chromatography-mass spectrometer (7890B and 5977B MSD, Agilent Technologies) was used for plastic identification and semi-quantification. Pyrolysis was performed at a temperature from 150 to 600 °C (1 min). The transfer line until the gas chromatograph was maintained at 300 °C. The GC injector operated in split mode with a 100:1 ratio at a temperature of 300 °C. Pyrolysis products were separated using He (1.5 mL/min) as the carrier gas in the HP-5 capillary column (30 m length \times 0.32 mm i.d. \times 0.25 μ m film thickness; Agilent). The GC oven program was as follows: 2 min at 40 °C, then increased up to 325 °C at 10 °C/min and held for 2 min. The GC-MS interface temperature was fixed at 280 °C. The mass spectrometer operated under electron ionization mode (70 eV); the source temperature was kept at 230 °C. The acquisition was performed under scan mode ranging from 40 to 400 m/z. The pyrolytic products used as indicators of the presence of PS are indicated in Table 8 including the most specific m/z ions selected for each compound.

Table 8. Characteristic pyrolytic products obtained for polystyrene and m/z ions selected as indicators for each peak.

Polymer	Pyrolytic Products	Indicator Ions (m/z)
PS	Styrene *	104, 78, 51
13	3-Butene-1,3-diyldibenzene (Styrene dimer)	91, 104, 130

91, 117, 194

* Compound used for quantification.

Although it is known that styrene can be generated from other sources, it was selected as the quantifying peak in this study as the recoveries in the real samples were satisfactory (see Supplementary Materials S2).

The quantification of polymers was conducted by injecting calibration curves using specific standards. The description of the preparation of the standards and validation of the method is given in Supplementary Materials S2. The limit of detection and quantification (LOD and LOQ) were defined according to the matrix (activated sludge and permeate) and the volume treated, also referred to in Supplementary Materials S2.

The treatment and analysis of both types of samples were conducted under strict protocols to avoid cross-contamination and altered results (see Supplementary Materials S1).

2.5. Membrane Characterization

2.5.1. RIS Analysis

To understand the fouling mechanism during the studied processes, the resistance-in-series (RIS) analysis was realized following the model proposed by [190]:

$$R_t = \frac{TMP}{J\,\mu} \tag{8}$$

where J is the permeate flux of the fouled membrane [m³ m⁻² s⁻¹], TMP is the transmembrane pressure [Pa], and μ is the permeate viscosity [Pa s] at the operating temperature. By the end of the studied period, the membranes were removed from the bioreactor and physically cleaned by rinsing with tap water and soft mechanical cleaning following the procedure of Rodríguez-Sáez et al. [85]. The cleaned membrane was then immersed in clean water and exposed to the same operational filtration conditions as during the experiment in order to measure the resistance to filtration in clean water ($R_{t.c.w}$):

$$R_{t,cw} = \frac{TMP_{cw}}{J_{cw} \,\mu} \tag{9}$$

where J_{cw} is the permeate flux of the cleaned membrane [m³ m⁻² s⁻¹] measured with clean water, TMP_{cw} is the transmembrane pressure [Pa], and μ is the permeate viscosity [Pa s] at the operating temperature.

The total resistance is expressed as follows in Equation (10):

$$R_t = R_m + R_{pb} + R_c \tag{10}$$

where R_m , R_{pb} , and R_c represent the membrane, the pore blocking, and cake layer resistance contributions, respectively. The total resistance $R_{t,cw}$ during clean water operation can be expressed as (Equation (11)):

$$R_{t,cw} = R_m + R_{nh} \tag{11}$$

Fouling resistance (R_f) is defined as the total fouling resistance excluding the membrane resistance R_m (Equation (12)):

$$R_f = R_c + R_{pb} \tag{12}$$

2.5.2. Scanning Electron Microscopy (SEM)

Scanning electron microscopy (SEM) using the S-8000 Model (Hitachi) image device was employed to observe the morphology of the membrane surfaces and the fouling degree of the studied membranes after the physical cleaning of the membranes at the end of the experiment. Preceding the microscopy analysis, the membrane samples were dried by heating at $50\,^{\circ}\text{C}$ for $48\,\text{h}$.

2.5.3. Confocal Laser Scanning Microscopy (CLSM)

The membranes were also observed under a confocal laser scanning microscope (CLSM Leica SP5, Leica Microsystems). Each membrane was cut into pieces of 5 mm \times 5 mm (i.e., the membrane from the MBR-Control system and the other from the MBR-PS system) and three different areas were examined. The resulting images were analyzed by ImageJ software (Version 1.51n). The 3D projection images of the particles were constructed by the ImageJ 3Dviewer plugin.

3. Results

3.1. Activated sludge

3.1.1. Changes to Settleability of Sludge and SMP

MLSS and SVI were measured periodically to characterize the settleability capacity of the sludge. SVI values were calculated with n = 3 (i.e., a dilution 1:3 of mixed liquor: permeate water) to obtain representative values (i.e., values below 400 mL/g MLSS). The SVI decreased from 218.3 mL/g MLSS (day 1) to 199.2 mL/g MLSS (day 39) in the MBR-Control, while the SVI in the MBR-PS decreased from 206.2 mL/g MLSS (day 1) to 202.9 mL/g MLSS (day 39). Even though the variation in SVI in MBR-PS was <2% compared to <9% in the MBR-Control, which might have been influenced by the plastic mass accumulation in the reactor, the results showed that the presence of polystyrene nanospheres in the mixed liquor did not significantly affect the settleability in terms of the volumetric index. This is in concordance with results obtained for the low concentration of nano-sized PS (213.7 \pm 1.7 nm) by Xu et al. [191]. However, physical changes such as a variation in the color were observed since the employed PS nanospheres had a fluorescent dye

incorporated in the particles. The color of the sludge changed from brown to reddish, which may indicate the absorption of NPs to the activated sludge flocs. Li et al. [192] studied the effect of short-term exposure to polystyrene nanoparticles on activated sludge performance. They also observed a color shift of the activated sludge from dark brown to light yellow and attributed it to the adsorption of the white PS-NPs by the activated sludge.

Soluble microbial products (SMPs) are the most direct indicator relating to membrane fouling [193]. SMPs are also reported in the literature as soluble extracellular polymeric substances (S-EPSs) and mainly consist in the portion of EPSs that are not associated with the microbial cell but are solubilized in the mixed liquor [194]. SMPs are related to cell lysis, substrate metabolism, and biomass growth [195], which can be affected by many influencing factors such as the substrate type, nutrient content, solid retention time, presence of toxic substances, the shear rate of a reactor, and salinity [196]. The major components of SMPs are carbohydrates (SMPc) and proteins (SMPp) [197]. Therefore, the SMP concentration, expressed as SMPc and SMPp, were determined at three different moments of the experiment: (1) at the beginning, (2) at the end of the first period of PS addition, and (3) at the end of the experiment with the MF membrane (day 39).

In the first stage of the experiment (i.e., up to 20 mg PS L⁻¹), the obtained concentrations of SMPc were 1.54 mg L⁻¹ and 1.15 mg L⁻¹ while the SMPp values were 4.06 mg L⁻¹ and 5.58 mg L⁻¹ in the MBR-Control and MBR-PS, respectively. The values obtained in both the MBR-Control and MBR-PS reactors showed no significant difference in the average SMP values, which means that the presence of PS nanospheres at a low concentration did not provoke any biomass disruption. Previous reports have shown the toxicity of NPs as a dose-dependent manner, where low concentrations of PS-NPs (0.1, 1, 5, 10, and 50 mg L^{-1}) did not exhibit obvious toxicity [198,199]. However, even though the levels of SMPs observed in the biomass flocs during the course of this study were relatively low, at the end of the 39-day experiment, when the accumulation of PS-NPs was higher (i.e., around 60 mg L^{-1}), the behavior changed. The most significant variation was observed in the carbohydrate measurements. The increase in the SMPc values in the MBR-PS was double compared with the control. While the MBR-Control increased more than 2.5 times, the MBR-PS showed more than five times the SMPc increment, most probably due to the protective responses of bacteria under nanoplastic stress. A similar behavior was observed by Tang et al. [200], who studied the influence of three different PS nanoplastic concentrations (PS-0.1, PS-1, and PS-10 mg L⁻¹) on the S-EPS variation [200]. They observed an increase in S-EPSs in all of the studied reactors after exposure to low doses of PS-NPs. They concluded that the production of S-EPSs on the bacteria cell surfaces helped to protect them from harm when they exposed to PS-NPs [200].

Regarding the protein concentrations, they remained almost constant in both cases, obtaining values of 3.99 mg L⁻¹ and 4.93 mg L⁻¹ in the MBR-Control and

MBR-PS, respectively. Wang et al. [196] observed that a relatively lower concentration (0.14–0.30 g L^{-1}) of polypropylene microspheres (500 μ m) in an 84-day experiment stimulated the release of SMP [201]. Similarly, the content of S-EPS was increased slightly after PS-NP (100 mg L^{-1}) exposure in the study conducted by Qian et al. [202], which agrees with the results in the current study.

3.1.2. Microbial Community Analysis

Microbial communities were examined using microscopy observations and metagenomic analysis. The initial conditions of the experiment were similar for both reactors under investigation, where the predominant bacteria observed in both reactors were identified as morphotypes 0803/0914 and 0092. These morphotypes are associated with the phylum Chloroflexi. This finding aligns with the expected abundance of Chloroflexi in urban WWTPs, from which the utilized sludge was obtained. During the subsequent sample observations (i.e., intermediate sample), the relative abundance of the initial morphotypes remained, along with the presence of type 1851, which also appeared in the Chloroflexi phylum. However, morphotype 0092 was observed only in the control reactor. At the conclusion of the experiment, the bacterial community in the MBR-Control maintained was similar to that at the intermediate sample. In contrast, in the MBR-PS, there was a noticeable change in the bacterial community, specifically with the observation of morphotype 0041/0675, replacing the previous observation of morphotype 1851.

16 S rRNA gene sequencing was also investigated (1) at the beginning, (2) at the end of the first period of PS addition, and (3) at the 39th day. Bacterial communities were dominated by Proteobacteria in both reactors (average of 30.99% of 16S rRNA gene reads) during the study. This result is in agreement with Rehman et al. [203], who studied the composition and functional potential of the microbial communities of a lab-scale MBR system with a submerged ultrafiltration (UF) membrane configuration. As Figure 22 shows, other major groups were the Planctomycetota (15.11%), Bacteroidota (13.45%), Chloroflexi (8.61%), Verrucomicrobiota (6.33%), Patescibacteria (5.67%), Actinobacteriota (4.24%), Actinobacteriota (3.07%), Myxococcota (2.42%), Gemmatimonadota (1.45%), Nitrospirota (1.44%), and Bdellovibrionota (1.42%) (Figure 22a). Previous studies have also observed the same phyla predominance in conventional activated sludge reactors [204,205].

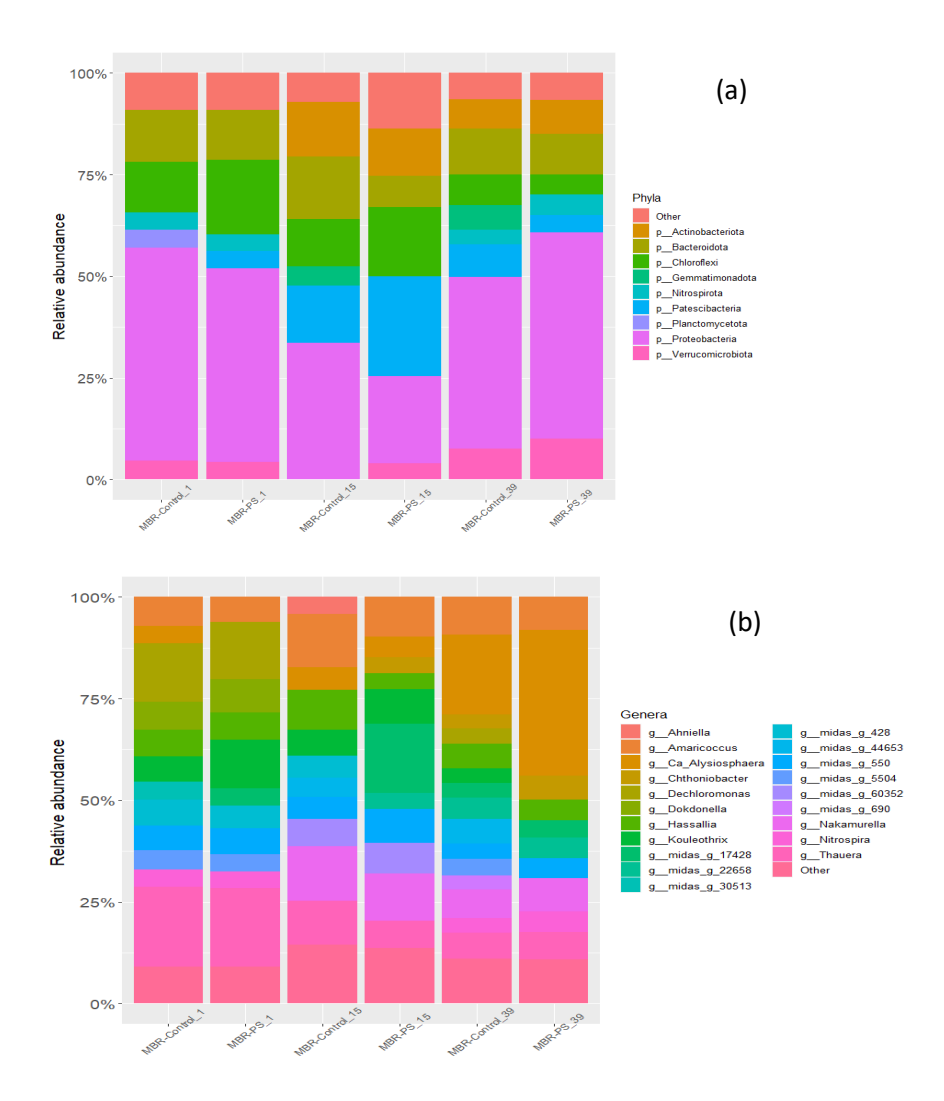


Figure 22. Bacterial community composition at the phylum level (a) and genera level (b) in both reactors (i.e., MBR-Control and MBR-PS) sampled on the initial day (day 1st), on day 15, and day 39.

Minor changes were observed with the most abundant phylum Proteobacteria along with Planctomycetota, and Verrucomicrobiota. At the same intermediate sample, the relative abundance of Proteobacteria dropped from 31% to 25%, from 15% to 13% in the case of Planctomycetota, and from 7% to 5% for Verrucomicrobiota. In the last sample analyzed (day 39), all phylum recovered the relative abundance of the initial values obtained in the control reactor. Furthermore, the results shown in Figure 22 suggest that the presence of PS at low concentrations (first stage of treatment) and for a short period have more effect on the bacterial community than higher concentrations for a longer time. In the cluster analysis of Figure 23, the adaptation capability of the medium to the pollutant presence over time was more noticeable.

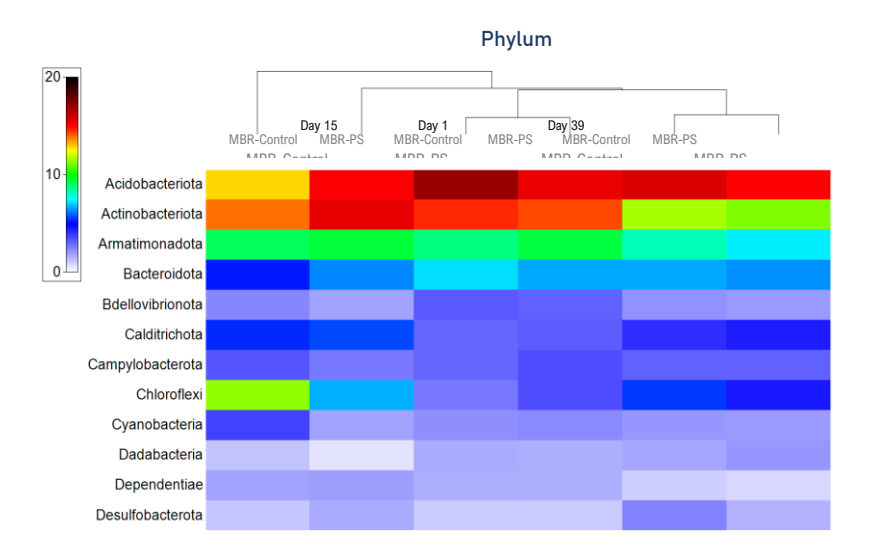


Figure 23. Heat-map of the bacterial community composition at the phylum level with cluster analysis. The color intensity in each panel shows the percentage in a sample, referring to the color key at the left.

The relative abundance of Patescibacteria increased from 3% to 7% and 11% in MBR-Control and MBR-PS, respectively, when the PS remained at low concentrations (stage I). Alvim et al. [206] have recently studied the effect of PS 100 nm size on the activated sludge in a sequencing batch reactor. The same results were found with the Patescibacteria phylum at low concentrations of nanoplastic. Other studies also agree with the enrichment of Patescibacteria in the presence of plastic [200] and suggested this phylum as a possible bacterial biomarker for plastic contamination [206]. Even though there are similar findings in terms of the abundance of some bacterial communities in the presence of NPs, a direct comparison between the Conventional Activated Sludge (CAS) and MBR systems behavior is not straightforward. This is due to the relatively longer operational time and higher MLSS concentration associated with MBR technology compared to CAS [207]. Consequently, the cumulative impact of nanoplastics could diverge from conventional sludge technologies, potentially leading to variations in bacterial relative abundance fluctuations. In our study, at the end of the second cycle of PS addition, the relative abundance of Patescibacteria decreased again up to 5 % in both reactors, while the accumulation and homogeneity of the nanoplastic in the MBR increased. Given the intermittent addition of PS, the results suggest that the bacterial community is capable of adapting following a period of rest.

3.2. Membrane Operation

3.2.1. Permeate Quality

The experiment (once the addition of PS started) was conducted with an MF membrane (nominal diameter of 0.4 µm) for 39 days, followed by testing the UF

membranes including c-UF and r-UF for two weeks for each one. Table 9 summarizes the characteristics of the effluents of both MBRs, where the results are expressed in average values and their respective standard deviations (±SD).

Table 9. Average effluent of	quality and removal	capacity of MBR.
-------------------------------------	---------------------	------------------

	pН	CE	COD	%R	TOC	%R	Total N	%R
	pm	(µS/cm)	(mg/L)	(COD)	(mg/L)	(TOC)	(mg/L)	(TN)
				M	F			
MBR-	7.90 ± 0.20	564.92 ± 0.17	10.28 ± 2.30	97.44 ± 1.82	2.28 ± 0.65	97.88 ± 2.00	15.63 ± 4.50	49.60 ± 14.52
Control	7.90 ± 0.20	304.92 ± 0.17	10.28 ± 2.30	97. 44 ± 1.62	2.28 ± 0.03	97.88 ± 2.00	13.03 ± 4.30	49.00 ± 14.32
MBR-	7.91 ± 0.12	518.08 ± 0.17	8.84 ± 3.05	97.80 ± 0.76	1.83 ± 0.61	98.38 ± 0.84	18.75 ± 3.45	39.52 ± 11.14
PS	7.91 ± 0.12	318.08 ± 0.17	8.84 ± 3.03	97.80 ± 0.70	1.83 ± 0.01	96.36 ± 0.64	16.75 ± 5.45	39.32 ± 11.14
				c-U	J F			
MBR-	7.91 ± 0.10	482.60 ± 0.10	8.48 ± 1.39	97.89 ± 0.35	2.05 ± 0.82	98.46 ± 0.62	12.75 ± 2.50	50.96 ± 9.62
Control	7.91 ± 0.10	402.00 ± 0.10	0.40 ± 1.39	97.89 ± 0.33	2.03 ± 0.82	98.40 ± 0.02	12.75 ± 2.50	30.90 ± 9.02
MBR-	7.93 ± 0.12	452.80 ± 0.08	9.18 ± 0.59	97.71 ± 0.15	1.98 ± 0.33	98.51 ± 0.25	18.00 ± 2.65	30.77 ± 10.18
PS	7.75 ± 0.12	432.00 ± 0.00	7.10 ± 0.57	77.71 ± 0.13	1.70 ± 0.33	76.51 ± 0.25	10.00 ± 2.03	30.77 ± 10.16
				r-U	J F			
MBR-	7.80 ± 0.08	440.75 ± 0.02	5.33 ± 0.67	98.61 ± 0.17	1.19 ± 0.12	99.09 ± 0.10	14.55 ± 1.67	46.18 ± 4.64
Control	7.80 ± 0.00	440.75 ± 0.02	3.33 ± 0.07	76.01 ± 0.17	1.17 ± 0.12	77.07 ± 0.10	14.55 ± 1.07	40.10 ± 4.04
MBR-	7.92 ± 0.08	516.25 ± 0.09	5.88 ± 1.17	98.47 ± 0.34	1.07 ± 0.27	99.18 ± 0.21	18.25 ± 4.11	32.01 ± 17.18
PS	1.72 ± 0.06	310.23 ± 0.09	3.00 ± 1.17	70.47 ± 0.34	1.07 ± 0.27)).10 ± 0.21	10.23 ± 4.11	32.01 ± 17.16

In general terms, the effluents from both the MBR-Control and MBR-PS reactors were very similar in terms of characteristics. A percentage of COD removal above 97% was obtained in both reactors (MBR-Control and MBR-PS) for all membranes, which represents a high purification capacity. Results showed that the presence of nanoplastics (PS) did not affect the remediation capacity of the MBR for organic matter. Similar high removal efficiencies (effluent COD: 20.2 ± 10.2- 23.8 ± 13.4 mg L⁻¹) were previously achieved by Maliwan et al. [208] during their study of different MP additions (0, 7, 15, and 75 MPs/L, respectively). Furthermore, other studies related to biological wastewater treatment have reported COD removal efficiencies of sequencing batch reactor (SBR) during an experimental time above 90% [206], and 97.35 \pm 0.81% (n = 33) of COD removal was obtained in SBR-MP, representing a high purification capacity of the reactor in the presence of polyethylene microbeads [209]. It is also worth noticing that the r-UF showed a higher removal efficiency compared to commercial ones, despite the results summarized in Table 7. The chlorination transformation process modified key surface characteristics [210], particularly achieving a MWCO of 30,000 Da, which could influence the observed COD removal efficiency.

The quality of permeate streams from samples obtained from the three types of membranes (i.e., MF, r-UF, and c-UF) was also verified in terms of PS presence. Before conducting the Pyr-GC-MS analysis, a pre-concentration step was carried out to enhance the detectability of trace nanoplastics. The pre-concentrated permeate samples were analyzed from a larger initial volume from 5 to 8 L, as explained in Section 2.4.3. According to the results, no presence of PS was detected, since all

values were below the limit of detection (LOD: ranging from 0.013 to 0.067 $\mu g \ mL^{-1}$). Consequently, the rejection capacity of the MBR toward PS nanoplastics was 100% with all of the studied membranes.

In addition, the verification of PS concentration in sludge was conducted weekly. Since the comparison study of membrane operation occurred sequentially (i.e., r-UF following c-UF), four measurements using Py-GC-MS were controlled. Each time, the Py-GC-MS analyses were performed on both types of samples (i.e., from MBR-Control and MBR-PS) to confirm the presence of PS in the sludge.

As could be verified, the PS concentration was kept almost constant (Table 10) during the comparative study. Accordingly, Mitrano et al. [179] reported that PS-NPs have the propensity to rapidly transition from the aqueous phase to the sludge phase within a short timeframe. Consequently, the swift formation of the cake layer and the strong adsorption capability of activated sludge for PS-NPs can act as a physical barrier, hindering the movement of additional nanoparticles and limiting their ability to contribute significantly to pore blocking.

Table 10. Summary of the PS quantification in sludge by Py-GC/MS.

	c-UF M	lembrane	r-UF Me	embrane
	Initial Point Second Week		Third Week	Fourth Week
Conc. PS (mg L^{-1})	52.86	52.31	55.03	55.27

3.2.2. Transmembrane Pressure (TMP) Evolution

The effect of the presence of PS was noticeable in the transmembrane pressure (TMP) increment. Figure 24 shows the TMP evolution over the experimental time for the three studied membranes.

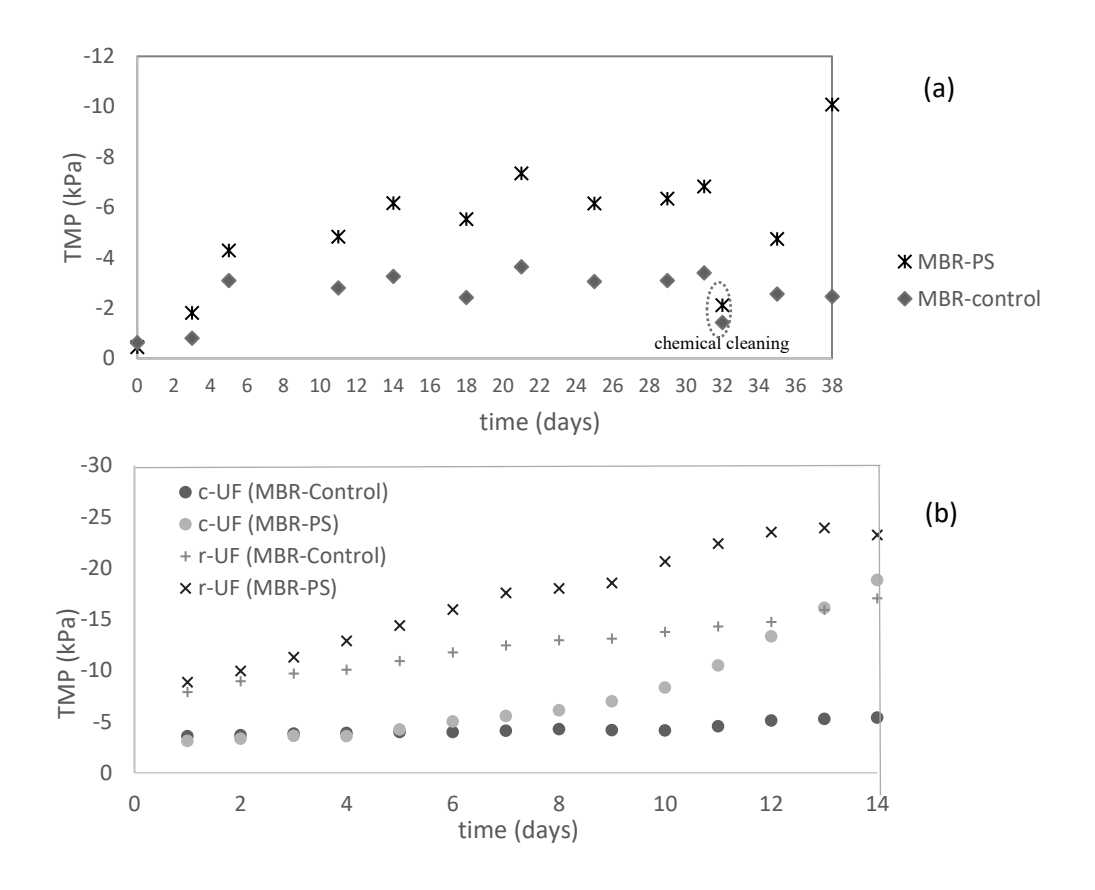


Figure 24. Variation of the transmembrane pressure (TMP) over the experimental time of the (a) microfiltration membrane (the highlighted TMP values on the 32nd day relate to chemical cleaning of the membranes) and (b) ultrafiltration membranes (comparison between

As can be observed in Figure 24, the overall increase in TMP in the MBR-PS with the increment of PS addition was higher than in the MBR-Control (i.e., no presence of PS) for the three membranes employed. This indicates that nanoplastics contribute significantly to membrane fouling over time.

For the case of the MF membrane (Figure 24a), throughout the experimental period, regular physical cleaning of the membranes was carried out weekly, along with a single chemical clean at the conclusion of polystyrene (PS) addition (day 32). It is important to note that the inflection points in Figure 24a correspond to the instances of membrane cleaning. Finally, the system kept running without PS addition for another week. Toward the end of the evaluated time, while the TMP in the MBR-Control increased less than two times, the growth of the TMP in the MBR-PS was almost five times higher than the initial TMP. This behavior shows the interactions between NPs and the membrane, which enhanced the membrane fouling and consequently the overall process performance of the wastewater treatment by MBR.

Subsequent to the 39-day period of the experiment, a comparative study of the UF membranes (c-UF and r-Uf) was carried out. The membrane fouling of c-UF and r-UF induced by the presence/absence of PS was studied, with the results given in Figure 24b. It was observed in Figure 24b that while r-UF exhibited a lineal ($R^2 > 0.97$ for both r-UF membranes) TMP increase, with the TMP of the membrane from MBR-PS higher than that from the MBR-Control, the TMP of the c-UF membrane behaved differently. After day 8, the c-UF submerged in MBR-PS presented a sharp TMP increase. On the other hand, the r-UF submerged in MBR-PS tended to stabilize. This stabilization is a promising result and could be attributed to the NaClO treatment used in the recycling process, which modifies the membrane-surface properties, potentially reducing its susceptibility to biofouling [83,85].

3.2.3. RIS Analysis and Surface Characterizations

Figure 25 reports the RIS model outputs of the three membranes: MF, c-UF, and r-UF. The presented R_c values include both reversible and irreversible cake layer resistance, whereas the R_f values comprise the resistances of the cake layer and the pore-blocking mechanism.

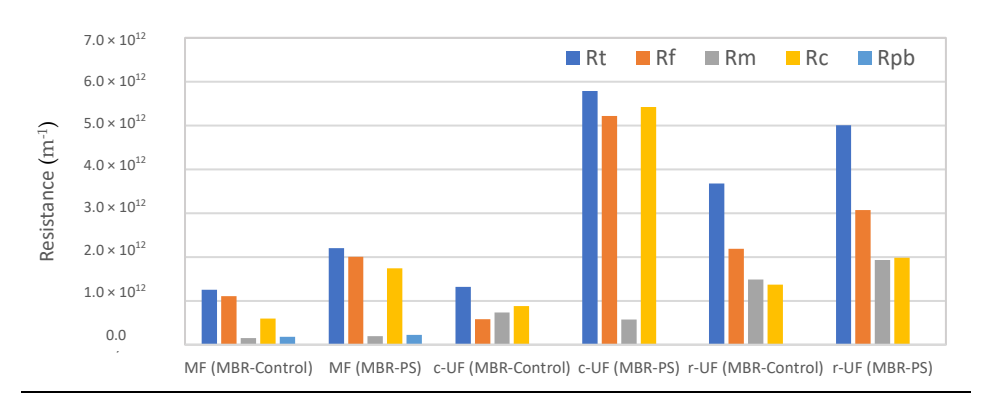


Figure 25. Resistances of the MF, commercial UF (c-UF), and recycled UF (r-UF) membranes in the control (MBR-Control) and the experimental (MBR-PS) reactors. R_t : total resistance; R_r : fouling resistance; R_m : membrane resistance; R_c : cake layer resistance; R_p b: pore blocking resistance.

The major contribution to the total resistance was from the cake layer resistance (Rc) across all three membrane types assessed (MF, c-UF, and r-UF), as depicted in Figure 25.

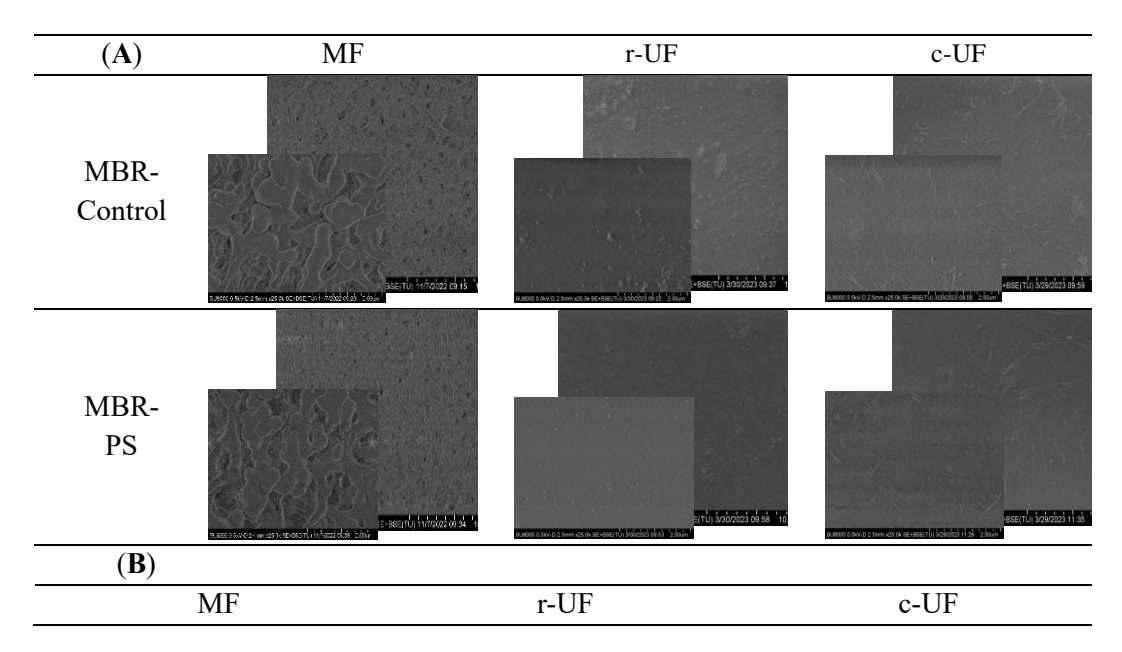
For the case of MF (0.4 μ m), one might have hypothesized a significant increase in the pore blocking resistance (Rpb) of the membrane due to the accumulation of the nanospheres (116 nm) inside the membrane. However, the primary contribution to the overall resistance originates from Rc (cake layer formation). This suggests that even with larger pores, the formation of a cake layer by SMPs (explained in section 3.1.1) and potential biofilm can significantly impede flow. The major SMP release is directly linked to the formation of the cake layer. During filtration, SMPs are believed to adsorb onto the membrane surface, blocking membrane pores and/or forming a gel

layer on the surface. This process provides a potential nutrient source for biofilm formation, thereby increasing resistance to permeate flow [194].

On the other hand, it is important to note that the Rm of the r-UF membrane was the highest value among the compared membranes, as depicted in Fig. 26. This difference can be attributed to the intrinsic properties of the recycled membranes, which experience a manufacturing process (transformation from EoL to r-UF), involving the removal of the first layer and the emergence the polyethersulfone layer after use. Additionally, the r-UF membrane has the smallest pore size, as Table 1 depicts, which results in higher resistance to water permeation. However, a close examination of the fouling resistance behavior reveals a tendency of r-UF towards lower values of Rf than those of the c-UF membrane (as shown in Fig. 26). This reinforces the previous observation of potential fouling reduction benefits associated with recycled UF membranes and aligns with the TMP evolution explained in the previous section. Thus, the application of r-UF membranes in a flat sheet configuration within an aMBR system for both in absence and in presence of NPs demonstrates promising results.

3.2.4. Membrane Characterization

To support the previous observations, two different techniques after the physical clean at the end of each assessment were employed. Figure 26 shows the SEM micrographs of the MF and UF membranes (A) and the three-dimension (3D) projections from the confocal micrograph (B).



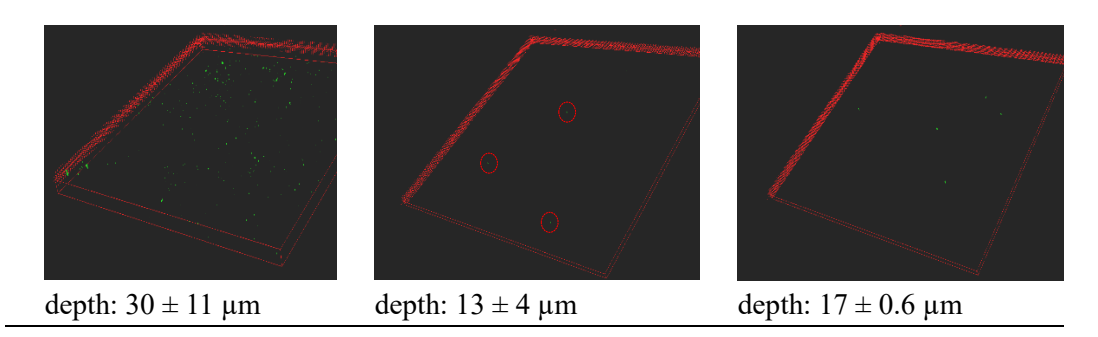


Figure 26. (A) Membrane surface micrographs of the membranes at the end of the experiment after the physical clean: membranes from the MBR-Control (second row) and membranes from MBR-PS (third row). (B) 3D projection from confocal laser scanning microscopy of the MBR-PS membranes. Green dots in the 3D projection of the membranes represent the PS nanoparticles.

SEM images of the studied membrane surfaces did not reveal any visible evidence of PS deposition or attachment. To obtain a more comprehensive understanding of potential PS fouling, confocal microscopy was employed as a complementary technique. Unlike SEM, 3D imaging confocal microscopy allows for depth profiling, which can reveal PS particles that may have penetrated the membrane structure.

Confocal images from the MBR-Control samples were not presented because no fluorescent particles were observed, resulting in entirely black images devoid of fluorescent dots. This absence of fluorescent signals in the control samples served as the baseline, confirming that any fluorescent dots observed in other samples can be attributed to PS particles. A 3D projection from the confocal microscope showed the portion of infiltrated nanoplastics adhered within the pores of the MF membrane. This aligns with prior studies by Abdelrasoul et al. [167], who reported the fouling effect of small particles falling within the critical size range, which is defined as the size range between 1/6 and 1/2 of the pore diameter. This fouling leads to particle attachments in the internal wall of the membrane pores, decreasing the membrane effective pore size [167]. However, in the current study, the portion of nanoplastics that infiltrated was very small, and consequently did not significantly contribute to the internal pore blocking. For the case of the UF membranes, the CLSM images exhibited a significantly lower attachment of PS nanospheres on their surfaces after the physical cleaning protocol was conducted.

The analysis of the 3D projection from CLSM provides insights into the depth of PS penetration into the different membrane structures (Figure 26B). For MF membranes, the depth of the PS-containing layers was around 30 μm . In contrast, the depth of the PS layers was approximately half for the UF membranes. This difference revealed the more effective sieving capability of both UF membranes in preventing the passage of PS nanoplastics compared to the MF membrane.

Nevertheless, it is worth noting that the fouling contribution of the presence of PS may vary over time, influenced by potential interactions between the nanoparticles

and their accumulation within the membrane. Further research should be conducted to investigate the long-term effects of these NPs.

4. Conclusions

This study demonstrates that aerobic membrane bioreactors are highly effective in removing nanoparticles from wastewater, achieving over 97% COD removal in both the control and PS-exposed reactors. However, the presence of nano-sized PS particles negatively affected the membrane performance, enhancing the fouling phenomena and increasing the transmembrane pressure. This impact was particularly evident in changes in the soluble microbial products, especially carbohydrates, which are key contributors to fouling. The recycled UF membrane showed lower fouling tendencies than the commercial UF membranes, highlighting the potential benefits of surface modifications. Despite these challenges, aerobic MBRs remain a promising solution for NP removal, though membrane fouling requires further attention.

5. Supplementary Materials

S1. Quality Control

To ensure the reliability and accuracy of our experimental setup, a series of quality control measures were implemented during the collection, processing, and analysis of samples.

Laboratory Attire and Hygiene:

Laboratory personnel wore cotton lab coats to minimize the risk of introducing external contaminants. Gloves were worn throughout the sample processing procedures to prevent contamination from skin contact.

Sample Handling:

During filtration, a glass cover was placed on top of the filtration unit to shield the samples from airborne particles. Prior to use, all containers used for sample processing were cleaned with distilled water.

Process Blanks:

A process blank was prepared by replicating all steps of sample digestion, filtration, and storage without actual sample material. This blank was processed in parallel with the samples to monitor for any potential contamination introduced during the experimental procedures. The inclusion of process blanks enabled the identification and correction of any contamination sources, ensuring the integrity of the experimental results.

Cross-Contamination Prevention during Analysis:

During Py-GC-MS analysis, blank runs were conducted between each sample analysis. These blank runs were essential to detect and eliminate any residual contamination from previous samples, thereby preventing cross-contamination and ensuring the accuracy of subsequent measurements.

S2. Preparation of Standards and Instrumental Validation Py-GC-MS

- Preparation of Standards and the Calibration Curve

PS dissolved in THF was used as standard for the quantification with the Py-GC-MS. 20 mg of PS was dissolved in 1 mL of THF using ultrasound for 20 minutes and the resulting solution of 20 mg mL⁻¹ was used for the preparation of the calibration stocks by dilution. From the stocks of 2000, 200 and 20 mg mL⁻¹, different volumes were taken to prepare the different calibration points directly into the pyrolysis tubes. Before injecting them into the system, the solvent was allowed to evaporate. The specific conditions to prepare the six calibration points (from 0.1 to 5 μ g of PS) are indicated in Table S2.

Table S 2. Preparation of the calibration curve.

PS (µg)	Stock used (mg/L)	μL from the stock
0,1	20	5
0,2	20	10
0,5	200	2,5
1	200	5
2	200	10
5	2000	2,5

- Validation

Validation of the method was performed in terms of instrumental repeatability, linearity, accuracy and precision, and limits of detection (LOD) and quantification (LOQ).

The instrumental repeatability was tested by injecting replicates of the PS standard at two masses, 0.1 and 2 μ g. Relative standard deviation (RSD) was satisfactory (less than 10-15%).

Linearity was tested in the range 0.1 to $5\,\mu g$ (higher masses saturate the detector), and adjusted to a quadratic regression with a regression coefficient greater than 0.99. Figure S8 shows the calibration curve obtained.

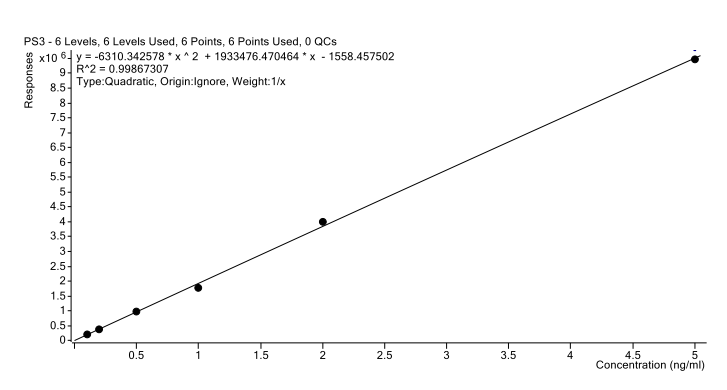


Figure S 8. Calibration curve for PS from 0.1 to 5 μg.

The instrumental LOQ for PS was established at the lowest level of the calibration curve, i.e., the minimum value with an RSD less than 20%, a signal at least 10 times higher than the blank, and a linear trend with the other points. The LOD was established at a concentration in which the signal is at least three times higher than the signal of the blank.

Accuracy and precision were evaluated by studying recoveries from spiked samples subjected to the pre-treatment.

For permeate, validation was carried out with 100, 200, and 500 mL fortified with different concentrations of PS, from 0.2 to 1 mg/L (according to the filtered volume). An average recovery of 124% was obtained for this process, and 8% of RSD from the three replicates.

For the activated sludge matrix, a volume of 100 mL was fortified at 10 mg/L and the average %R obtained was over 90%. Precision was not as good as RSD was 30%.

The limits of detection and quantification for each matrix were established according to the instrumental values, the volume of the sample treated and the possible presence of PS signal in the blank samples. Table S3 shows the LOQ and LOD established in each case.

Table S 3. Instrumental LOQ and LOD established for each matrix.

	Volume (mL)	LOQ (ug/mL)	LOD (ug/mL)
Activated sludge	100	10	3
Permeate	100 - 500	0.04 - 0.2	0.013 - 0.067

CHAPTER VI:

General conclusions and future research

CHAPTER VI: General conclusions and future research

The compendium of scientific articles in this doctoral thesis investigates potential applications for indirect recycling of end-of-life (EoL) RO membranes, specifically their transformation into NF, UF, and AEM membranes. While these recycled membranes have been extensively characterized in previous works to understand their properties, their practical applications require further investigation. This research is particularly timely as water scarcity and quality degradation have emerged as critical global challenges, with 2.2 billion people lacking access to safely managed drinking water services. This global crisis requires the use of non-traditional water sources, including wastewater, seawater, and brackish water. Additionally, the emergence of new contaminants, particularly nanoplastics and other micropollutants, presents significant challenges to conventional water treatment systems. In response to these interconnected challenges, this thesis investigated the application of membrane processes in wastewater treatment systems, with a particular focus on saline wastewater treatment, fouling behavior, and nanoplastic removal. The main conclusions from this doctoral thesis can be summarized as follows.

Chapter III focused on the implementation of recycled membranes for saline wastewater treatment. The research validated the effectiveness of recycled membranes compared to commercial alternatives and demonstrated a successful application of these membranes in treating saline urban wastewater for crop irrigation purposes. The rNF membrane exhibited high selective rejection of divalent ions, while the recycled anion exchange membrane rAEM achieved demineralization rates comparable to commercial membranes. Both recycled NF and ED membrane processes demonstrated their feasibility for treating saline urban wastewater, marking the first successful application of recycled membranes in this context. Importantly, the quality of treated effluents from both processes met the requirements for irrigation purposes, particularly in managing salt content and maintaining appropriate nutrient balance, thus validating their suitability for agricultural applications.

Chapter IV was centered on studying the fouling behavior of ultrafiltration membranes in the presence of PS nanoparticles, comparing both commercial and recycled membranes. In the investigation of ultrafiltration membrane fouling, the OCT analysis revealed important insights into fouling behavior across different membrane types. The study demonstrated that the combination of PS and BSA resulted in reduced PS deposition on membrane surfaces. Notably, regenerated cellulose membranes achieved 100% permeability recovery after physical cleaning. The research established clear correlations between membrane properties and fouling behavior, with material composition, surface charge characteristics, and molecular weight cut-off significantly influencing filtration performance and fouling tendencies. Consequently, RC membranes were selected for the subsequent pretreatment of the MBR permeates.

Chapter V, the final experiment, focused on emerging pollutants removal through MBR systems, yielded significant findings. The aerobic MBR system proved highly effective in nanoparticles removal, achieving over 97% COD removal in both control and PS-exposed reactors. Although the presence of nano-sized PS particles increased

fouling and transmembrane pressure, recycled UF membranes demonstrated superior performance with lower fouling tendencies compared to commercial UF membranes under these challenging conditions.

These comprehensive findings validate the potential of recycled membranes across multiple applications, from treating saline wastewater for irrigation to managing fouling in the presence of nanoparticles and removing emerging contaminants in MBR systems. The research demonstrates that recycled membranes not only match but can exceed the performance of commercial alternatives in specific applications. These results strongly support the implementation of sustainable water treatment solutions aligned with circular economy principles, offering practical pathways for more efficient and environmentally conscious wastewater management strategies.

Future research lines

The future research directions identified in this thesis highlight several key areas that warrant further investigation to advance the field of recycled membrane technology. These research lines emerge from the findings and limitations encountered during the current investigation, pointing toward critical areas for development.

The primary focus should prioritize **evaluating the applicability** of recycled membrane performance **with real urban wastewater**, as current studies have largely relied on synthetic conditions. Such studies would provide critical insights into how recycled membranes perform under realistic operational conditions, including the presence of mixed contaminants, fluctuating water quality, and varying flow rates.

Scaling up studies represent another crucial avenue for research, essential for transitioning this technology from laboratory to industrial applications.

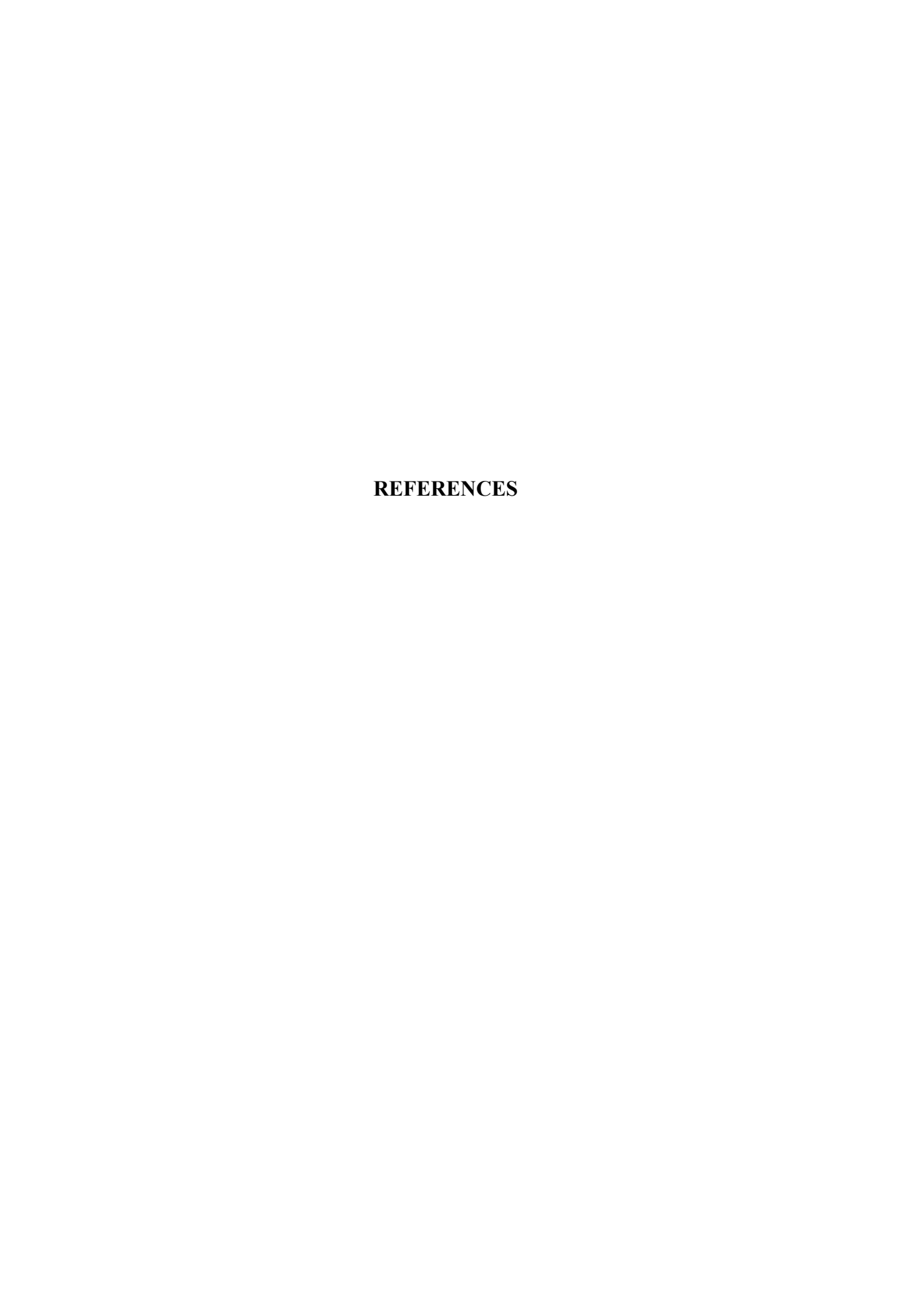
Furthermore, **long-term experiments** are essential to assess the durability and sustainability of recycled membranes over extended periods of use. These studies should investigate issues such as the membranes' lifespan, degradation mechanisms, cleaning requirements, and the overall impact of operational stresses. Additionally, further investigation is needed to understand the behavior of recycled UF membranes in MBR systems, particularly the potential integration of recycled UF membranes with **anaerobic processes**, which presents another promising research direction.

The behavior of **UF membranes in MBR systems** treating emerging contaminants requires further investigation, particularly given the **complex interactions** between microplastics, pharmaceutical compounds, and antimicrobial resistance. Microplastics present a unique challenge as they can serve as ideal substrates for microbial colonization and biofilm formation. These "plastisphere" environments create favorable conditions for bacterial growth and, more critically, facilitate the horizontal transfer of antibiotic resistance genes (ARGs).

Finally, a **deeper understanding of membrane fouling mechanisms** remains crucial for optimizing the long-term performance and sustainability of membrane systems. These

research directions collectively aim to bridge the gap between current knowledge and practical implementation, ultimately advancing the field of sustainable membrane technology.

By addressing these factors, future research can help to establish recycled membranes as a reliable and cost-effective alternative for wastewater treatment in real applications.



References

- Mekonnen, M.M.; Hoekstra, A.Y. Four Billion People Facing Severe Water Scarcity. Science Advances 2016, 2.
- He, C.; Liu, Z.; Wu, J.; Pan, X.; Fang, Z.; Li, J.; Bryan, B.A. Future Global Urban Water Scarcity and Potential Solutions. *Nature Communications* 2021 12:1 2021, 12, 1–11, doi:10.1038/s41467-021-25026-3.
- 3. Noto, L. V.; Cipolla, G.; Francipane, A.; Pumo, D. Climate Change in the Mediterranean Basin (Part I): Induced Alterations on Climate Forcings and Hydrological Processes. *Water Resources Management* **2023**, *37*, 2287–2305, doi:10.1007/S11269-022-03400-0/TABLES/3.
- Mishra, R.K.M. Fresh Water Availability and Its Global Challenge Available online: https://bjmas.org/index.php/bjmas/article/view/455/993 (accessed on 8 May 2024).
- Noto, L. V.; Cipolla, G.; Pumo, D.; Francipane, A. Climate Change in the Mediterranean Basin (Part II): A Review of Challenges and Uncertainties in Climate Change Modeling and Impact Analyses. Water Resources Management 2023, 37, 2307–2323, doi:10.1007/S11269-023-03444-W/FIGURES/1.
- Tortajada, C.; van Rensburg, P. Drink More Recycled Wastewater. *Nature 2021* 577:7788 2019, 577, 26–28, doi:10.1038/d41586-019-03913-6.
- 7. Ishraq Emran, Md.G.; Barma, R.; Hussain Khan, A.; Roy, M. Reasons behind the Water Crisis and Its Potential Health Outcomes. *European Journal of Development Studies* **2021**, doi:10.24018/ejdevelop.YEAR.VOL.ISSUE.ID.
- 8. Contaminantes Emergentes Available online: https://www.miteco.gob.es/es/agua/temas/estado-y-calidad-de-las-aguas/contaminantes-emergentes.html (accessed on 12 December 2024).
- 9. Greenlee, L.F.; Lawler, D.F.; Freeman, B.D.; Marrot, B.; Moulin, P. Reverse Osmosis Desalination: Water Sources, Technology, and Today's Challenges. *Water Res* **2009**, *43*, 2317–2348, doi:10.1016/J.WATRES.2009.03.010.
- Almasoudi, S.; Jamoussi, B. Desalination Technologies and Their Environmental Impacts: A Review. Sustainable Chemistry One World 2024, 1, 100002, doi:10.1016/J.SCOWO.2024.100002.
- Somashekar, V.; Anand, A.V.; Hariprasad, V.; Elsehly, E.M.; Kapulu, M. Advancements in Saline Water Treatment: A Review. *Water Reuse* 2023, 13, 475–491, doi:10.2166/WRD.2023.065.
- Jones, E.; Qadir, M.; van Vliet, M.T.H.; Smakhtin, V.; Kang, S. mu The State of Desalination and Brine Production: A Global Outlook. *Science of The Total Environment* 2019, 657, 1343–1356, doi:10.1016/J.SCITOTENV.2018.12.076.
- 13. Habieeb, A.R.; Kabeel, A.E.; Sultan, G.I.; Abdelsalam, M.M. Advancements in Water Desalination Through Artificial Intelligence: A Comprehensive Review of AI-Based Methods for Reverse Osmosis Membrane Processes. *Water Conservation Science and Engineering* **2023**, *8*, 1–18, doi:10.1007/S41101-023-00227-7/FIGURES/6.
- Jodar-Abellan, A.; López-Ortiz, M.I.; Melgarejo-Moreno, J. Wastewater Treatment and Water Reuse in Spain. Current Situation and Perspectives. Water 2019, Vol. 11, Page 1551 2019, 11, 1551, doi:10.3390/W11081551.
- Srivastava, A.; Parida, V.K.; Majumder, A.; Gupta, B.; Gupta, A.K. Treatment of Saline Wastewater Using Physicochemical, Biological, and Hybrid Processes: Insights into Inhibition Mechanisms, Treatment Efficiencies and Performance Enhancement. *J Environ Chem Eng* 2021, 9, 105775, doi:10.1016/J.JECE.2021.105775.

- DesalData Available online: https://www.desaldata.com/ (accessed on 14 May 2024).
- 17. Emerging Pollutants in Wastewater: An Increasing Threat Available online: https://www.unep.org/events/unep-event/emerging-pollutants-wastewater-increasing-threat (accessed on 4 July 2024).
- 18. Liu, W.; Zeng, M.; Li, Y.; Chen, G.; Wen, J.; Wang, J. Deciphering the Research of Micro(Nano)Plastics: An in-Depth Bibliometric Expedition into Ecotoxicological Impacts and Research Trends. *TrAC Trends in Analytical Chemistry* **2024**, *172*, 117608, doi:10.1016/J.TRAC.2024.117608.
- 19. Microplastics European Commission Available online: https://environment.ec.europa.eu/topics/plastics/microplastics_en#law (accessed on 4 July 2024).
- Mandala, G.; Mishra, S. A Review on Emerging Micro and Nanoplastic Pollutants, Heavy Metals and Their Remediation Techniques. *Nanofabrication* 2023, 8, 1–18, doi:https://doi.org/10.37819/nanofab.008.302.
- Lares, M.; Ncibi, M.C.; Sillanpää, M.; Sillanpää, M. Occurrence, Identification and Removal of Microplastic Particles and Fibers in Conventional Activated Sludge Process and Advanced MBR Technology. Water Res 2018, 133, 236– 246, doi:10.1016/J.WATRES.2018.01.049.
- Talvitie, J.; Mikola, A.; Setälä, O.; Heinonen, M.; Koistinen, A. How Well Is Microlitter Purified from Wastewater? – A Detailed Study on the Stepwise Removal of Microlitter in a Tertiary Level Wastewater Treatment Plant. Water Res 2017, 109, 164–172, doi:10.1016/J.WATRES.2016.11.046.
- 23. Egea-Corbacho, A.; Martín-García, A.P.; Franco, A.A.; Quiroga, J.M.; Røjgaard Andreasen, R.; Koustrup Jørgensen, M.; Morten Lykkegaard, C. Occurrence, Identification and Removal of Microplastics in a Wastewater Treatment Plant Compared to an Advanced MBR Technology: Full-Scale Pilot Plant. J Environ Chem Eng 2023, 2213–3437.
- Cavazzoli, S.; Ferrentino, R.; Scopetani, C.; Monperrus, M.; Andreottola, G.; Cavazzoli, S.; Ferrentino, R.; Andreottola, G.; Scopetani, C. Analysis of Micro-and Nanoplastics in Wastewater Treatment Plants: Key Steps and Environmental Risk Considerations. *Environ Monit Assess* 2023, 195, 1483, doi:10.1007/s10661-023-12030-x.
- Chen, Z.; Shi, X.; Zhang, J.; Wu, L.; Wei, W.; Ni, B.J. Nanoplastics Are Significantly Different from Microplastics in Urban Waters. *Water Res X* 2023, 19, 100169, doi:10.1016/J.WROA.2023.100169.
- Abdeljaoued, A.; Ruiz, B.L.; Tecle, Y.-E.; Langner, M.; Bonakdar, N.; Bleyer, G.; Stenner, P.; Vogel, N. Efficient Removal of Nanoplastics from Industrial Wastewater through Synergetic Electrophoretic Deposition and Particle-Stabilized Foam Formation., doi:10.1038/s41467-024-48142-2.
- Ramasamy, B.S.S.; Palanisamy, S. A Review on Occurrence, Characteristics, Toxicology and Treatment of Nanoplastic Waste in the Environment. Environmental Science and Pollution Research 2021, 28, 43258–43273, doi:10.1007/S11356-021-14883-6/METRICS.
- 28. Mustapha, S.; Tijani, J.O.; Elabor, R.; Salau, R.B.; Egbosiuba, T.C.; Amigun, A.T.; Shuaib, D.T.; Sumaila, A.; Fiola, T.; Abubakar, Y.K.; et al. Technological Approaches for Removal of Microplastics and Nanoplastics in the Environment. *J Environ Chem Eng* **2024**, *12*, 112084, doi:10.1016/J.JECE.2024.112084.
- Xu, J.L.; Thomas, K. V.; Luo, Z.; Gowen, A.A. FTIR and Raman Imaging for Microplastics Analysis: State of the Art, Challenges and Prospects. *TrAC*

- *Trends in Analytical Chemistry* **2019**, *119*, 115629, doi:10.1016/J.TRAC.2019.115629.
- Sullivan, G.L.; Gallardo, J.D.; Jones, E.W.; Hollliman, P.J.; Watson, T.M.; Sarp, S. Detection of Trace Sub-Micron (Nano) Plastics in Water Samples Using Pyrolysis-Gas Chromatography Time of Flight Mass Spectrometry (PY-GCToF). *Chemosphere* 2020, 249, 126179, doi:10.1016/J.CHEMOSPHERE.2020.126179.
- 31. Fries, E.; Dekiff, J.H.; Willmeyer, J.; Nuelle, M.T.; Ebert, M.; Remy, D. Identification of Polymer Types and Additives in Marine Microplastic Particles Using Pyrolysis-GC/MS and Scanning Electron Microscopy. *Environ Sci Process Impacts* **2013**, *15*, 1949–1956, doi:10.1039/C3EM00214D.
- Molina, S.; Ocaña-Biedma, H.; Rodríguez-Sáez, L.; Landaburu-Aguirre, J. Experimental Evaluation of the Process Performance of MF and UF Membranes for the Removal of Nanoplastics. *Membranes (Basel)* 2023, 13, 683, doi:10.3390/MEMBRANES13070683.
- 33. Li, P.; Li, Q.; Hao, Z.; Yu, S.; Liu, J. Analytical Methods and Environmental Processes of Nanoplastics. *Journal of Environmental Sciences* **2020**, *94*, 88–99, doi:10.1016/j.jes.2020.03.057.
- 34. Li, P.; Liu, J. Micro(Nano)Plastics in the Human Body: Sources, Occurrences, Fates, and Health Risks. *Environ Sci Technol* **2023**, *58*, 3078, doi:10.1021/ACS.EST.3C08902/ASSET/IMAGES/LARGE/ES3C08902_000 4.JPEG.
- Shen, M.; Zhao, Y.; Liu, S.; Hu, T.; Zheng, K.; Wang, Y.; Lian, J.; Meng, G. Recent Advances on Micro/Nanoplastic Pollution and Membrane Fouling during Water Treatment: A Review. Science of the Total Environment 2023, 881, 163467, doi:10.1016/j.scitotenv.2023.163467.
- 36. Al Aani, S.; Mustafa, T.N.; Hilal, N. Ultrafiltration Membranes for Wastewater and Water Process Engineering: A Comprehensive Statistical Review over the Past Decade. *Journal of Water Process Engineering* 2020, 35, 101241, doi:10.1016/J.JWPE.2020.101241.
- 37. Abdullah, N.; Rahman, M.A.; Othman, M.H.D.; Jaafar, J.; Ismail, A.F. Membranes and Membrane Processes: Fundamentals. *Current Trends and Future Developments on (Bio-) Membranes: Photocatalytic Membranes and Photocatalytic Membrane Reactors* **2018**, 45–70, doi:10.1016/B978-0-12-813549-5.00002-5.
- 38. Basic Principles of Membrane Technology Marcel Mulder Google Libros Available online: https://books.google.es/books?hl=es&lr&id=y2_wCAAAQBAJ&oi=fnd&pg =PA1&dq=membrane+technology+and+applications&ots=X9dWjd_hLK&si g=_UkABAUgrYeChgUTyfNJdU-k2Qk&redir_esc=y#v=onepage&q=membrane%20technology%20and%20ap plications&f=false (accessed on 2 July 2024).
- Diem, T.; Nguyen, T.; Altıok, E.; Siekierka, A.; Pietrelli, A.; Yalcınkaya, F. Preparation and Characterization of Microfiltration Membrane by Utilization Non-Solvent Induced Phase Separation Technique Article Info. *Journal of Membrane Science and Research* 2023, 9, 1995689, doi:10.22079/JMSR.2023.1995689.1594.
- Gul, A.; Hruza, J.; Yalcinkaya, F. Fouling and Chemical Cleaning of Microfiltration Membranes: A Mini-Review. *Polymers 2021, Vol. 13, Page 846* 2021, 13, 846, doi:10.3390/POLYM13060846.
- 41. Kammakakam, I.; Lai, Z. Next-Generation Ultrafiltration Membranes: A Review of Material Design, Properties, Recent Progress, and Challenges.

- Chemosphere **2023**, 316, 137669, doi:10.1016/J.CHEMOSPHERE.2022.137669.
- Sánchez-Arévalo, C.M.; Vincent-Vela, C.; Luján-Facundo, M.-J.; Alvarez-Blanco, S. Ultrafiltration with Organic Solvents: A Review on Achieved Results, Membrane Materials and Challenges to Face. *Process Safety and Environmental Protection* 2023, 177, 118–137, doi:10.1016/j.psep.2023.06.073.
- Maroufi, N.; Hajilary, N. Nanofiltration Membranes Types and Application in Water Treatment: A Review. 2023, 9, 142, doi:10.1007/s40899-023-00899-v.
- 44. Hilal, N.; A1-Zoubp, H.; Darwish, N.A.; Mohammad, A.W.; Arabi, M.A. A Comprehensive Review of Nanofiltration Membranes: Treatment, Pretreatment, Modelling, and Atomic Force Microscopy. *Desalination* 2004, 170, 281–308, doi:10.1016/j.desal.2004.01.007.
- 45. Gohil, P.P.; Desai, H.; Kumar, A.; Kumar, R. Current Status and Advancement in Thermal and Membrane-Based Hybrid Seawater Desalination Technologies. **2023**, doi:10.3390/w15122274.
- Lee, K.P.; Arnot, T.C.; Mattia, D. A Review of Reverse Osmosis Membrane Materials for Desalination—Development to Date and Future Potential. J Memb Sci 2011, 370, 1–22, doi:10.1016/J.MEMSCI.2010.12.036.
- Wu, J.; He, J.; Quezada-Renteria, J.A.; Le, J.; Au, K.; Guo, K.; Xiao, M.; Wang, X.; Dlamini, D.; Fan, H.; et al. Polyamide Reverse Osmosis Membrane Compaction and Relaxation: Mechanisms and Implications for Desalination Performance. *J Memb Sci* 2024, doi:10.1016/j.memsci.2024.122893.
- 48. McCutcheon, J.R.; Mauter, M.S. Fixing the Desalination Membrane Pipeline. *Science* (1979) **2023**, 380, 242–244, doi:10.1126/SCIENCE.ADE5313.
- Baker, R.W. MEMBRANE TECHNOLOGY AND APPLICATIONS Second Edition;
- Molina Martínez, S. Preparación de Membranas Porosas a Partir de Poliamidas Aromáticas Hidrofilicas. Estudios de Aplicación En Operaciones de Ultrafiltración y Pervaporación., University Complutense of Madrid, 2013.
- 51. Terna Iorhemen, O.; Hamza, R.A.; Tay, J.H. Membrane Bioreactor (MBR) Technology for Wastewater Treatment and Reclamation: Membrane Fouling. *Membranes (Basel)* **2016**, doi:10.3390/membranes6020033.
- Sutrisna, P.D.; Riadi, L.; Buana, P.C.W.; Khoiruddin, K.; Boopathy, R.; Wenten, I.G.; Siagian, U.W.R. Membrane and Membrane-Integrated Processes for Nanoplastics Removal and Remediation. *Polym Degrad Stab* 2024, 220, 110635, doi:10.1016/J.POLYMDEGRADSTAB.2023.110635.
- 53. Le-Clech, P.; Chen, V.; Fane, T.A.G. Fouling in Membrane Bioreactors Used in Wastewater Treatment. *J Memb Sci* **2006**, *284*, 17–53, doi:10.1016/J.MEMSCI.2006.08.019.
- 54. Du, X.; Shi, Y.; Jegatheesan, V.; Haq, I.U. A Review on the Mechanism, Impacts and Control Methods of Membrane Fouling in MBR System. *Membranes (Basel)* **2020**, doi:10.3390/membranes10020024.
- 55. Yamamoto, K.; Hiasa, M.; Mahmood, T.; Matsuo, T. DIRECT SOLID-LIQUID SEPARATION USING HOLLOW FIBER MEMBRANE IN AN ACTIVATED SLUDGE AERATION TANK. Water Pollution Research and Control Brighton 1988, 43–54, doi:10.1016/B978-1-4832-8439-2.50009-2.
- Van Der Bruggen, B.; Koninckx, A.; Vandecasteele, C. Separation of Monovalent and Divalent Ions from Aqueous Solution by Electrodialysis and Nanofiltration. Water Res 2004, 38, 1347–1353, doi:10.1016/j.watres.2003.11.008.

- Strathmann, H. *Ion-Exchange Membrane Separation Prosses*; Volume 9.;
 Membrane Science and Technology Series, 2004; ISBN 044450236X.
- 58. Strathmann, H. Ion-Exchange Membrane Separation Processes | 978-0-444-50236-0 | Elsevier. **2004**, 360.
- Luo, T.; Abdu, S.; Wessling, M. Selectivity of Ion Exchange Membranes: A Review. 2018, doi:10.1016/j.memsci.2018.03.051.
- He, Z.; Miller, D.J.; Kasemset, S.; Paul, D.R.; Freeman, B.D. The Effect of Permeate Flux on Membrane Fouling during Microfiltration of Oily Water. J Memb Sci 2017, 525, 25–34, doi:10.1016/J.MEMSCI.2016.10.002.
- Jepsen, K.L.; Bram, M.V.; Pedersen, S.; Yang, Z. Membrane Fouling for Produced Water Treatment: A Review Study From a Process Control Perspective. Water 2018, Vol. 10, Page 847 2018, 10, 847, doi:10.3390/W10070847.
- 62. Marselina, Y.; Lifía; Le-Clech, P.; Stuetz, R.M.; Chen, V. Characterisation of Membrane Fouling Deposition and Removal by Direct Observation Technique. *J Memb Sci* **2009**, *341*, 163–171, doi:10.1016/J.MEMSCI.2009.06.001.
- Huisman, K.T.; Blankert, B.; Horn, H.; Wagner, M.; Vrouwenvelder, J.S.; Bucs, S.; Fortunato, L. Noninvasive Monitoring of Fouling in Membrane Processes by Optical Coherence Tomography: A Review. *J Memb Sci* 2024, 692, 122291, doi:10.1016/J.MEMSCI.2023.122291.
- 64. Landaburu-Aguirre, J.; García-Pacheco, R.; Molina, S.; Rodríguez-Sáez, L.; Rabadán, J.; García-Calvo, E. Fouling Prevention, Preparing for Re-Use and Membrane Recycling. Towards Circular Economy in RO Desalination. *Desalination* **2016**, *393*, 16–30, doi:10.1016/j.desal.2016.04.002.
- Senán-Salinas, J.; Blanco, A.; García-Pacheco, R.; Landaburu-Aguirre, J.; García-Calvo, E. Prospective Life Cycle Assessment and Economic Analysis of Direct Recycling of End-of-Life Reverse Osmosis Membranes Based on Geographic Information Systems. *J Clean Prod* 2021, 282, 124400, doi:10.1016/J.JCLEPRO.2020.124400.
- Judd, S.J. Membrane Technology Costs and Me. Water Res 2017, 122, 1–9, doi:10.1016/J.WATRES.2017.05.027.
- 67. Senán-Salinas, J.; Blanco, A.; García-Pacheco, R.; Landaburu-Aguirre, J.; García-Calvo, E. Prospective Life Cycle Assessment and Economic Analysis of Direct Recycling of End-of-Life Reverse Osmosis Membranes Based on Geographic Information Systems. *J Clean Prod* **2021**, *282*, 124400, doi:10.1016/J.JCLEPRO.2020.124400.
- Khaled, M.; Noby, H.; Mansor, E.S.; Elshazly, A.H.; Aissa, W.A. Waste High Impact Polystyrene (HIPS) Microfiltration Membranes for Water Treatment: A Thorough Experimental Study. *Environmental Quality Management* 2022, doi:10.1002/tqem.21948.
- 69. Yang, Z.; Lü, F.; Zhang, H.; Wang, W.; Shao, L.; Ye, J.; He, P. Is Incineration the Terminator of Plastics and Microplastics? *J Hazard Mater* **2021**, *401*, 123429, doi:10.1016/J.JHAZMAT.2020.123429.
- Lejarazu-Larrañaga, A.; Landaburu-Aguirre, J.; Senán-Salinas, J.; Ortiz, J.M.; Molina, S. Thin Film Composite Polyamide Reverse Osmosis Membrane Technology towards a Circular Economy. *Membranes 2022, Vol. 12, Page 864* 2022, 12, 864, doi:10.3390/MEMBRANES12090864.
- 71. Krook, J.; Svensson, N.; Eklund, M. Landfill Mining: A Critical Review of Two Decades of Research. *Waste Management* **2012**, *32*, 513–520, doi:10.1016/J.WASMAN.2011.10.015.
- 72. EUROPEAN COMMISSION EUR-Lex 52019DC0640 EN EUR-Lex Available online: https://eur-lex.europa.eu/legal-

- content/EN/TXT/?qid=1576150542719&uri=COM%3A2019%3A640%3AFI N (accessed on 3 May 2022).
- 73. Lim, Y.J.; Goh, K.; Kurihara, M.; Wang, R. Seawater Desalination by Reverse Osmosis: Current Development and Future Challenges in Membrane Fabrication A Review. *J Memb Sci* **2021**, *629*, 119292, doi:10.1016/J.MEMSCI.2021.119292.
- Lejarazu-Larrañaga, A.; Landaburu-Aguirre, J.; Senán-Salinas, J.; Ortiz, J.M.;
 Molina, S. Thin Film Composite Polyamide Reverse Osmosis Membrane
 Technology towards a Circular Economy. *Membranes 2022, Vol. 12, Page 864* 2022, 12, 864, doi:10.3390/MEMBRANES12090864.
- 75. Rodríguez, J.J.; Jiménez, V.; Trujillo, O.; Veza, J. Reuse of Reverse Osmosis Membranes in Advanced Wastewater Treatment. *Desalination* **2002**, *150*, 219–225, doi:10.1016/S0011-9164(02)00977-3.
- Lawler, W.; Bradford-Hartke, Z.; Cran, M.J.; Duke, M.; Leslie, G.; Ladewig, B.P.; Le-Clech, P. Towards New Opportunities for Reuse, Recycling and Disposal of Used Reverse Osmosis Membranes. *Desalination* 2012, 299, 103–112, doi:10.1016/J.DESAL.2012.05.030.
- 77. Coutinho de Paula, E.; Amaral, M.C.S. Extending the Life-Cycle of Reverse Osmosis Membranes: A Review. *Waste Management and Research* **2017**, *35*, 456–470, doi:10.1177/0734242X16684383.
- 78. Molina, S.; Landaburu-Aguirre, J.; Rodríguez-Sáez, L.; García-Pacheco, R.; de la Campa, J.G.; García-Calvo, E. Effect of Sodium Hypochlorite Exposure on Polysulfone Recycled UF Membranes and Their Surface Characterization. *Polym Degrad Stab* **2018**, *150*, 46–56, doi:10.1016/j.polymdegradstab.2018.02.012.
- García-Pacheco, R.; Landaburu-Aguirre, J.; Molina, S.; Rodríguez-Sáez, L.;
 Teli, S.B.; García-Calvo, E. Transformation of End-of-Life RO Membranes into NF and UF Membranes: Evaluation of Membrane Performance. *J Memb Sci* 2015, 495, 305–315, doi:10.1016/j.memsci.2015.08.025.
- García-Pacheco, R.; Landaburu-Aguirre, J.; Terrero-Rodríguez, P.; Campos, E.; Molina-Serrano, F.; Rabadán, J.; Zarzo, D.; García-Calvo, E. Validation of Recycled Membranes for Treating Brackish Water at Pilot Scale. *Desalination* 2018, 433, 199–208, doi:10.1016/J.DESAL.2017.12.034.
- 81. Contreras-Martínez, J.; García-Payo, C.; Khayet, M. Electrospun Nanostructured Membrane Engineering Using Reverse Osmosis Recycled Modules: Membrane Distillation Application. *Nanomaterials* 2021, Vol. 11, Page 1601 2021, 11, 1601, doi:10.3390/NANO11061601.
- 82. Contreras-Martínez, J.; García-Payo, C.; Arribas, P.; Rodríguez-Sáez, L.; Lejarazu-Larrañaga, A.; García-Calvo, E.; Khayet, M. Recycled Reverse Osmosis Membranes for Forward Osmosis Technology. *Desalination* **2021**, *519*, 115312, doi:10.1016/J.DESAL.2021.115312.
- 83. Morón-López, J.; Nieto-Reyes, L.; Senán-Salinas, J.; Molina, S.; El-Shehawy, R. Recycled Desalination Membranes as a Support Material for Biofilm Development: A New Approach for Microcystin Removal during Water Treatment. Science of The Total Environment 2019, 647, 785–793, doi:10.1016/J.SCITOTENV.2018.07.435.
- Morón-López, J.; Nieto-Reyes, L.; Molina, S.; Lezcano, M.Á. Exploring Microcystin-Degrading Bacteria Thriving on Recycled Membranes during a Cyanobacterial Bloom. Science of The Total Environment 2020, 736, 139672, doi:10.1016/J.SCITOTENV.2020.139672.
- 85. Rodríguez-Sáez, L.; Patsios, S.I.; Senán-Salinas, J.; Landaburu-Aguirre, J.; Molina, S.; García-Calvo, E. A Novel Application of Recycled Ultrafiltration

- Membranes in an Aerobic Membrane Bioreactor (AMBR): A Proof-of-Concept Study. *Membranes (Basel)* **2022**, *12*, 218, doi:10.3390/MEMBRANES12020218.
- Rodríguez-Sáez, L.; Landaburu-Aguirre, J.; García-Calvo, E.; Molina, S. Application of Recycled Ultrafiltration Membranes in an Aerobic Membrane Bioreactor (AMBR): A Validation Study. *Membranes (Basel)* 2024, 14, 149, doi:10.3390/membranes14070149.
- 87. Ortiz De Lejarazu Larrañaga, A. Anion-Exchange Membranes from End of Life Reverse Osmosis Membranes: Indirect Recycling Approach for a Circular Water Sector. Programa de Doctorado en Hidrología y Gestión de los Recursos Hídricos, Universidad de Alcalá.: Alcalá de Henares, 2022.
- Lejarazu-Larrañaga, A.; Ortiz, J.M.; Molina, S.; Zhao, Y.; García-Calvo, E. Nitrate-Selective Anion Exchange Membranes Prepared Using Discarded Reverse Osmosis Membranes as Support. *Membranes (Basel)* 2020, 10, 1–18, doi:10.3390/membranes10120377.
- 89. Lejarazu-Larrañaga, A.; Molina, S.; Ortiz, J.M.; Riccardelli, G.; García-Calvo, E. Influence of Acid/Base Activation Treatment in the Performance of Recycled Electromembrane for Fresh Water Production by Electrodialysis. Chemosphere 2020, 248, 126027, doi:10.1016/J.CHEMOSPHERE.2020.126027.
- Lejarazu-Larrañaga, A.; Ortiz, J.M.; Molina, S.; Pawlowski, S.; Galinha, C.F.; Otero, V.; García-Calvo, E.; Velizarov, S.; Crespo, J.G. Nitrate Removal by Donnan Dialysis and Anion-Exchange Membrane Bioreactor Using Upcycled End-of-Life Reverse Osmosis Membranes. *Membranes 2022, Vol. 12, Page 101* 2022, *12*, 101, doi:10.3390/MEMBRANES12020101.
- Ortiz, A.; Larrañaga, L. Anion-Exchange Membranes from End-of-Life Reverse Osmosis Membranes: Indirect Recycling Approach for a Circular Water Sector. TESIS DOCTORAL, 2022.
- 92. Willis, R.M.; Stewart, R.A.; Williams, P.R.; Hacker, C.H.; Emmonds, S.C.; Capati, G. Residential Potable and Recycled Water End Uses in a Dual Reticulated Supply System. *Desalination* **2011**, *272*, 201–211, doi:10.1016/J.DESAL.2011.01.022.
- Racar, M.; Dolar, D.; Karadakić, K.; Čavarović, N.; Glumac, N.; Ašperger, D.; Košutić, K. Challenges of Municipal Wastewater Reclamation for Irrigation by MBR and NF/RO: Physico-Chemical and Microbiological Parameters, and Emerging Contaminants. Science of The Total Environment 2020, 722, 137959, doi:10.1016/J.SCITOTENV.2020.137959.
- 94. Srivastava, A.; Parida, V.K.; Majumder, A.; Gupta, B.; Gupta, A.K. Treatment of Saline Wastewater Using Physicochemical, Biological, and Hybrid Processes: Insights into Inhibition Mechanisms, Treatment Efficiencies and Performance Enhancement. *J Environ Chem Eng* **2021**, *9*, 105775, doi:10.1016/J.JECE.2021.105775.
- R.S Ayers; D.W. Westcot Water Quality for Agriculture; California, USA, 1985; Vol. 1; ISBN 9251022631.
- Nor Naimah Rosyadah Ahmad, Wei Lun Ang, Choe Peng Leo, Abdul Wahab Mohammad, N.H. Current Advances in Membrane Technologies for Saline Wastewater Treatment: A Comprehensive Review. *Desalination* 2021, 517, 115170.
- 97. Goodman, N.B.; Taylor, R.J.; Xie, Z.; Gozukara, Y.; Clements, A. A Feasibility Study of Municipal Wastewater Desalination Using Electrodialysis Reversal to Provide Recycled Water for Horticultural Irrigation. *Desalination* **2013**, *317*, 77–83, doi:10.1016/J.DESAL.2013.02.010.

- 98. Chojnacka, K.; Witek-Krowiak, A.; Moustakas, K.; Skrzypczak, D.; Mikula, K.; Loizidou, M. A Transition from Conventional Irrigation to Fertigation with Reclaimed Wastewater: Prospects and Challenges. *Renewable and Sustainable Energy Reviews* **2020**, *130*, 109959, doi:10.1016/J.RSER.2020.109959.
- Anis, S.F.; Hashaikeh, R.; Hilal, N. Microfiltration Membrane Processes: A Review of Research Trends over the Past Decade. *Journal of Water Process Engineering* 2019, 32, 100941, doi:10.1016/J.JWPE.2019.100941.
- 100. Al Aani, S.; Mustafa, T.N.; Hilal, N. Ultrafiltration Membranes for Wastewater and Water Process Engineering: A Comprehensive Statistical Review over the Past Decade. *Journal of Water Process Engineering* 2020, 35, 101241, doi:10.1016/J.JWPE.2020.101241.
- Mohammad, A.W.; Teow, Y.H.; Ang, W.L.; Chung, Y.T.; Oatley-Radcliffe, D.L.; Hilal, N. Nanofiltration Membranes Review: Recent Advances and Future Prospects. *Desalination* 2015, 356, 226–254, doi:10.1016/J.DESAL.2014.10.043.
- 102. Rodríguez, J.J.; Jiménez, V.; Trujillo, O.; Veza, J. Reuse of Reverse Osmosis Membranes in Advanced Wastewater Treatment. *Desalination* **2002**, *150*, 219–225, doi:10.1016/S0011-9164(02)00977-3.
- 103. Veza, J.M.; Rodriguez-Gonzalez, J.J. Second Use for Old Reverse Osmosis Membranes: Wastewater Treatment. *Desalination* 2003, 157, 65–72, doi:10.1016/S0011-9164(03)00384-9.
- 104. García-Pacheco, R.; Landaburu-Aguirre, J.; Molina, S.; Rodríguez-Sáez, L.; Teli, S.B.; García-Calvo, E. Transformation of End-of-Life RO Membranes into NF and UF Membranes: Evaluation of Membrane Performance. *J Memb Sci* 2015, 495, 305–315, doi:10.1016/j.memsci.2015.08.025.
- 105. Molina, S.; García-Pacheco, R.; Rodríguez-Sáez, L.; E. García-Calvo, E.C.; Zarzo, D.; González, J.; Abajo, J. Transformation of End-of-Life RO Membranes into Recycled NF and UF Membranes, Surface Characterization. *Idawc15* 2015.
- 106. Ahmed, J.; Jamal, Y. A Pilot Application of Recycled Discarded RO Membranes for Low Strength Gray Water Reclamation. *Environmental Science and Pollution Research* 2021, 28, 34042–34050, doi:10.1007/S11356-020-11117-Z/FIGURES/10.
- García-Pacheco, R.; Landaburu-Aguirre, J.; Terrero-Rodríguez, P.; Campos, E.; Molina-Serrano, F.; Rabadán, J.; Zarzo, D.; García-Calvo, E. Validation of Recycled Membranes for Treating Brackish Water at Pilot Scale. *Desalination* 2018, 433, 199–208, doi:10.1016/J.DESAL.2017.12.034.
- 108. Lejarazu-Larrañaga, A.; Molina, S.; Ortiz, J.M.; Navarro, R.; García-Calvo, E. Circular Economy in Membrane Technology: Using End-of-Life Reverse Osmosis Modules for Preparation of Recycled Anion Exchange Membranes and Validation in Electrodialysis. *J Memb Sci* 2020, 593, 117423, doi:10.1016/j.memsci.2019.117423.
- 109. Lejarazu-Larrañaga, A.; Ortiz, J.M.; Molina, S.; Zhao, Y.; García-Calvo, E. Nitrate-Selective Anion Exchange Membranes Prepared Using Discarded Reverse Osmosis Membranes as Support. *Membranes (Basel)* 2020, 10, 1–18, doi:10.3390/membranes10120377.
- García-Pacheco, R.; Lawler, W.; Landaburu-Aguirre, J.; García-Calvo, E.; Le-Clech, P. 4.14 End-of-Life Membranes: Challenges and Opportunities. In Comprehensive Membrane Science and Engineering; Elsevier, 2017; pp. 293–310.

- 111. Baker, R.W.; Wijmans, J.G.; Huang, Y. Permeability, Permeance and Selectivity: A Preferred Way of Reporting Pervaporation Performance Data. *J Memb Sci* **2010**, *348*, 346–352, doi:10.1016/J.MEMSCI.2009.11.022.
- Mowlid Nur, H.; Yüzer, B.; Aydin, M.İ.; Aydin, S.; Öngen, A.; Selçuk, H. Desalination and Fate of Nutrient Transport in Domestic Wastewater Using Electrodialysis Membrane Process. 2018, 24–26, doi:10.5004/dwt.2019.24984.
- 113. Strathmann, H. Electrodialysis, a Mature Technology with a Multitude of New Applications. **2010**, doi:10.1016/j.desal.2010.04.069.
- 114. Baker, R.W.; Wijmans, J.G.; Huang, Y. Permeability, Permeance and Selectivity: A Preferred Way of Reporting Pervaporation Performance Data. *J Memb Sci* **2010**, *348*, 346–352, doi:10.1016/J.MEMSCI.2009.11.022.
- 115. Mowlid Nur, H.; Yüzer, B.; Aydin, M.İ.; Aydin, S.; Öngen, A.; Selçuk, H. Desalination and Fate of Nutrient Transport in Domestic Wastewater Using Electrodialysis Membrane Process. 2018, 24–26, doi:10.5004/dwt.2019.24984.
- 116. Gherasim, C.V.; Křivčík, J.; Mikulášek, P. Investigation of Batch Electrodialysis Process for Removal of Lead Ions from Aqueous Solutions. Chemical Engineering Journal 2014, 256, 324–334, doi:10.1016/J.CEJ.2014.06.094.
- 117. Merkel, A.; Ashrafi, A.M.; Ečer, J. Bipolar Membrane Electrodialysis Assisted PH Correction of Milk Whey. J Memb Sci 2018, 555, 185–196, doi:10.1016/J.MEMSCI.2018.03.035.
- Chemical and Physical Characteristics of Standard Soils According to GLP Available online: https://www.lufa-speyer.de/ (accessed on 30 March 2022).
- 119. Driscoll, W.C. Robustness of the ANOVA and Tukey-Kramer Statistical Tests. *Comput Ind Eng* **1996**, *31*, 265–268, doi:10.1016/0360-8352(96)00127-1.
- 120. American Public Health Association; American Water Works Association; Water Environment Federation APHA Method 4500-NO3: Standard Methods for the Examination of Water and Wastewater; American Public Health Association: Washington DC, USA, 1992; Vol. 552; ISBN ISBN 0-87553-207-1
- 121. Service, O.S.University.E.; Extension, W.S.University.; Extension, U. of Idaho.; Hopkins, B.G.; Horneck, D.A.; Stevens, R.G.; Ellsworth, J.W.; Sullivan, Dan M. (Dan Matthew), 1954-; Extension, P.N.C. Managing Irrigation Water Quality for Crop Production in the Pacific Northwest Available online:
 - https://ir.library.oregonstate.edu/concern/administrative_report_or_publicatio ns/w3763710v?locale=en (accessed on 14 February 2022).
- 122. Xu, X.; He, Q.; Ma, G.; Wang, H.; Nirmalakhandan, N.; Xu, P. Selective Separation of Mono- and Di-Valent Cations in Electrodialysis during Brackish Water Desalination: Bench and Pilot-Scale Studies. *Desalination* **2018**, *428*, 146–160, doi:10.1016/j.desal.2017.11.015.
- 123. Cowan, D.A.; Brown, J.H. Effect of Turbulence on Limiting Current in Electrodialysis Cells.
- 124. Strathmann, H. *Ion-Exchange Membrane Separation Prosses*; Volume 9.; Membrane Science and Technology Series, 2004; ISBN 044450236X.
- 125. Lightfoot, E.N. Membrane Separations Technology: Principles and Applications. *Chem Eng Sci* **1996**, *51*, 325–326, doi:10.1016/s0009-2509(96)90039-1.
- 126. Mohammadi, R.; Ramasamy, D.L.; Sillanpää, M. Enhancement of Nitrate Removal and Recovery from Municipal Wastewater through Single-and Multi-

- Batch Electrodialysis: Process Optimisation and Energy Consumption. *Desalination* **2021**, *498*, 114726, doi:10.1016/j.desal.2020.114726.
- 127. Cifuentes-Araya, N.; Pourcelly, G.; Bazinet, L. Impact of Pulsed Electric Field on Electrodialysis Process Performance and Membrane Fouling during Consecutive Demineralization of a Model Salt Solution Containing a High Magnesium/Calcium Ratio. *J Colloid Interface Sci* **2011**, *361*, 79–89, doi:10.1016/J.JCIS.2011.05.044.
- 128. Lejarazu-Larrañaga, A.; Ortiz, J.M.; Molina, S.; Pawlowski, S.; Galinha, C.F.; Otero, V.; García-Calvo, E.; Velizarov, S.; Crespo, J.G. Nitrate Removal by Donnan Dialysis and Anion-Exchange Membrane Bioreactor Using Upcycled End-of-Life Reverse Osmosis Membranes. *Membranes* 2022, Vol. 12, Page 101 2022, 12, 101, doi:10.3390/MEMBRANES12020101.
- 129. Senán-Salinas, J.; García-Pacheco, R.; Landaburu-Aguirre, J.; García-Calvo, E. Recycling of End-of-Life Reverse Osmosis Membranes: Comparative LCA and Cost-Effectiveness Analysis at Pilot Scale. Resour Conserv Recycl 2019, 150, 104423, doi:10.1016/J.RESCONREC.2019.104423.
- Dolar, D.; Racar, M.; Košutić, K. Municipal Wastewater Reclamation and Water Reuse for Irrigation by Membrane Processes. *Chem Biochem Eng Q* 2019, 33, 417–425, doi:10.15255/CABEQ.2018/1571.
- 131. Gündoğdu, M.; Jarma, Y.A.; Kabay, N.; Pek, T.; Yüksel, M. Integration of MBR with NF/RO Processes for Industrial Wastewater Reclamation and Water Reuse-Effect of Membrane Type on Product Water Quality. *Journal of Water Process Engineering* 2019, 29, 100574, doi:10.1016/j.jwpe.2018.02.009.
- 132. Petek, M.; Krvavica, L.; Karažija, T.; Žlabur, J.Š.; Ćustić, M.H. Macroelements Status in Lettuce Affected by Different Forms of Phosphorus Fertilization. *Scientific Papers. Series B, Horticulture* **2020**, *LXIV*, 227–234.
- 133. López, A.; Javier, G.A.; Fenoll, J.; Hellín, P.; Flores, P. Chemical Composition and Antioxidant Capacity of Lettuce: Comparative Study of Regular-Sized (Romaine) and Baby-Sized (Little Gem and Mini Romaine) Types. *Journal of Food Composition and Analysis* 2014, 33, 39–48, doi:10.1016/J.JFCA.2013.10.001.
- 134. Broadley, M.R.; Seginer, I.; Burns, A.; Escobar-Gutiérrez, A.J.; Burns, I.G.; White, P.J. The Nitrogen and Nitrate Economy of Butterhead Lettuce (Lactuca Sativa Var. Capitata L.). J Exp Bot 2003, 54, 2081–2090, doi:10.1093/JXB/ERG222.
- 135. Solaiman, Z.M.; Yang, H.; Archdeacon, D.; Tippett, O.; Tibi, M.; Whiteley, A.S. Humus-Rich Compost Increases Lettuce Growth, Nutrient Uptake, Mycorrhizal Colonisation, and Soil Fertility. *Pedosphere* 2019, 29, 170–179, doi:10.1016/S1002-0160(19)60794-0.
- 136. European Parliament and Council Concerning the Registration, Evaluation, Authorisation and Restriction of Chemicals (REACH) as Regards Synthetic Polymer Microparticles.
- 137. Gigault, J.; Halle, A. ter; Baudrimont, M.; Pascal, P.Y.; Gauffre, F.; Phi, T.L.; El Hadri, H.; Grassl, B.; Reynaud, S. Current Opinion: What Is a Nanoplastic? *Environmental Pollution* **2018**, 235, 1030–1034, doi:10.1016/J.ENVPOL.2018.01.024.
- 138. Lares, M.; Ncibi, M.C.; Sillanpää, M.; Sillanpää, M. Occurrence, Identification and Removal of Microplastic Particles and Fibers in Conventional Activated Sludge Process and Advanced MBR Technology. Water Res 2018, 133, 236–246, doi:10.1016/J.WATRES.2018.01.049.
- 139. Talvitie, J.; Mikola, A.; Setälä, O.; Heinonen, M.; Koistinen, A. How Well Is Microlitter Purified from Wastewater? A Detailed Study on the Stepwise

- Removal of Microlitter in a Tertiary Level Wastewater Treatment Plant. *Water Res* **2017**, *109*, 164–172, doi:10.1016/J.WATRES.2016.11.046.
- 140. Alimi, O.S.; Farner Budarz, J.; Hernandez, L.M.; Tufenkji, N. Microplastics and Nanoplastics in Aquatic Environments: Aggregation, Deposition, and Enhanced Contaminant Transport. *Environ Sci Technol* **2018**, *52*, 1704–1724, doi:10.1021/ACS.EST.7B05559/SUPPL FILE/ES7B05559 SI 001.PDF.
- 141. Golgoli, M.; Khiadani, M.; Shafieian, A.; Sen, T.K.; Hartanto, Y.; Johns, M.L.; Zargar, M. Microplastics Fouling and Interaction with Polymeric Membranes: A Review. *Chemosphere* 2021, 283, 131185, doi:10.1016/J.CHEMOSPHERE.2021.131185.
- 142. Elsaid, K.; Olabi, A.G.; Abdel-Wahab, A.; Elkamel, A.; Alami, A.H.; Inayat, A.; Chae, K.-J.; Abdelkareem, M.A. Membrane Processes for Environmental Remediation of Nanomaterials: Potentials and Challenges. *Science of The Total Environment* 2023, 879, 162569, doi:10.1016/j.scitotenv.2023.162569.
- Landaburu-Aguirre, J. Polymeric Membranes for Micronanoplastic Sampling and Removal from Water Effluents. *Polymer Science: Peer Review Journal* 2022, 4, doi:10.31031/PSPRJ.2022.04.000591.
- 144. Wan, H.; Shi, K.; Yi, Z.; Ding, P.; Zhuang, L.; Mills, R.; Bhattacharyya, D.; Xu, Z. Removal of Polystyrene Nanoplastic Beads Using Gravity-Driven Membrane Filtration: Mechanisms and Effects of Water Matrices. *Chemical Engineering Journal* 2022, 450, 138484, doi:10.1016/J.CEJ.2022.138484.
- 145. Wang, J.; Cahyadi, A.; Wu, B.; Pee, W.; Fane, A.G.; Chew, J.W. The Roles of Particles in Enhancing Membrane Filtration: A Review. *J Memb Sci* 2020, 595, 117570, doi:10.1016/J.MEMSCI.2019.117570.
- 146. Enfrin, M.; Lee, J.; Le-Clech, P.; Dumee, L.F. Kinetic and Mechanistic Aspects of Ultrafiltration Membrane Fouling by Nano-and Microplastics. *J Memb Sci* 2020, 601, 117890, doi:10.1016/j.memsci.2020.117890.
- 147. Ayoubian Markazi, S.; Karimi, M.; Yousefi, B.; Sadati, M.; Khoramshahi, H.; Khoee, S.; Karimi, M.R. Experimental and Modeling Study on the Simultaneous Fouling Behavior of Micro/Nanoplastics and Bovine Serum Albumin in Ultrafiltration Membrane Separation. *J Environ Chem Eng* **2023**, *11*, 109354, doi:10.1016/J.JECE.2023.109354.
- 148. Sharma, A.; Kumari, S.; Chopade, R.L.; Pandit, P.P.; Rai, A.R.; Nagar, V.; Awasthi, G.; Singh, A.; Awasthi, K.K.; Sankhla, M.S. An Assessment of the Impact of Structure and Type of Microplastics on Ultrafiltration Technology for Microplastic Remediation. *Sci Prog* 2023, 106, 1–20, doi:10.1177/00368504231176399.
- 149. Cifuentes-Cabezas, M.; Bohórquez-Zurita, J.L.; Gil-Herrero, S.; Vincent-Vela, M.C.; Mendoza-Roca, J.A.; Álvarez-Blanco, S. Deep Study on Fouling Modelling of Ultrafiltration Membranes Used for OMW Treatment: Comparison Between Semi-Empirical Models, Response Surface, and Artificial Neural Networks. Food Bioproc Tech 2023, 16, 2126–2146, doi:10.1007/S11947-023-03033-0.
- 150. Di Bella, G.; Lee, S.; Cho, H.; Choi, Y.; Lee, S. Membranes Application of Optical Coherence Tomography (OCT) to Analyze Membrane Fouling under Intermittent Operation. *Membrane* **2023**, *392*, 13, doi:10.3390/membranes13040392.
- 151. Zou, S.; Wang, Y.N.; Wicaksana, F.; Aung, T.; Wong, P.C.Y.; Fane, A.G.; Tang, C.Y. Direct Microscopic Observation of Forward Osmosis Membrane Fouling by Microalgae: Critical Flux and the Role of Operational Conditions. *J Memb Sci* 2013, 436, 174–185, doi:10.1016/J.MEMSCI.2013.02.030.

- 152. Xi, C.; Marks, D.L.; Schlachter, S.; Luo, W.; M.D., S.A.B. High-Resolution Three-Dimensional Imaging of Biofilm Development Using Optical Coherence Tomography. *J Biomed Opt* **2006**, *11*, 034001, doi:10.1117/1.2209962.
- Wagner, M.; Taherzadeh, D.; Haisch, C.; Horn, H. Investigation of the Mesoscale Structure and Volumetric Features of Biofilms Using Optical Coherence Tomography. *Biotechnol Bioeng* 2010, 107, 844–853, doi:10.1002/BIT.22864.
- 154. Haisch, C.; Niessner, R. Visualisation of Transient Processes in Biofilms by Optical Coherence Tomography. Water Res 2007, 41, 2467–2472, doi:10.1016/J.WATRES.2007.03.017.
- 155. Im, S.J.; Viet, N.D.; Jang, A. Real-Time Monitoring of Forward Osmosis Membrane Fouling in Wastewater Reuse Process Performed with a Deep Learning Model. *Chemosphere* 2021, 275, 130047, doi:10.1016/J.CHEMOSPHERE.2021.130047.
- 156. Trinh, T.A.; Li, W.; Chew, J.W. Internal Fouling during Microfiltration with Foulants of Different Surface Charges. J Memb Sci 2020, 602, 117983, doi:10.1016/J.MEMSCI.2020.117983.
- 157. Han, Q.; Trinh, T.A.; Chew, J.W. Cake Formation of Bidisperse Suspensions in Dead-End Microfiltration. **2019**, doi:10.1016/j.memsci.2019.01.048.
- Lay, H.T.; Wang, R.; Chew, J.W. Membrane Fouling by Mixtures of Oppositely Charged Particles. *J Memb Sci* **2021**, *625*, 119093, doi:10.1016/j.memsci.2021.119093.
- 159. Park, J.; Lee, S.; You, J.; Park, S.; Ahn, Y.; Jung, W.; Cho, K.H. Evaluation of Fouling in Nanofiltration for Desalination Using a Resistance-in-Series Model and Optical Coherence Tomography. *Science of the Total Environment* **2018**, *642*, 349–355, doi:10.1016/j.scitotenv.2018.06.041.
- 160. Molina, S.; García-Pacheco, R.; Rodríguez-Sáez, L.; E. García-Calvo, E.C.; Zarzo, D.; González, J.; Abajo, J. Transformation of End-of-Life RO Membranes into Recycled NF and UF Membranes, Surface Characterization. *Idawc15* 2015.
- 161. EUROPEAN COMMISSION EUR-Lex 52019DC0640 EN EUR-Lex Available online: https://eur-lex.europa.eu/legal-content/EN/TXT/?qid=1576150542719&uri=COM%3A2019%3A640%3AFI N (accessed on 3 May 2022).
- García-Pacheco, R. Nanofiltration and Ultrafiltration Membranes from End-of-Life Reverse Osmosis Membranes: A Study of Recycling, 2017.
- 163. Mohamed, M.A.; Salleh, W.N.W.; Jaafar, J.; Ismail, A.F.; Abd. Mutalib, M.; Jamil, S.M. Feasibility of Recycled Newspaper as Cellulose Source for Regenerated Cellulose Membrane Fabrication. *J Appl Polym Sci* 2015, *132*, 42684, doi:10.1002/APP.42684.
- Molina, S.; Carretero, P.; Teli, S.B.; De la Campa, J.G.; Lozano, Á.E.; De Abajo, J. Hydrophilic Porous Asymmetric Ultrafiltration Membranes of Aramid-g-PEO Copolymers. *J Memb Sci* 2014, 454, 233–242, doi:10.1016/J.MEMSCI.2013.11.025.
- 165. Li, W.; Liu, X.; Wang, Y.-N.; Chong, T.H.; Tang, C.Y.; Fane, A.G. Analyzing the Evolution of Membrane Fouling via a Novel Method Based on 3D Optical Coherence Tomography Imaging. *Environ. Sci. Technol.* 2016, 50, 6930–6939, doi:10.1021/acs.est.6b00418.
- 166. Guo, Y.; Tang, N.; Lu, L.; Li, N.; Hu, T.; Guo, J.; Zhang, J.; Zeng, Z.; Liang, J. Aggregation Behavior of Polystyrene Nanoplastics: Role of Surface Functional

- Groups and Protein and Electrolyte Variation. **2023**, doi:10.1016/j.chemosphere.2023.140998.
- Abdelrasoul, A.; Doan, H.; Lohi, A. A Mechanistic Model for Ultrafiltration Membrane Fouling by Latex. J Memb Sci 2013, 433, 88–99, doi:10.1016/j.memsci.2013.01.003.
- 168. Contreras, A.E.; Kim, A.; Li, Q. Combined Fouling of Nanofiltration Membranes: Mechanisms and Effect of Organic Matter. *J Memb Sci* **2009**, *327*, 87–95, doi:10.1016/J.MEMSCI.2008.11.030.
- 169. Zin, G.; Penha, F.M.; Rezzadori, K.; Silva, F.L.; Guizoni, K.; Petrus, J.C.C.; Oliveira, J.V.; Di Luccio, M. Fouling Control in Ultrafiltration of Bovine Serum Albumin and Milk by the Use of Permanent Magnetic Field. *J Food Eng* 2016, 168, 154–159, doi:10.1016/J.JFOODENG.2015.07.033.
- Wu, S.; Hua, X.; Ma, B.; Fan, H.; Miao, R.; Ulbricht, M.; Hu, C.; Qu, J. Three-Dimensional Analysis of the Natural-Organic-Matter Distribution in the Cake Layer to Precisely Reveal Ultrafiltration Fouling Mechanisms. *Environ Sci Technol* 2021, 55, 5442–5452, doi:10.1021/ACS.EST.1C00435/SUPPL FILE/ES1C00435 SI 004.MPG.
- 171. Tanudjaja, H.J.; Anantharaman, A.; Qi, A.; Ng, Q.; Ma, Y.; Begüm Tanis-Kanbur, M.; Zydney, A.L.; Chew, J.W. A Review of Membrane Fouling by Proteins in Ultrafiltration and Microfiltration. *Journal of Water Process Engineering* **2022**, *50*, 103294, doi:10.1016/j.jwpe.2022.103294.
- 172. Ma, B.; Wu, G.; Li, W.; Miao, R.; Li, X.; Wang, P. Roles of Membrane–Foulant and Inter/Intrafoulant Species Interaction Forces in Combined Fouling of an Ultrafiltration Membrane. Science of The Total Environment 2019, 652, 19–26, doi:10.1016/J.SCITOTENV.2018.10.229.
- 173. Tian, J.-Y.; Ernst, M.; Cui, F.; Jekel, M. Effect of Particle Size and Concentration on the Synergistic UF Membrane Fouling by Particles and NOM Fractions. *J Memb Sci* **2013**, *446*, 1–9, doi:10.1016/j.memsci.2013.06.016.
- 174. Plastics the Facts 2022 Plastics Europe Available online: https://plasticseurope.org/knowledge-hub/plastics-the-facts-2022-2/.
- 175. Gigault, J.; Halle, A. ter; Baudrimont, M.; Pascal, P.Y.; Gauffre, F.; Phi, T.L.; El Hadri, H.; Grassl, B.; Reynaud, S. Current Opinion: What Is a Nanoplastic? *Environmental Pollution* **2018**, 235, 1030–1034, doi:10.1016/J.ENVPOL.2018.01.024.
- 176. Gigault, J.; El Hadri, H.; Nguyen, B.; Grassl, B.; Rowenczyk, L.; Tufenkji, N.; Feng, S.; Wiesner, M. Nanoplastics Are Neither Microplastics nor Engineered Nanoparticles. *Nature Nanotechnology 2021 16:5* **2021**, *16*, 501–507, doi:10.1038/s41565-021-00886-4.
- 177. Talvitie, J.; Mikola, A.; Koistinen, A.; Setälä, O. Solutions to Microplastic Pollution Removal of Microplastics from Wastewater Effluent with Advanced Wastewater Treatment Technologies. *Water Res* **2017**, *123*, 401–407, doi:10.1016/J.WATRES.2017.07.005.
- 178. Mohana, A.A.; Rahman, M.; Sarker, S.K.; Haque, N.; Gao, L.; Pramanik, B.K. Nano/Microplastics: Fragmentation, Interaction with Co-Existing Pollutants and Their Removal from Wastewater Using Membrane Processes.

 Chemosphere 2022, 309, 136682, doi:10.1016/J.CHEMOSPHERE.2022.136682.
- 179. Mitrano, D.M.; Beltzung, A.; Frehland, S.; Schmiedgruber, M.; Cingolani, A.; Schmidt, F. Synthesis of Metal-Doped Nanoplastics and Their Utility to Investigate Fate and Behaviour in Complex Environmental Systems. *Nature Nanotechnology* 2019 14:4 2019, 14, 362–368, doi:10.1038/s41565-018-0360-3.

- 180. Doddy Sutrisna, P.; Riadi, L.; Cipta Buana, P.W.; Khoiruddin, K.; Boopathy, R.; Gede Wenten, I.; Siagian, U.W. Journal Pre-Proof Membrane and Membrane-Integrated Processes for Nanoplastics Removal and Remediation. 2023, doi:10.1016/j.polymdegradstab.2023.110635.
- Bodzek, M.; Pohl, A.; Bodzek, M. Possibilities of Removing Microplastics from the Aquatic Environment Using Membrane Processes. 2022, 14–16, doi:10.5004/dwt.2023.29154.
- 182. Lv, L.; Zhou, F.; Wang, Z.; Wu, K.; Li, X.; Liao, W. The Current State and Future Opportunities of Micro- and Nano-Plastics Removal in Wastewater Treatment Plants. *Journal of Water Process Engineering* **2024**, *63*, 105462, doi:10.1016/J.JWPE.2024.105462.
- 183. Alvim, C.B.; Ferrer-Polonio, E.; Bes-Piá, M.A.; Mendoza-Roca, J.A.; Fernández-Navarro, J.; Alonso-Molina, J.L.; Amorós-Muñoz, I. Effect of Polystyrene Nanoplastics on the Activated Sludge Process Performance and Biomass Characteristics. A Laboratory Study with a Sequencing Batch Reactor. *J Environ Manage* **2023**, *329*, doi:10.1016/J.JENVMAN.2022.117131.
- 184. Zhou, C. shuang; Wu, J. wen; Ma, W. li; Liu, B. feng; Xing, D. feng; Yang, S. shan; Cao, G. li Responses of Nitrogen Removal under Microplastics versus Nanoplastics Stress in SBR: Toxicity, Microbial Community and Functional Genes. *J Hazard Mater* 2022, 432, 128715, doi:10.1016/J.JHAZMAT.2022.128715.
- 185. Bai, Z.; Zhang, Y.; Cheng, L.; Zhou, X.; Wang, M. Nanoplastics Pose a Greater Effect than Microplastics in Enhancing Mercury Toxicity to Marine Copepods. *Chemosphere* **2023**, *325*, doi:10.1016/J.CHEMOSPHERE.2023.138371.
- 186. Rice, E.W.; Baird, R.B.; Eaton, A.D. Standard Methods for the Examination of Water and Wastewater; American Public Health Association, Washington, D.C., 2017; Vol. 23rd Edition; ISBN 9780875532875.
- 187. Frølund, B.; Palmgren, R.; Keiding, K.; Nielsen, P.H. Extraction of Extracellular Polymers from Activated Sludge Using a Cation Exchange Resin. *Water Res* **1996**, *30*, 1749–1758, doi:10.1016/0043-1354(95)00323-1.
- 188. Zuriaga-Agustí, E.; Bes-Piá, A.; Mendoza-Roca, J.A.; Alonso-Molina, J.L. Influence of Extraction Methods on Proteins and Carbohydrates Analysis from MBR Activated Sludge Flocs in View of Improving EPS Determination. Sep Purif Technol 2013, 112, 1–10, doi:10.1016/J.SEPPUR.2013.03.048.
- 189. Bretas Alvim, C.; Bes-Piá, M.A.; Mendoza-Roca, J.A. Separation and Identification of Microplastics from Primary and Secondary Effluents and Activated Sludge from Wastewater Treatment Plants. Chemical Engineering Journal 2020, 402, doi:10.1016/J.CEJ.2020.126293.
- 190. Di Bella, G.; Di Trapani, D.; Judd, S. Fouling Mechanism Elucidation in Membrane Bioreactors by Bespoke Physical Cleaning. *Sep Purif Technol* **2018**, *199*, 124–133, doi:10.1016/J.SEPPUR.2018.01.049.
- 191. Xu, J.; Wang, X.; Zhang, Z.; Yan, Z.; Zhang, Y. Effects of Chronic Exposure to Different Sizes and Polymers of Microplastics on the Characteristics of Activated Sludge. Science of the Total Environment 2021, 783, doi:10.1016/J.SCITOTENV.2021.146954.
- 192. Li, H.; Xu, S.; Wang, S.; Yang, J.; Yan, P.; Chen, Y.; Guo, J.; Fang, F. New Insight into the Effect of Short-Term Exposure to Polystyrene Nanoparticles on Activated Sludge Performance. *Journal of Water Process Engineering* 2020, 38, 101559, doi:10.1016/J.JWPE.2020.101559.
- 193. Deng, L.; Guo, W.; Ngo, H.H.; Zhang, H.; Wang, J.; Li, J.; Xia, S.; Wu, Y. Biofouling and Control Approaches in Membrane Bioreactors. *Bioresour Technol* **2016**, *221*, 656–665, doi:10.1016/J.BIORTECH.2016.09.105.

- 194. Gkotsis, P.K.; Zouboulis, A.I. Biomass Characteristics and Their Effect on Membrane Bioreactor Fouling. *Molecules 2019, Vol. 24, Page 2867* **2019**, *24*, 2867, doi:10.3390/MOLECULES24162867.
- 195. Kunacheva, C.; Stuckey, D.C. Analytical Methods for Soluble Microbial Products (SMP) and Extracellular Polymers (ECP) in Wastewater Treatment Systems: A Review. *Water Res* **2014**, *61*, 1–18, doi:10.1016/J.WATRES.2014.04.044.
- 196. Wang, Z.; Gao, M.; Wang, Z.; She, Z.; Chang, Q.; Sun, C.; Zhang, J.; Ren, Y.; Yang, N. Effect of Salinity on Extracellular Polymeric Substances of Activated Sludge from an Anoxic–Aerobic Sequencing Batch Reactor. *Chemosphere* 2013, 93, 2789–2795, doi:10.1016/J.CHEMOSPHERE.2013.09.038.
- 197. Lin, H.; Zhang, M.; Wang, F.; Meng, F.; Liao, B.Q.; Hong, H.; Chen, J.; Gao, W. A Critical Review of Extracellular Polymeric Substances (EPSs) in Membrane Bioreactors: Characteristics, Roles in Membrane Fouling and Control Strategies. *J Memb Sci* 2014, 460, 110–125, doi:10.1016/J.MEMSCI.2014.02.034.
- 198. González-Fernández, C.; Tallec, K.; Le Goïc, N.; Lambert, C.; Soudant, P.; Huvet, A.; Suquet, M.; Berchel, M.; Paul-Pont, I. Cellular Responses of Pacific Oyster (Crassostrea Gigas) Gametes Exposed in Vitro to Polystyrene Nanoparticles. *Chemosphere* 2018, 208, 764–772, doi:10.1016/J.CHEMOSPHERE.2018.06.039.
- 199. Wu, Y.; Wang, J.; Zhao, T.; Sun, M.; Xu, M.; Che, S.; Pan, Z.; Wu, C.; Shen, L. Polystyrene Nanoplastics Lead to Ferroptosis in the Lungs. *J Adv Res* **2023**, doi:10.1016/J.JARE.2023.03.003.
- 200. Tang, S.; Qian, J.; Wang, P.; Lu, B.; He, Y.; Yi, Z.; Zhang, Y. Exposure to Nanoplastic Induces Cell Damage and Nitrogen Inhibition of Activated Sludge: Evidence from Bacterial Individuals and Groups. *Environmental Pollution* 2022, 306, doi:10.1016/J.ENVPOL.2022.119471.
- 201. Wang, Q.Y.; Li, Y.L.; Liu, Y.Y.; Zhou, Z.; Hu, W.J.; Lin, L.F.; Wu, Z.C. Effects of Microplastics Accumulation on Performance of Membrane Bioreactor for Wastewater Treatment. *Chemosphere* 2022, 287, 131968, doi:10.1016/J.CHEMOSPHERE.2021.131968.
- 202. Qian, J.; He, X.; Wang, P.; Xu, B.; Li, K.; Lu, B.; Jin, W.; Tang, S. Effects of Polystyrene Nanoplastics on Extracellular Polymeric Substance Composition of Activated Sludge: The Role of Surface Functional Groups. *Environmental Pollution* 2021, 279, doi:10.1016/J.ENVPOL.2021.116904.
- 203. Ur Rehman, Z.; Fortunato, L.; Cheng, T.; Leiknes, T. Metagenomic Analysis of Sludge and Early-Stage Biofilm Communities of a Submerged Membrane Bioreactor. Science of the Total Environment journal 2020, doi:10.1016/j.scitotenv.2019.134682.
- 204. Zhang, B.; Xu, X.; Zhu, L. Structure and Function of the Microbial Consortia of Activated Sludge in Typical Municipal Wastewater Treatment Plants in Winter. Scientific Reports 2017 7:1 2017, 7, 1–11, doi:10.1038/s41598-017-17743-x.
- 205. Simonsen Dueholm, M.; Nierychlo, M.; Skytte Andersen, K.; Rudkjøbing, V.; Knutsson, S.; MiDAS Global Consortium, the; Albertsen, M.; Halkjaer Nielsen, P. MiDAS 4: A Global Catalogue of Full-Length 16S RRNA Gene Sequences and Taxonomy for Studies of Bacterial Communities in Wastewater Treatment Plants. bioRxiv 2021, 2021.07.06.451231, doi:10.1101/2021.07.06.451231.
- Alvim, C.B.; Ferrer-Polonio, E.; Bes-Piá, M.A.; Mendoza-Roca, J.A.;
 Fernández-Navarro, J.; Alonso-Molina, J.L.; Amorós-Muñoz, I. Effect of

- Polystyrene Nanoplastics on the Activated Sludge Process Performance and Biomass Characteristics. A Laboratory Study with a Sequencing Batch Reactor. *J Environ Manage* **2023**, *329*, doi:10.1016/J.JENVMAN.2022.117131.
- 207. Olivier Lefebvre; Kok Kwang Ng; Kai Yin Tang; How Yong Ng Membrane Biological Reactors: Theory, Modeling, Design, Management and Applications to Wastewater Reuse Available online: https://www.researchgate.net/publication/277565753_Membrane_Biological_Reactors_Theory_Modeling_Design_Management_and_Applications_to_Wastewater Reuse.
- 208. Maliwan, T.; Pungrasmi, W.; Lohwacharin, J. Effects of Microplastic Accumulation on Floc Characteristics and Fouling Behavior in a Membrane Bioreactor. J. Hazard Mater 2021, 411, 124991, doi:10.1016/J.JHAZMAT.2020.124991.
- 209. Bretas Alvim, C.; Castelluccio, S.; Ferrer-Polonio, E.; Bes-Piá, M.A.; Mendoza-Roca, J.A.; Fernández-Navarro, J.; Alonso, J.L.; Amorós, I. Effect of Polyethylene Microplastics on Activated Sludge Process Accumulation in the Sludge and Influence on the Process and on Biomass Characteristics. *Process Safety and Environmental Protection* 2021, 148, 536–547, doi:10.1016/J.PSEP.2020.10.014.
- 210. Morón -López, J.; Nieto-Reyes, L.; Aguado, S.; El-Shehawy, R.; Molina, S. Recycling of End-of-Life Reverse Osmosis Membranes for Membrane Biofilms Reactors (MBfRs). Effect of Chlorination on the Membrane Surface and Gas Permeability. Jesús Mor on-L Opez. 2019, doi:10.1016/j.chemosphere.2019.05.108.